

①

NAVAL POSTGRADUATE SCHOOL

Monterey, California

AD-A283 211



THESIS

AN ANALYSIS OF EDDY RESOLVING GLOBAL OCEAN
MODELS IN THE SOUTHERN OCEAN

by

Rosemarie O'Carroll

March 1994

Thesis Advisor:

Albert J. Semtner

Approved for public release; distribution is unlimited.

DTIC
ELECTE
AUG 1 1 1994
S B D

13498
94-25249



DTIC QUALITY INSPECTED 1

94 8 10 016

REPORT DOCUMENTATION PAGE			Form Approved OMB No. 0704	
Public reporting burden for this collection of information is estimated to average 1 hour per response, including the time for reviewing instruction, searching existing data sources, gathering and maintaining the data needed, and completing and reviewing the collection of information. Send comments regarding this burden estimate or any other aspect of this collection of information, including suggestions for reducing this burden, to Washington headquarters Services, Directorate for Information Operations and Reports, 1215 Jefferson Davis Highway, Suite 1204, Arlington, VA 22202-4302, and to the Office of Management and Budget, Paperwork Reduction Project (04-0188) Washington DC 20503.				
1. AGENCY USE ONLY (Leave blank)		2. REPORT DATE March, 1994	3. REPORT TYPE AND DATES COVERED Master's Thesis	
4. TITLE AND SUBTITLE AN ANALYSIS OF EDDY RESOLVING GLOBAL OCEAN MODELS IN THE SOUTHERN OCEAN			5. FUNDING NUMBERS	
6. AUTHOR(S) Rosemarie Helen O'Carroll				
7. PERFORMING ORGANIZATION NAME(S) AND ADDRESS(ES) Naval Postgraduate School Monterey CA 93943-5000			8. PERFORMING ORGANIZATION REPORT NUMBER	
9. SPONSORING/MONITORING AGENCY NAME(S) AND ADDRESS(ES)			10. SPONSORING/MONITORING AGENCY REPORT NUMBER	
11. SUPPLEMENTARY NOTES The views expressed in this thesis are those of the author and do not reflect the official policy or position of the Department of Defense or the U.S. Government.				
12a. DISTRIBUTION/AVAILABILITY STATEMENT Approved for public release; distribution is unlimited.			12b. DISTRIBUTION CODE A	
13. ABSTRACT (maximum 200 words) <p>Comparisons between the two model runs, a half degree resolution and a quarter degree resolution of the Semtner-Chervin eddy-resolving global ocean model, and the Hydrographic Atlas of the Southern Ocean (Olters et al., 1993) observations are conducted by analyzing horizontal and vertical sections.</p> <p>The quarter degree model, employing a Mercator grid, was interpolated forward from the half degree model initialization. For the last three years of the model run time, the resolution was improved to 0.25° on average and ECMWF winds were used. Also, no deep restoring in the last three years is introduced into the model. Another difference between the half degree model and the quarter degree model is that in the latter, the bathymetry is unsmoothed, so that not only is the resolution finer, the topography is more realistic.</p> <p>The model is shown to produce very realistic circulation and temperature and salinity distributions. Volume transport and meridional volume and heat transports are also calculated.</p> <p>The quarter degree model shows marked improvement over the half degree model although both models have salinities to the south and near the surface which are higher than those observed. This could be due to errors in surface flux parametrizations. Improvement in this area and in vertical resolution of the model will improve this global three dimensional model.</p> <p>More thermohaline observations in the Southern Ocean as is being attempted by WOCE (World Ocean Circulation Experiment) will also help achieve more accurate simulation of deep convection resulting in a more realistic abyssal circulation.</p>				
14. SUBJECT TERMS Ocean Modeling, Southern Ocean			15. NUMBER OF PAGES 135	
			16. PRICE CODE	
17. SECURITY CLASSIFICATION OF REPORT Unclassified	18. SECURITY CLASSIFICATION OF THIS PAGE Unclassified	19. SECURITY CLASSIFICATION OF ABSTRACT Unclassified	20. LIMITATION OF ABSTRACT UL	

Approved for public release; distribution is unlimited.

An Analysis of Eddy Resolving Global Ocean Models in the Southern Ocean

by

Rosemarie Helen O'Carroll
Lieutenant , United States Navy
B.S., Loyola University of Chicago , 1984

Submitted in partial fulfillment of the
requirements for the degree of

MASTER OF SCIENCE IN METEOROLOGY AND PHYSICAL OCEANOGRAPHY

from the

NAVAL POSTGRADUATE SCHOOL
March, 1994

Author:

Rosemarie O'Carroll

Rosemarie O'Carroll

Approved by:

Albert J. Semner

Albert J. Semner, Thesis Advisor

Stephen F. Ackley

Stephen F. Ackley, Second Reader

Robert H. Bouckie Jr.

Curtis A. Collins, Chairman
Department of Oceanography

Abstract

Comparisons between the two model runs, a half degree resolution and a quarter degree resolution of the Semtner-Chervin eddy-resolving global ocean model, and the Hydrographic Atlas of the Southern Ocean (Olbers et al., 1993) observations are conducted by analyzing horizontal and vertical sections.

The quarter degree model, employing a Mercator grid, was interpolated forward from the half degree model initialization. For the last three years of the model run time, the resolution was improved to 0.25° on average and ECMWF winds were used. Also, no deep restoring in the last three years is introduced into the model. Another difference between the half degree model and the quarter degree model is that in the latter, the bathymetry is unsmoothed, so that not only is the resolution finer, the topography is more realistic.

The model is shown to produce very realistic circulation and temperature and salinity distributions. Volume transport and meridional volume and heat transports are also calculated.

The quarter degree model shows marked improvement over the half degree model although both models have salinities to the south and near the surface which are higher than those observed. This could be due to errors in surface flux parametrizations. Improvement in this area and in vertical resolution of the model will improve this global three dimensional model.

More thermohaline observations in the Southern Ocean as is being attempted by WOCE (World Ocean Circulation Experiment) will also help achieve more accurate simulation of deep convection resulting in a more realistic abyssal circulation.

TABLE OF CONTENTS

I. INTRODUCTION AND BACKGROUND	1
A. THE ANTARCTIC REGION	2
1. Geography and Meteorology	2
2. The Antarctic Circumpolar Current	5
3. Upwelling	9
4. Water Masses	9
5. Heat Flux	12
B. MODEL BACKGROUND	13
1. Overview	13
2. Semtner - Chervin Model	14
3. Observations	18
II. DATA PRESENTATION/COMPARISON	21
A. DRAKE PASSAGE/BRAZILIAN-MALVINAS CONFLUENCE	22
1. Area Temperature and Salinity (100 m)	22
2. Vertical Sections	26
3. Circulation Comparisons	30
4. Potential Vorticity	32
B. CENTRAL ATLANTIC/ AGULHAS CURRENT REGION	36
1. Area Temperature and Salinity (100 m)	36
2. Vertical Sections	40
3. Circulation	43
4. Potential Vorticity	47
C. KERGUELEN PLATEAU/CROZET BASIN AREA	50
1. Area Temperature and Salinity (100 m)	50
2. Vertical Sections	51
3. Circulation	55
4. Potential Vorticity	60
D. ACC SOUTH OF AUSTRALIA	63
1. Area Temperature and Salinity (100 m)	63
2. Vertical Sections	66
3. Circulation	69
4. Potential Vorticity	69
E. MACQUARIE RIDGE/ROSS SEA	73

1. Area Temperature and Salinity (100 m)	73
2. Vertical Sections	76
3. Circulation	79
4. Potential Vorticity	79
F. CENTRAL PACIFIC	83
1. Area Temperature and Salinity Charts (100 m)	83
2. Vertical Sections	83
3. Circulation	87
4. Potential Vorticity	91
G. WEDDELL SEA	93
1. Vertical Sections	95
2. Area 4000 m Temperature	96
3. Circulation	96
H. THE TOTAL ACC	101
1. Transports	101
III CONCLUSIONS	117
LIST OF REFERENCES	119
INITIAL DISTRIBUTION LIST	123

Accession For	
NTIS GRA&I	<input checked="checked" type="checkbox"/>
DTIC TAB	<input type="checkbox"/>
Unannounced	<input type="checkbox"/>
Justification	
By	
Distribution/	
Availability Codes	
Dist	Avail and/or Special
A-1	

LIST OF FIGURES

Figure 1.1	Map of Antarctica showing the 3000 m isobath and the floating Ice Shelf	3
Figure 1.2	Average atmospheric pressure map for July	6
Figure 1.3	Average surface positions of Southern Ocean Fronts	8
Figure 1.4	Schematic cross section of Southern Ocean circulation	11
Figure 1.5	Geometry of the model domain	15
Figure 1.6	Distribution of observation stations with temperature and salinity data	20
Figure 2.1	100 m Temperature charts for area 90°W to 30°W	23
Figure 2.2	100 m Salinity Charts for area 90°W to 30°W	25
Figure 2.3	Vertical Temperature sections along 69°W	27
Figure 2.4	Vertical Salinity sections along 69°W	28
Figure 2.5	Surface Circulation for area 90°W to 30°W	31
Figure 2.6	Deep Circulation for area 90°W to 30°W	33
Figure 2.7	Potential Vorticity for area 90°W to 30°W	35
Figure 2.8	100 m Temperature charts for area 30°W to 30°E	37
Figure 2.9	100 m Salinity Charts for area 30°W to 30°E	39
Figure 2.10	Vertical Temperature sections along 30°W	41
Figure 2.11	Vertical Salinity sections along 30°W	42
Figure 2.12	Vertical Temperature sections along 25° E	44
Figure 2.13	Vertical salinity sections along 25°E	45
Figure 2.14	Surface Circulation for area 30°W to 30°E	46
Figure 2.15	Deep Circulation for area 30°W to 30°E	48
Figure 2.16	Potential Vorticity for area 30°W to 30°E	49
Figure 2.17	100 m Temperature charts for area 30°E to 90°E	52
Figure 2.18	100 m Salinity Charts for area 30°E to 90°E	53
Figure 2.19	Vertical Temperature sections along 60°E	54
Figure 2.20	Vertical Salinity sections along 60°E	56
Figure 2.21	Surface Circulation for area 30°E to 90°E	57
Figure 2.22	Schematic Surface Circulation for area 30°E to 90°E	58
Figure 2.23	Deep Circulation for area 30°E to 90°E	59
Figure 2.24	Schematic Deep Circulation for area 30°E to 90°E	61
Figure 2.25	Potential Vorticity for area 30°E to 90°E	62
Figure 2.26	100 m Temperature charts for area 90°E to 150°E	64

Figure 2.27	100 m Salinity Charts for area 90°E to 150°E	65
Figure 2.28	Vertical Temperature sections along 130°E	67
Figure 2.29	Vertical Salinity sections along 130°E	68
Figure 2.30	Surface Circulation for area 90°E to 150 °E	70
Figure 2.31	Deep Circulation for area 90°E to 150 °E	71
Figure 2.32	Potential Vorticity for area 90°E to 150°E	72
Figure 2.33	100 m Temperature charts for area 150°E to 150°W	74
Figure 2.34	100 m Salinity Charts for area 150°E to 150°W	75
Figure 2.35	Vertical Temperature sections along 180°E	77
Figure 2.36	Vertical salinity sections along 180°E	78
Figure 2.37	Surface Circulation for area 150°E to 150°W	80
Figure 2.38	Deep Circulation for area 150°E to 150°W	81
Figure 2.39	Potential Vorticity for area 150°E to 150°W	82
Figure 2.40	100 m Temperature charts for area 150°W to 90°W	84
Figure 2.41	100 m Salinity Charts for area 150°W to 90°W	85
Figure 2.42	Vertical Temperature sections along 120°W	86
Figure 2.43	Vertical salinity sections along 120°W	88
Figure 2.44	Surface Circulation for area 150°W to 90°W	89
Figure 2.45	Deep Circulation for area 150°W to 90°W	90
Figure 2.46	Potential Vorticity for area 150°W to 90°W	92
Figure 2.47	Vertical Temperature sections along 72°S	94
Figure 2.48	Vertical Salinity sections along 72°S	97
Figure 2.49	4000 m Temperature charts for Weddell Sea Area	98
Figure 2.50	Surface Circulation in Weddell Sea Area	99
Figure 2.51	Deep Circulation in Weddell Sea Area	100
Figure 2.52	Meridional Transport	103
Figure 2.53	Meridional Heat Transport	105
Figure 2.54	Zonal Salinities	108
Figure 2.55	Polar 100 m Temperature Charts	
	(a) Olbers atlas data	110
	(b) Half degree model	111
	(c) Quarter degree model	112
Figure 2.56	Polar 100 m Salinity Charts	
	(a) Olbers atlas data	113

(b) Half degree model	114
Quarter degree model (c)	115

ACKNOWLEDGEMENT

Nothing in this world is created alone. Without the help and guidance given to me by an enormous number of people, this thesis would never have been written. My most sincere thanks go to Robin Tokmakian, Shirley Isakari, Anthony Craig, Jerry Davison, Pedro Tsai , Rost Parsons, Steve Ackley and Bert Semtner.

I would also like to take this opportunity to thank my mother and father for all their support through the years and my husband and daughter for their patience, love and support and for the joy they bring to my life.

I. INTRODUCTION AND BACKGROUND

The Antarctic region has always captured the imagination of man. Far away, cold, forbidding; it is the least studied area of the earth because of its remoteness and severe weather. The Southern Ocean which surrounds the Antarctic continent is unique in several ways:

It is the only global ocean. The Antarctic Circumpolar Current (ACC) blends all of the world's oceans together in a continual zonal flow around the Antarctic continent. Unlike the other major oceans, no meridional barrier is present to prevent the continuous flow of water. Processes occurring in the Antarctic can affect the global distribution of properties in the world's oceans.

Some of the densest water in the ocean is formed here. This water, termed Antarctic Bottom Water (AABW), flows north along the bottom of the ocean basins and can be found north of the equator. Antarctic Bottom Water, together with Circumpolar Deep Water and North Atlantic Deep Water create the thermohaline or vertical circulation of the world's oceans. The deep Antarctic convection sends both slowly moving and swifter western abyssal boundary currents equatorward. The main thermocline in the ocean is maintained by the resulting gentle upward flow.

Ocean dynamics and air sea interactions in the Southern Ocean frequently exert a global impact. The understanding of these processes is crucial to the development of climate prediction and the rational management of man's endeavors upon the earth (Nowlin, Klinck, 1986).

Computer simulation is the most promising tool available for enhancing the understanding of the global environment. Observations on a global scale are inadequate because it is difficult to make oceanographic measurements and place them on a common time base since the observations have to be made over several years to obtain global coverage. The resolution now possible with today's computers allows the study of ocean phenomena which we are only now beginning to observe in the environment, on a scale which is still not possible in the real ocean. This study examines the characteristics Southern Ocean as revealed by the Semtner-Chervin global ocean circulation model. (Semtner, 1992)

A. THE ANTARCTIC REGION

1. Geography and Meteorology

Antarctica is totally surrounded by the Southern Ocean (Figure 1.1.) The Southern Ocean is the world's only zonal sea with free boundaries to the north that extend into the South Pacific Ocean, the South Atlantic Ocean, and the Indian Ocean. This circumpolar ocean contains approximately 10% of all the world's sea water. Three distinct basins are close to the Antarctic continent: the Weddell Basin, the South-Indian Basin and the Southeast Pacific Basin. The Crozet Basin is separated from the South-Indian basin by the Kerguelan Plateau and from the Weddell Basin by the Crozet Plateau. The mid-ocean ridge system further encircles Antarctica and the continental basins to define four major basins. Each basin exceeds 4500 m in depth and is separated from each other by broad ridges and plateaus (Foldvik, 1988).

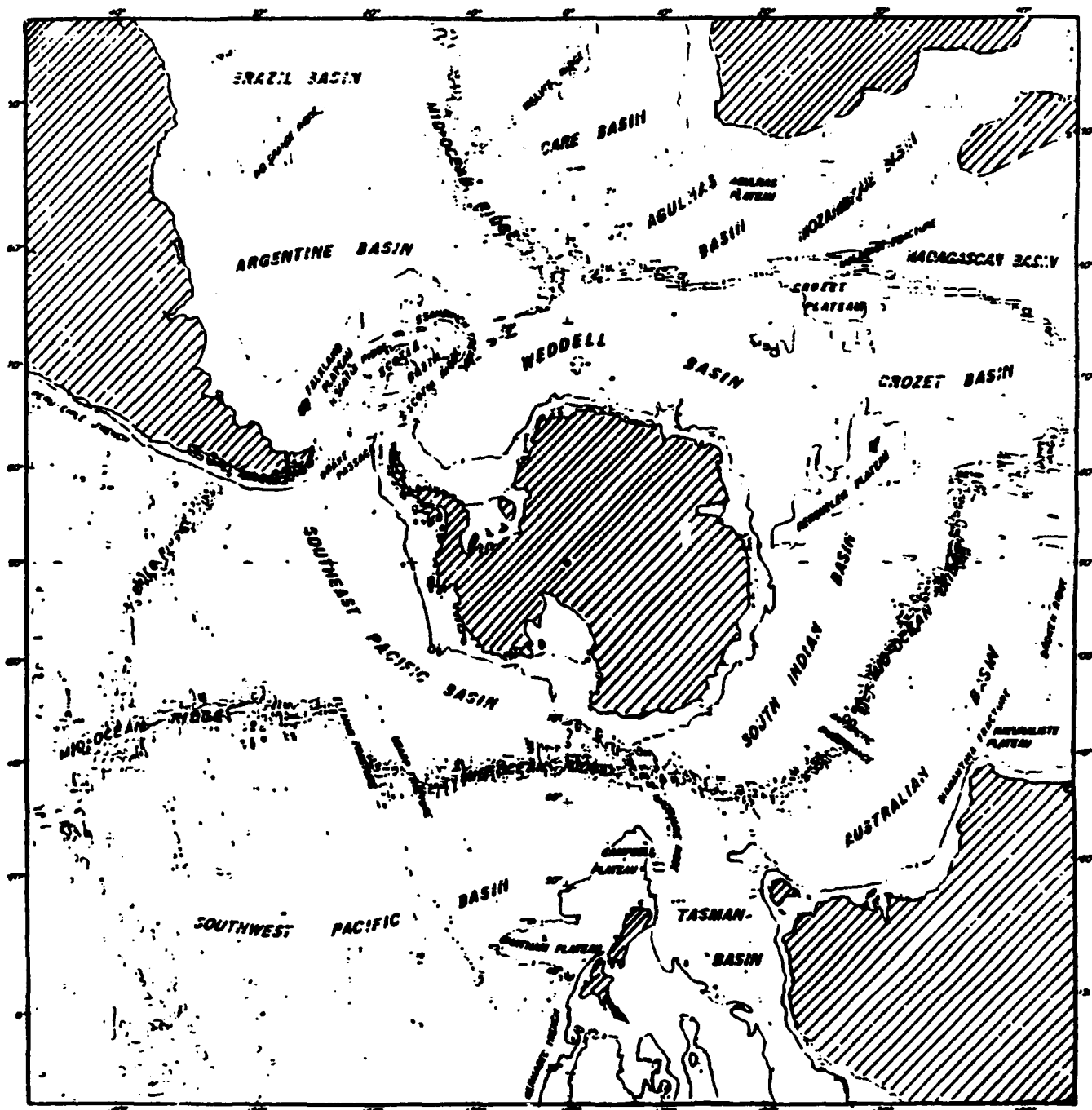


Figure 1.1 Map of Antarctica showing the 3000 m isobath and the floating ice shelf (Gordon, 1982)

The continental boundary to the south is special from a thermodynamic point of view. The Antarctic ice sheet moves slowly out from the interior towards the coastline where it ends as a vertical wall termed the ice barrier. Major portions of the ice sheet float as ice shelves on the sea over large areas, notably in the Ross Sea and the Weddell Sea (Ross Ice Shelf and the Filchner-Ronne Ice Shelf, respectively). The depth of the ice at the barrier varies with location but may exceed 400 m (Gordon, 1988).

The Drake Passage between South America and the Antarctic Peninsula is a narrow but deep choke point through which the ACC flows. This configuration provides a unique area to monitor the average properties of the circumpolar flow. The transport here represents the flow that is recirculated around the continent (Whitworth, 1982)

The Antarctic continent is the coldest region of the world. The ocean that encircles Antarctica not only establishes the major conduit between the three ocean basins but also isolates the polar continent of Antarctica from the warmer waters of the subtropics. It has been doing this for the last 25 million years, allowing a build up of a massive glacial ice cap resting on the Antarctic continent. This layer of fresh water glacial ice, with an average thickness of 3000 m and covering an area of $14 \times 10^6 \text{ km}^2$ comprises 91% of the Earth's continental ice. (Gordon, 1981)

The seasonality of the sea ice around Antarctica is dramatic. During the austral winter, sea ice completely surrounds the continent making an almost impassable barrier that extends northward from 65° S to 55° S in some locations, occupying about 60% of

the Southern Ocean ($20 \times 10^6 \text{ km}^2$). During the austral summer the ice melts to cover less than 10% of the Southern Ocean (Gordon, 1988).

The position of Antarctica influences the atmospheric circulation as great masses of cold air spread away from the dome of polar air over Antarctica. The boundary between the polar continental and the polar maritime air masses (the Antarctic coast) and the polar maritime and tropical maritime air masses (Polar Front at $\sim 50^\circ \text{S}$) represents an area of frequent and intense storm activity throughout the year. Storms generally are located north of 70°S and circle the continent from west to east. Lows forming along the Polar Front tend to move southeasterly towards the continent (Figure 1.2). The lack of a meridional barrier for atmospheric flow over the Southern Ocean leads to a basic zonal wind regime. These mean winds flow clockwise around the semi-permanent low pressure areas in both austral summer (January) and winter (July). Through zonal forcing of the sea surface, a westward flowing current the East Wind Drift is produced. North of the lows, the winds are westerly and produce an eastward surface circulation called the West Wind Drift (Karolyi, 1987).

2. The Antarctic Circumpolar Current

Through observations made in the last decade our concept of the dynamics and structure of the ACC has changed. The ACC is not a single broad flow but consists of four water masses, and multiple narrow jets imbedded in or associated with density fronts (the Subantarctic and Polar Fronts) which appear to be circumpolar in extent. Throughout most of the Southern Ocean the two jets run parallel to the mid-ocean ridge system that rings the Antarctic continent. Surface speeds in the jets are about 1.5 knots, considerably

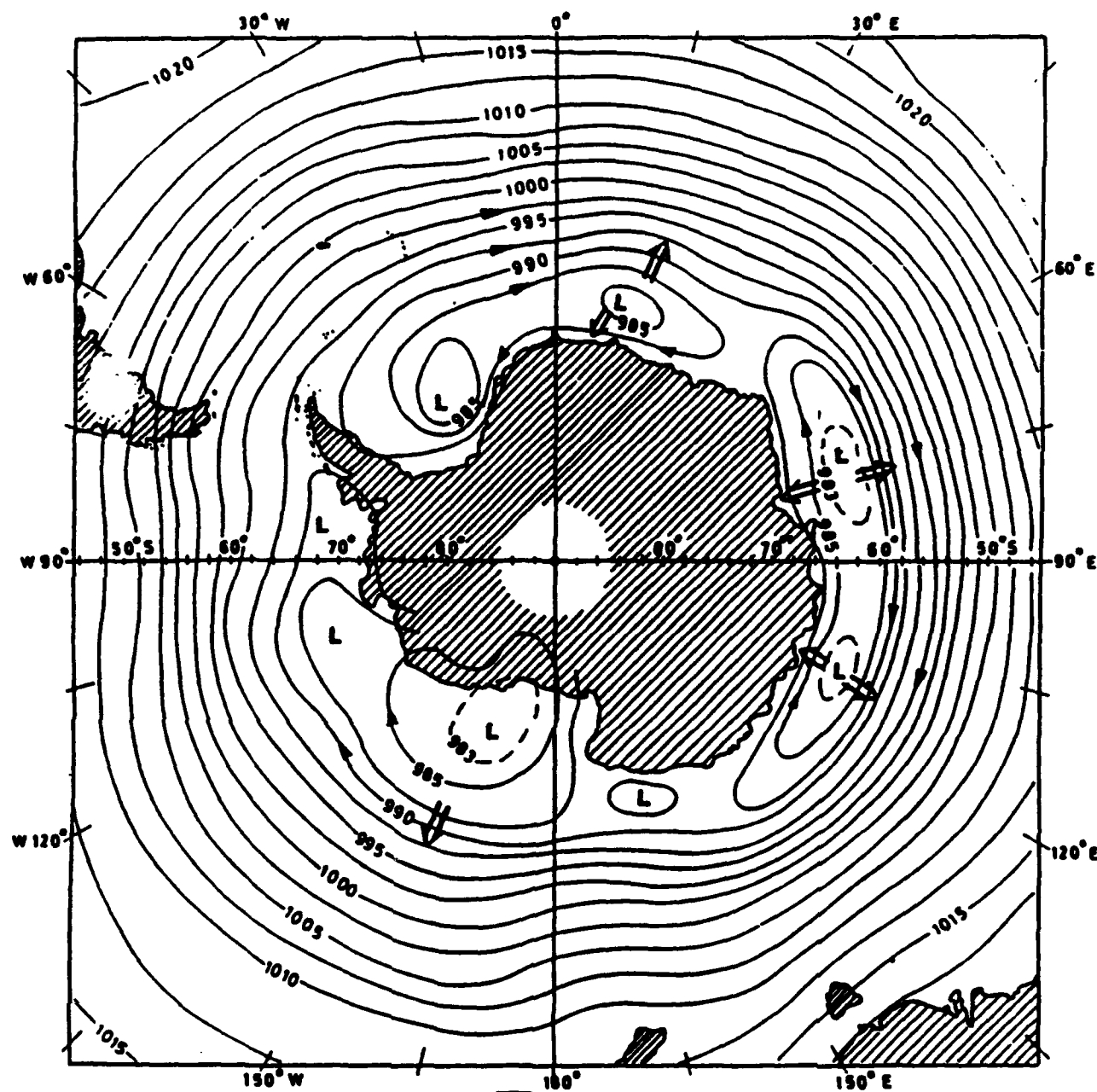


Figure 1.2 Average atmospheric pressure map for July (Foldvik, 1988) . The geostrophic wind direction is indicated on the isobars. The arrow shows the direction of the resulting Ekman transports in the upper ocean.

less than the Gulf Stream current where typical values are 3 to 4 kts and may reach 5 knots. But unlike the Gulf Stream, the eastward flow in the jets in the ACC extends all the way to the ocean bottom. The enormous volume of water that is transported by the ACC is accounted for by the great vertical extent of the ACC jet. Nowlin and Klinck (1986) report a mean transport through the Drake passage of 134 million cubic meters per second (Sverdrup, $Sv = 10^6 m^3/s$) with an uncertainty of 10% and a time variability estimated at 20%. The three narrow frontal regions carry most of the transport.

The current does not flow strictly along lines of latitude but tracks both to the north and south. Figure 1.3 depicts the positions of the surface fronts in the Southern Ocean. The most poleward excursions of the ACC are south of New Zealand, where the current is forced between the continental shelf and the mid-ocean ridge, and in the Drake passage. East of these two places the ACC turns to the north. Off the east coast of South America, the ACC reaches far enough north to collide with the warm southward flowing Brazil current.

The influence of the Southern Ocean on the rest of the world ocean depends on the ability of water properties to mix across the Antarctic Circumpolar Current. In the lower 2 or 3 kilometers this can be accomplished by deep boundary currents that breach the Antarctic Circumpolar Current belt. In the upper levels this task seems to fall primarily on large eddies and on northward surface water movement induced by the wind and coriolis effects.

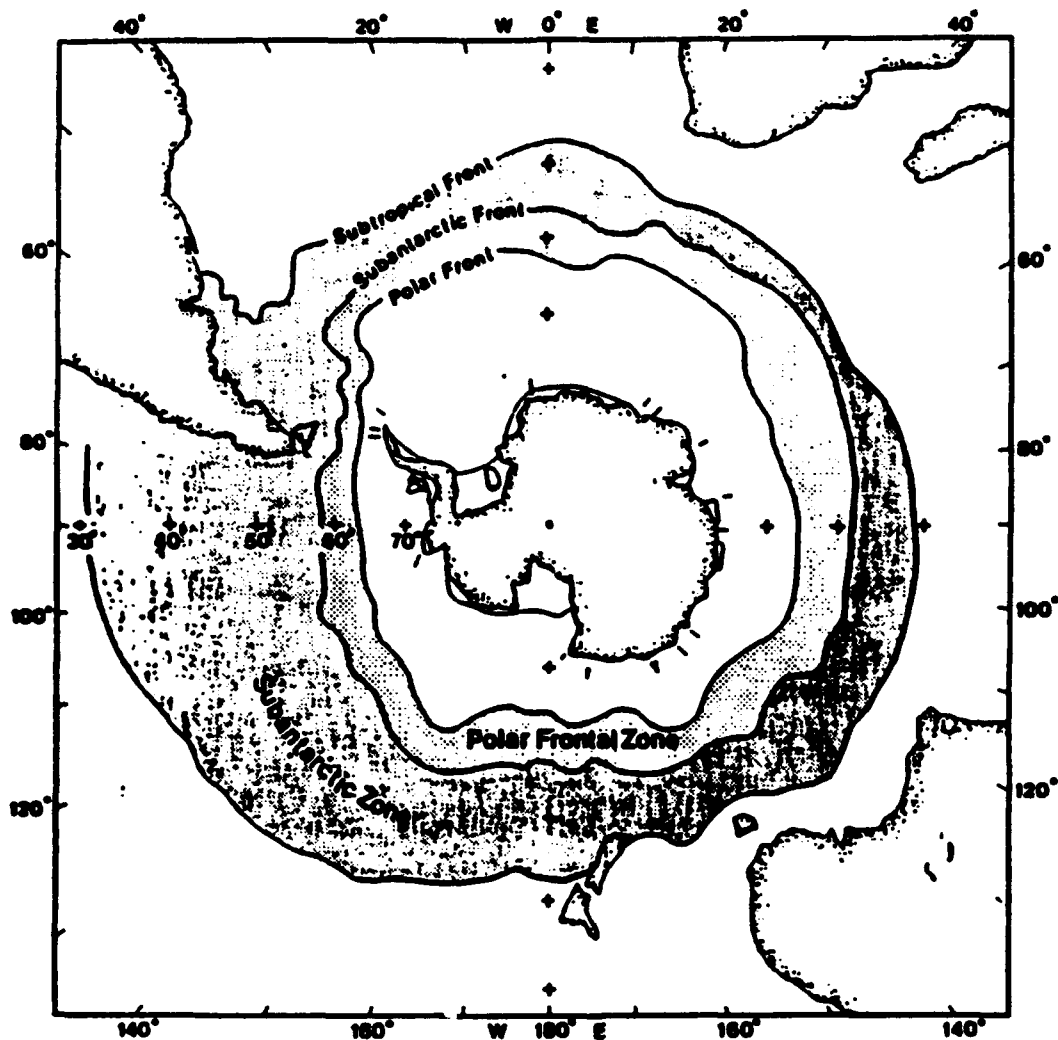


Figure 1.3 Average surface positions of Southern Ocean Fronts (Whitworth, 1982). Surface regimes of the Southern Ocean. Position of the Subtropical Front separating the subtropics from the Subantarctic Zone is after Deacon (1982). Locations of the Subantarctic Front and the Polar Front bounding the polar frontal zone are modified from a figure by Clifford (1983). The Antarctic Zone is south of the Polar Front. Summer ice extent is shown near Antarctica, as are locations where a water mass transition near the continental slope has been observed. (Clifford, 1983).

3. Upwelling

The wind-induced Ekman transports in the Southern Hemisphere are directed to the left of the wind stress. The southerly Ekman transport in the East Wind Drift and the northerly Ekman transport in the West Wind Drift give rise to divergence of the surface water. This area of divergence called the Antarctic Divergence Zone, facilitates the upwelling of deeper waters. Figure 1.4 shows a schematic meridional cross section of the upwelling deep water. The surface water moves north towards the Antarctic Convergence, also known as the Polar Front, where it sinks and contributes to the formation of low salinity intermediate waters of the worlds oceans. The induced upwelling of the relatively warm, saline, deep water necessitates a compensating southward flow of deep water. The deep water upwelling is 2 to 3 °C warmer than the winter surface water, which is near the freezing point. The surface water is continuously removed as about two thirds of it is transported northward to the circumpolar belt. A typical water parcel only resides in the surface layer for about two years. Any anomalies in temperature or salinity are quickly washed away (Foldvik, 1988).

4. Water Masses

Most water masses acquire their characteristics at the surface. The water properties are determined there by the local climate and when the water sinks along density surfaces, it carries those properties along with it.

During winter, cold water formed at the surface near the continent, extends to a depth of about 100 m. As one moves away from the continent into the Polar Frontal Zone, (see Figure 1.4) this fresh cold water sinks to a depth of about 500 m. North of the ACC,

this water continues to move equatorward , and sinks to a depth of 1000 m. This water mass, known as Subantarctic or Antarctic Intermediate Water (AAIW), spreads throughout the Southern Hemisphere.

The North Atlantic Deep Water flows south across the equator and is warmer but saltier than the AAIW, making it more dense. This is the water mass that is principally subject to upwelling at the Antarctic Divergence Zone. It continues to flow southward, mixing along the way with the underlying Circumpolar Deep Water.

The most voluminous water mass in the ACC is called Circumpolar Deep Water and is not of Antarctic origin. Water with salinity greater than 34.7 psu is Circumpolar Deep Water and constitutes more than half the water in the Drake Passage. Its high salinity can be traced directly back to the outflow from the Mediterranean Sea.

In the movement , rising, sinking and layering of the water masses in the region, temperature and salinity play complex and interchanging roles. While the water formed during the winter is cold, it is relatively fresh. The warmer but saltier Circumpolar Deep Water has a higher density and is located beneath the winter water. As a result of this, the temperature of the water between 200 and 500 m increases with depth.

Due to the extreme weather conditions that are found in the Antarctic, it should be no surprise that the densest water in the open ocean, Antarctic Bottom Water (AABW), is formed here. The density of AABW is about 27.9 (σ_t) and has a potential temperature less than 0 °C and a salinity between 34.6 and 34.7 psu. The surprising part is that 80% of

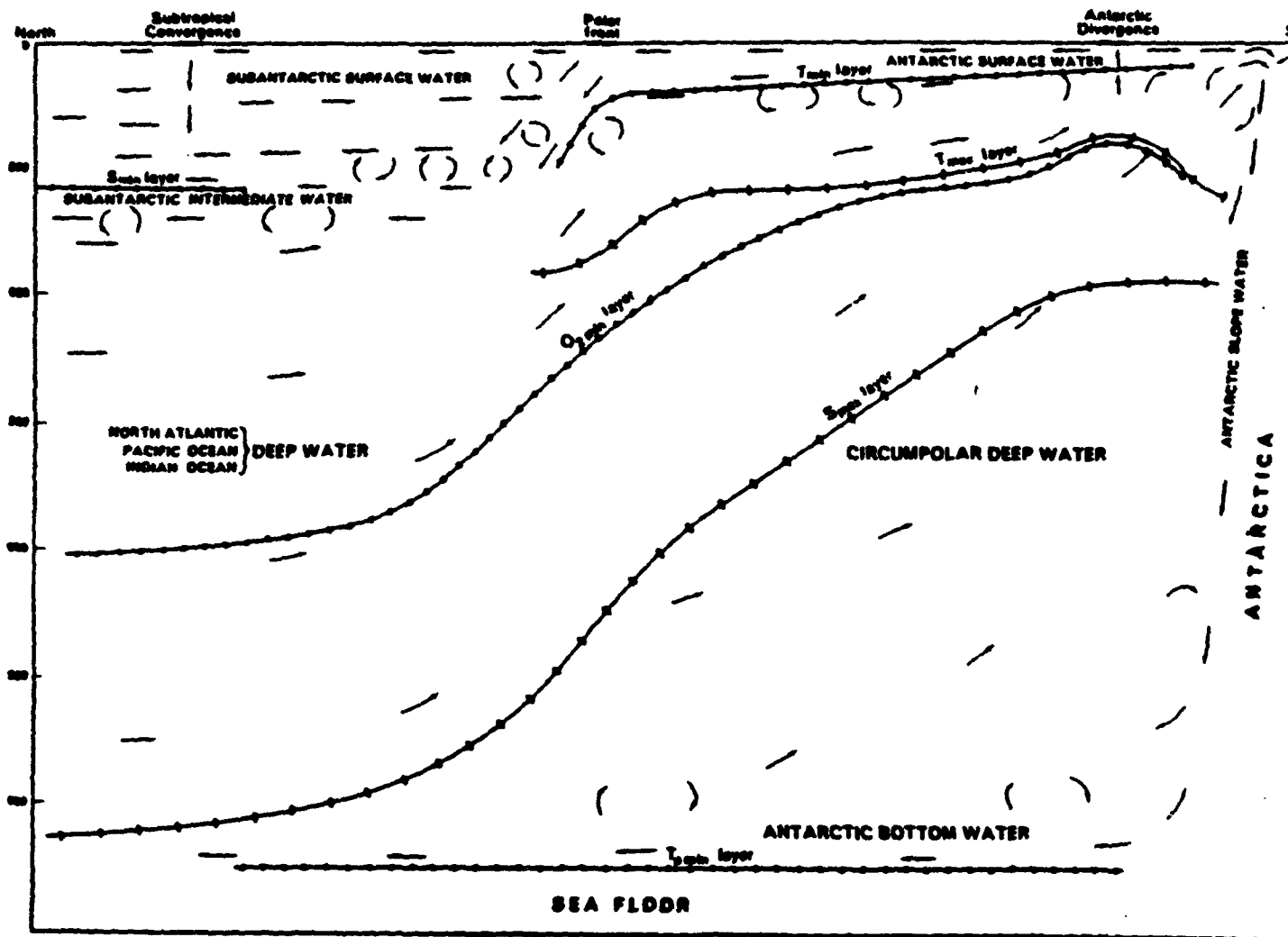


Figure 1.4 Schematic cross section of Southern Ocean circulation (Foldvik, 1988). Major Physical features of the Southern Ocean circulation are shown in this schematic cross section.

AABW is formed in one location in the Antarctic, the Weddell Sea . The formation rate is approximately 13 Sv (Gordon, 1988) .

When water is made cold enough, it becomes more dense than water of higher salinity, which is only slightly warmer. This is due to the non-linearity of the equation of state of sea water. The unique geography of the Weddell Sea, in particular the broad, deep ice shelf allows the water cooled at the surface, to sink and follow the contours along the shelf . This water is cooled still further by its contact with the underside of the glacial ice. Additionally the under ice bathymetry of the Weddell Sea forces a shallow inflow and a deep outflow which provides a larger driving force for the super cooled water. This dense, cold AABW, continues to sink and flows along the bottom of the major ocean basin where it is not impeded by ridges. It mixes to some extent with deep waters along its path. Its influence extends past the equator to 40° N in the Atlantic and 50° N in the Pacific. It is from this water that the major oceans derive their low temperatures.

(Foldvik, 1988)

5. Heat Flux

Associated with the water mass exchanges between the Southern Ocean and the rest of the global ocean is a significant poleward heat flux across 60° S estimated to be 5.4×10^{14} W (Gordon, 1988). This ocean heat withdrawn in the Southern Ocean is derived from the heat introduced into the deep water of the world's oceans by downward diffusion and deep convection of relatively warm salt water in the North Atlantic Ocean.

B. MODEL BACKGROUND

1. Overview

Ocean modeling is severely limited by computer power. Despite exponential growth in computer power, it is only recently, that we have been able to attempt to compute three-dimensional, realistic, physical ocean models. There are several reasons for this:

The primary length scale for geophysical fluids is the Rossby radius of deformation,

$R_o = (g' H)^{1/2} / 2 \Omega \sin(\phi)$ or the speed of the disturbance (internal wave) divided by the coriolis parameter. This is the distance internal gravity waves can travel before rotational effects impede the spreading of energy away from source regions (Gill, 1982). Numerical models require a grid size comparable to the Rossby radius of deformation to properly represent time-mean flows, and they require an even smaller grid size to represent a range of the most energetic eddies. The speed of a wave in the ocean is generally one tenth that of the atmosphere. The radii of the eddies that form are also smaller so that values vary from about 100 km near the equator to less than 10 km near the poles. The computational requirement for an ocean model that resolves currents and eddies is therefore ~ 1000 times that of a physically comparable atmospheric model. (Arakawa, 1982)

An additional desirable feature is the capability to perform extended simulations on climatic time scales. At present this can only be done by sacrificing grid resolution. Teraflop (10^{12} floating point operations per second) performance is needed to allow a proper treatment of the ocean in climate modeling.

The Semtner-Chervin model runs at slightly over 1.1Gflops (1 billion or 10^9 floating operations per second). The recent development that allowed for this kind of computational power is the parallel computer which uses multi-processors. The vector and multi-tasking

features of modern computers require that the code be written to exploit this architecture.

Hence, while the first realistic, physical computer code was written in 1969 by Bryan, it has undergone several transformations to optimize it for the emerging architectures of very fast computers.

Cox (1975) first accomplished mathematical modeling of the global ocean with realistic coastlines and bathymetry in 1975. Semtner reorganized the Bryan and Cox model for vector processing on longitudinal coordinates in 1974. In 1988 Semtner and Chervin modernized the 1974 code to use up to 64 processors. This was done by generating simultaneous tasks in the latitudinal coordinate. Almost all of the processor time is in use almost all of the time (99.64%). The end result is a code, which with performance scales with the number of processors on a given machine, has a relatively simple structure and bypasses the calculation of continental land masses. New physical and numerical packages developed by Cox (1984), such as bi-harmonic mixing and isopycnal mixing, were easily adapted to the modernized version of the 1974 code. Additional history of global ocean modeling can be found in Semtner (1986a and 1986b).

2. Semtner - Chervin Model

The simulations used in this study were run on the National Center for Atmospheric Research (NCAR) Cray supercomputer. The grid used was a 0.5° spacing in latitude and longitude for the half degree model with a maximum of 20 vertical levels in the deep ocean. The domain of the model is shown in Figure 1.5. A new simulation has recently completed with $.25^\circ$ horizontal spacing and 20 vertical levels, which was run on the 8 processor Cray supercomputer at NCAR. Some of those results will be compared to the original study. Both simulations were run using European Center for Medium range Weather Forecasting (ECMWF)

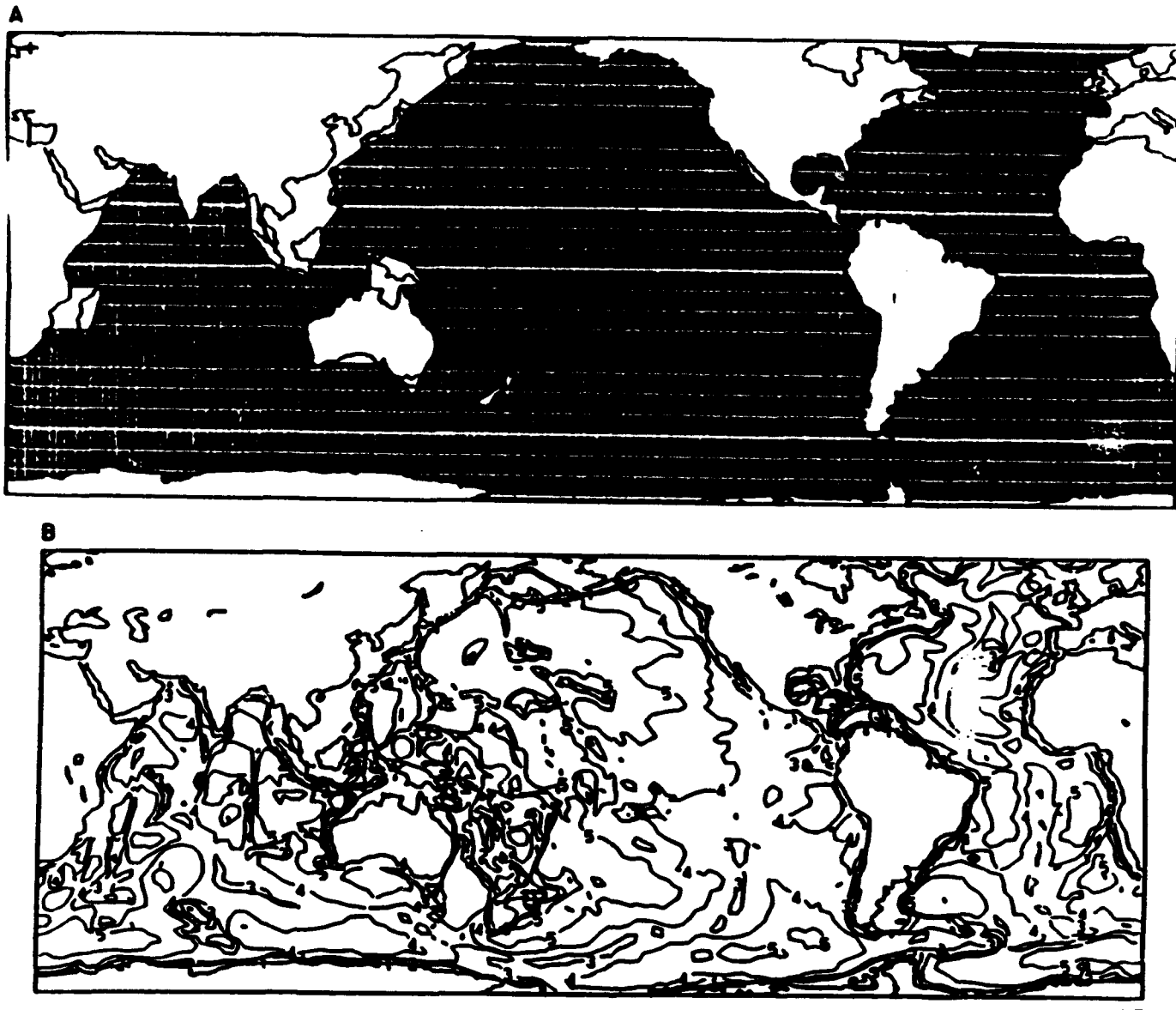


Figure 1.5 (a) Geometry of the half degree model domain (Semtner, 1992). The domain extends from 75°S to 65°N and through 360° of longitude with cyclic continuity at 20°E. Oceanic areas are shaded and land masses are white. The geographical outlines of coasts indicate where the model domain has been simplified by walling off inland seas and bays. Some islands have been submerged to become shoals. (b) Bottom topography of the half degree model domain (i.e. column depths), with a contour interval of 1 km, as constructed from bathymetric data with minor smoothing.

monthly average winds for the decade of the 1980's. Previous simulation runs used the monthly wind forcing from Hellerman and Rosenstein (1983). Both wind data sets were spline interpolated to daily values for updating of forcing every three days in the running model. The half degree model run with ECMWF winds was run on a two processor Cray at NCAR using Model Evaluation Consortium for Climate Assessment (MECCA) time.

The models were initialized with horizontally uniform profiles of temperature and salinity representative of mid-latitude conditions. The initial motion field was identically zero. The surface wind stress and forcing to Levitus temperature (T) and salinity (S) on a one month time scale was initiated with interior restoring to Levitus data on a one year time scale (Levitus, 1982). The half degree model was run for four years to obtain a relatively steady state in which the time rate of change of internal and external mode kinetic energy was less than 1% of the dominant forcing by the wind. Four e-folding times of Levitus forcing brought the interior T and S to within 2% of their equilibrium values.

This method of start-up was chosen to avoid shocking the model by initialization with observed data. This avoids the unphysical circulations that arise because of bottom pressure torques related to the slight incompatibility of observed data and model physics. A gentle spin-up of four years bypasses this problem. (Semtner, 1992)

Following the initial four years of integration the interior restoring time scale was changed to three years and an additional six years of integration were performed. This ends the first phase of integration, called the robust diagnostic phase. The use of the robust diagnostic method ensures that the simulated circulation will not experience a long term climatological drift. Then restoring to Levitus data was eliminated for model levels 2 through 10, which span the depth range of the main thermocline (25 m to 710 m). This begins the free thermocline

phase. The annual mean forcing with eddies phase commences at year 18 when scale selective bi-harmonic mixing in the horizontal replaces Laplacian mixing. The ECMWF wind forcing with eddies takes place during the last ten years of the model when the monthly average winds were spline interpolated to update forcing every three days in the running model. The culmination of the integration steps for the half degree model is this last phase, so that we will refer to this time period as years 1 - 10, leaving out the 22.5 year period of spin up to quasi-equilibrium conditions. These four phases are summarized in Table 1.1.

TABLE 1.1 INTEGRATION STRATEGY

Phases	robust diagnostic	free thermocline	annual w/ eddies	seasonal w/ eddies
years of integration time	0 —————>10	< —————>18<—	—————>22.5<	—————>32.5
restoring parameters	<—diagnostic>10	< —free thermocline	between 25m and 710 m	—————>32.5
horizontal mixing	0<—Laplacian mixing	—————>18<—	————biharmonic mixing	—————>32.5
wind forcing	0<—annual mean surface forcing	—————>22.5<	—ECMWF—	—————>32.5
data archiving	0<—infrequent archiving	—————>20.0<—	3 day archiving	—————>32.5

Vertical mixing is parameterized using the techniques of Pacanowski and Philander (1981). Surface fluxes of heat and salt are prescribed using the method of Haney (1971). Rather than explicitly prescribing either the sea surface temperature or the surface heat flux, a suitable climatological temperature is used as a set point in a negative feedback loop control system. At each time step of the integration, if the model temperature is colder (warmer) than climatology at a given point, it is then warmed (cooled) at a prescribed rate. The model incorporates a forcing term which applies this virtual heat flux towards the Levitus (1982) values on a monthly time

scale. Observed reference fields of surface temperature and salinity are from the climatology developed by Levitus (1982).

The change from Laplacian to bi-harmonic closure of the frictional and diffusive parameterization at year 18 of the simulation allows for the spontaneous generation of mesoscale eddies (Holland, 1978). If prescribed internal damping is sufficiently small, a horizontal grid spacing of 0.5° or less will allow the explicit representation of some instabilities which mix momentum, heat, salt and other properties in the ocean. Trial integrations with different values of the diffusion parameters led to a final choice of -2.5×10^{11} and $-7.5 \times 10^{11} \text{ m}^4/\text{s}$ for bi-harmonic viscosity and diffusion respectively. The model is 'sub-grid-resolving' and should begin to reproduce the state of the ocean from first principles.

The quarter degree model employs a mercator grid which was interpolated forward from the half degree model initialization, which used Hellerman and Rosenstein winds and a 5 year spin up time. For the last three years of the model run time, the resolution was improved to 0.25° on average and ECMWF winds were used. Also, no deep restoring in the last three years is introduced in the model. Another difference worth noting between the half degree model and the quarter degree model is that in the latter, the bathymetry is unsmoothed, so that not only is the resolution finer, the topography is more realistic.

3. Observations

The observed data presented here is from the Alfred Wegner Institute Southern Ocean Atlas (Olbers, et al., 1993). These data represent observations collected over a long period of time, although due to weather and operational restraints the data are primarily representative of summertime conditions. The data were converted to computer files and made available for those who purchased the atlas. This allowed for the manipulation of the presentation of the data to

match those of the model, allowing for direct comparisons. The resolution of the observed data is 1° by 1° longitude and latitude and has 38 vertical levels. The salinity is expressed in practical salinity units (psu) while the model salinity units are in parts per thousand (ppt). Figure 1.6 shows the stations that were used for the temperature and salinity data after quality control.

The Olbers et al. (1993) data base represents a large improvement over previous Southern Ocean atlases due to a tripling of the amount of data included. Russian data are now included as is new data collected over the past two decades. This resulted in an increase in temperature observations for example, to almost 400,000 observations compared to the Gordon and Molinelli (1982) Southern Ocean Atlas which had 167,000 observations after quality control screening was done.

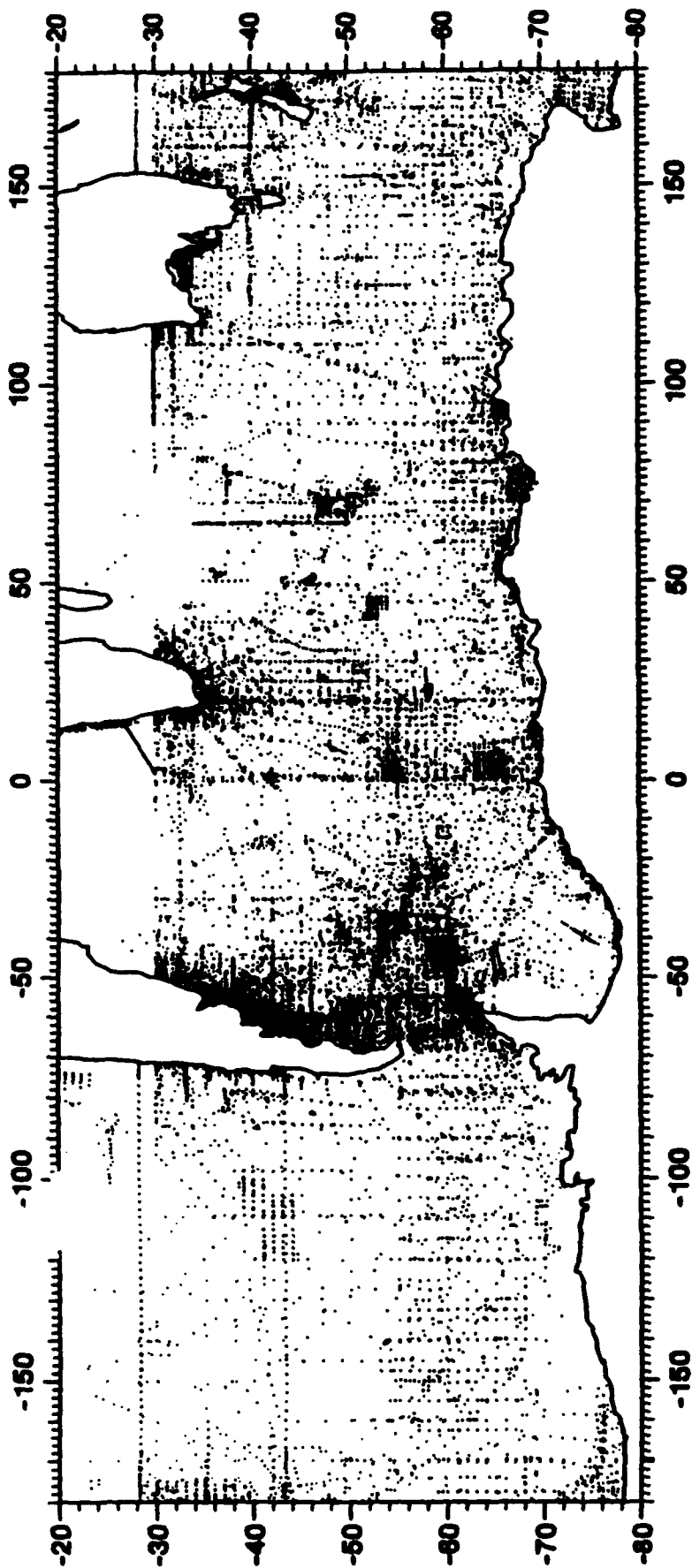


Figure 1.6 Distribution of observation stations with temperature and salinity data after quality control tests have been performed (olbers, 1993).

II DATA PRESENTATION/COMPARISON

I have divided the Antarctic Circumpolar region into six sections, each covering 60 degrees of longitude. The sections are as follows:

- A. 90°W - 30°W (Drake Passage)
- B. 30°W - 30°E (Central Atlantic/Agulhas Region)
- C. 30°E - 90°E (Agulhas Return/Crozet Basin)
- D. 90°E - 150°E (South of Australia)
- E. 150°E - 150°W (Macquarie Ridge/Ross Sea)
- F. 150°W - 90°W (Central Pacific)
- G. Weddell Sea
- H. Total Antarctic Circumpolar Current

Each section contains charts from the Semtner-Chervin half degree model and the quarter degree model run and the Southern Ocean Atlas (Olbers, et al. , 1992) data base. The charts presented here represent the mean of the last five years of the model run for the half degree model and the last three years of the model run for the quarter degree model.

Comparisons between the two model runs and the Atlas observations are conducted by analyzing horizontal and vertical sections . Horizontal sections are at 100 m depth for temperature and salinity analyses while for circulation they are near surface (37.5 m) and deep (3500 m).

A. DRAKE PASSAGE/BRAZILIAN-MALVINAS CONFLUENCE (90W - 30W)

This first section contains the Drake Passage, one of the most studied areas of the Antarctic Circumpolar Current .

1. Area Temperature and Salinity (100 m)

a. Temperature

The observational temperature charts of the area are only in fair agreement with the model solutions. (See Figures 2.1 a, b and c.) In the western portion of the region the half degree model shows a much stronger tongue of cooler water reaching northward just west of the western coast of South America. The quarter degree model solution exhibits the same tendency but is not as pronounced. The warmer tongue of water from the northern tropical regions is depicted further to the west in the models. In the observations, only the warmer tongue of water is depicted and the observations indicate that the tongue impinges on the western coast of South America.

Another difference between the half degree model and the observations is the presence of a large cold eddy just downstream from the Drake Passage. This is not present in the observations which depicts a more zonal temperature gradient. This also results in a much tighter temperature gradient in the Passage in the model solutions. The quarter degree model is closer to the observations in showing a much weaker eddy and a smaller northward excursion of cooler waters in the same vicinity. This can be traced to the enhanced bathymetry in the quarter degree model which will be more obvious in the surface and deep circulations shown later in this study.

The Brazilian-Malvinas Confluence is also much more vividly represented in the model solutions than in the observations, perhaps almost too strongly. This tight

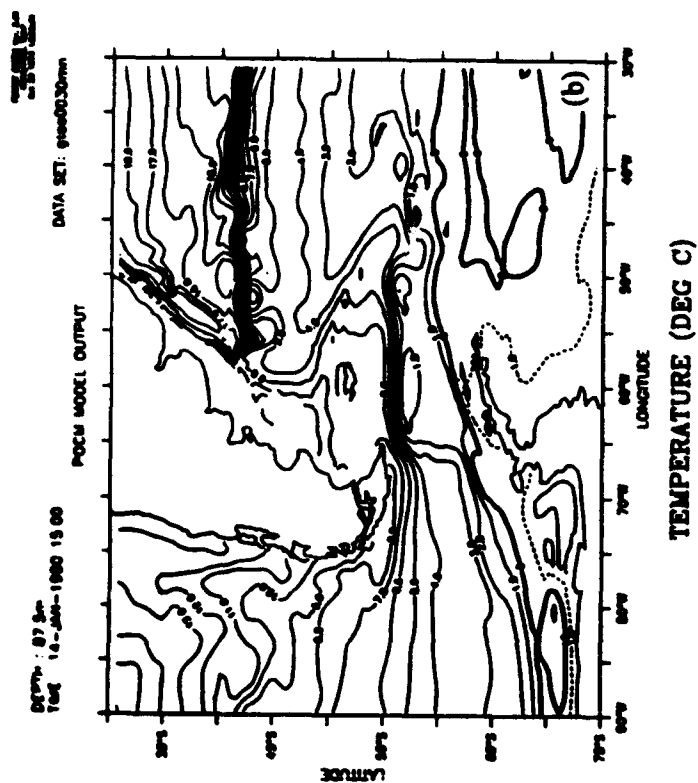
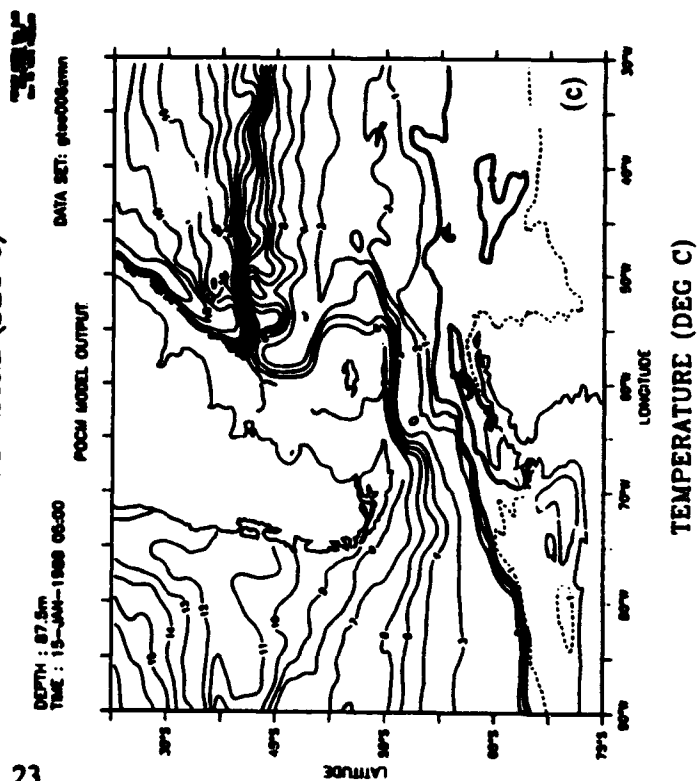
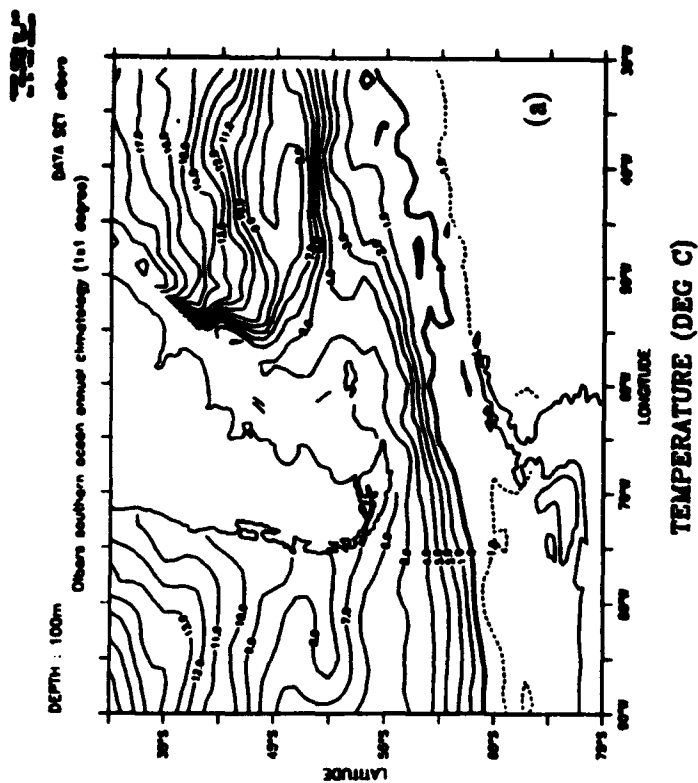


Figure 2.1 100 m Temperature charts for area 90°W to 30°W
a.) Atlas Data b.) Half Degree Model Solution
c.) Quarter Degree Model Solution

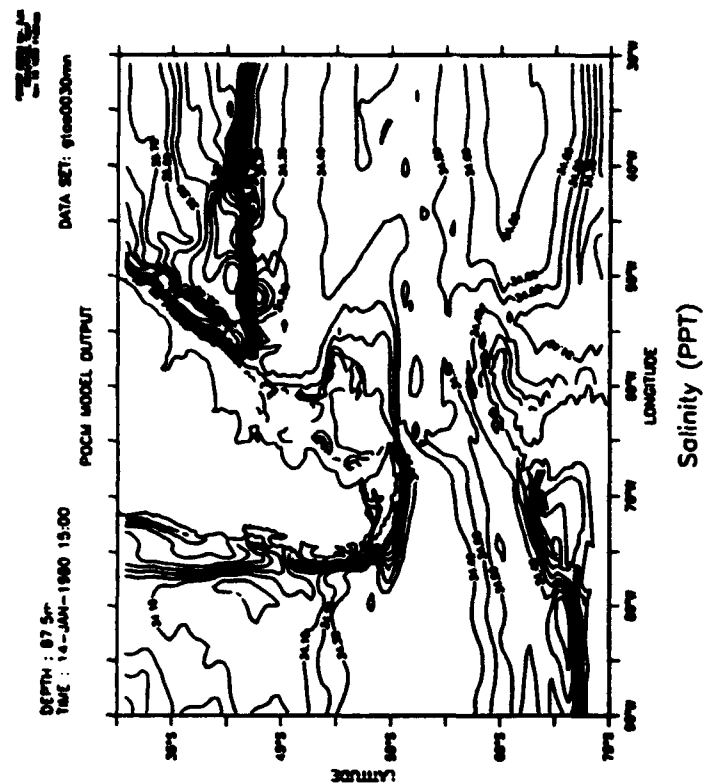
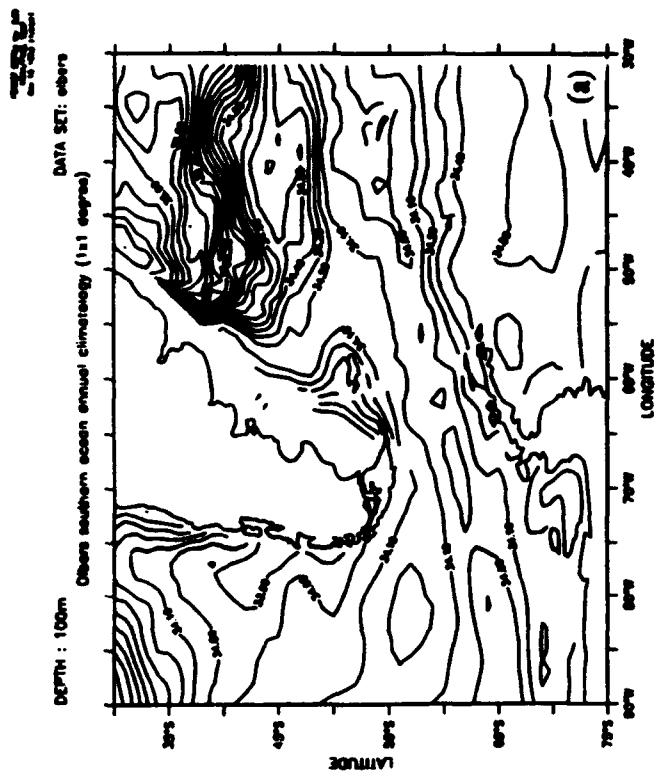
temperature gradient between 40°S and 45°S persists across the Atlantic and can be traced to the Agulhas Current system covered in the next section. The quarter degree model gradient is less tight than the half degree model. A cold tongue of water is present in the models along 53°W but in the observations is found farther east starting at 40°W.

The Weddell Sea, also shown in this region, appears to be more complex in the model solution than in the observational chart. Several pools of cooler water are shown in the model solution, while the observations show a large, slightly colder, homogeneous area in the Weddell Sea. This is perhaps related to the low density of observations in the area.

b. Salinity

In general, the observations to the south near Antarctica are less saline than shown in the models. (See Figures 2.2 a, b, and c.) In the models there are large salinity maxima on either side of the Antarctic Peninsula. In the observations, while salinity maxima are present, they are less well defined and at least 0.2 psu less saline and as much as .6 psu weaker to the west of the Peninsula.

Another major difference between the half degree model and the observations is the salinity gradient associated with the Brazilian - Malvinas Confluence. The gradient in the half degree model is much tighter and the higher salinity water is concentrated between 42°S and 40°S. The quarter degree model is in closer agreement with the observations. It also displays an interesting tongue of lower salinity water along the coast of Brazil, only hinted at in the observations and the half degree model, but fully resolved in the quarter degree model.



25

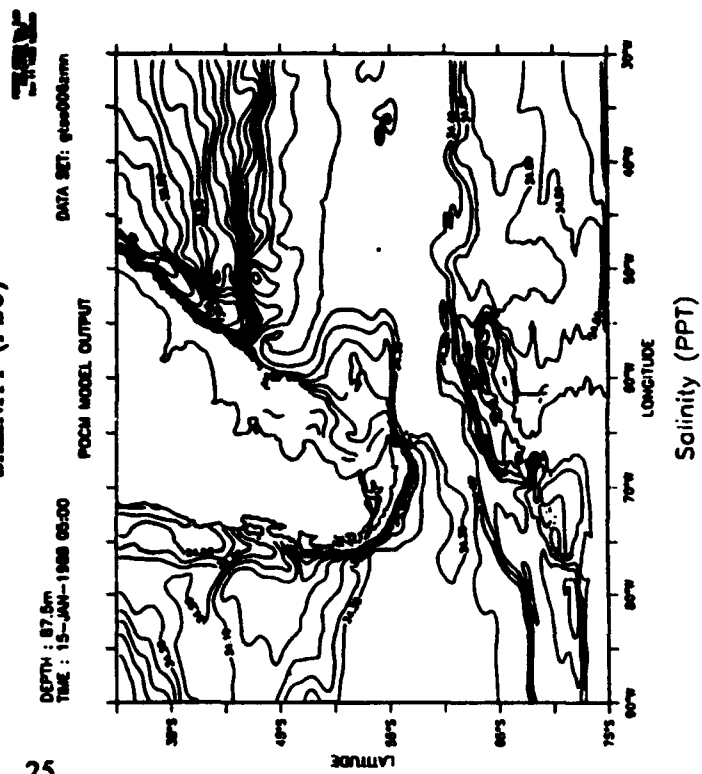
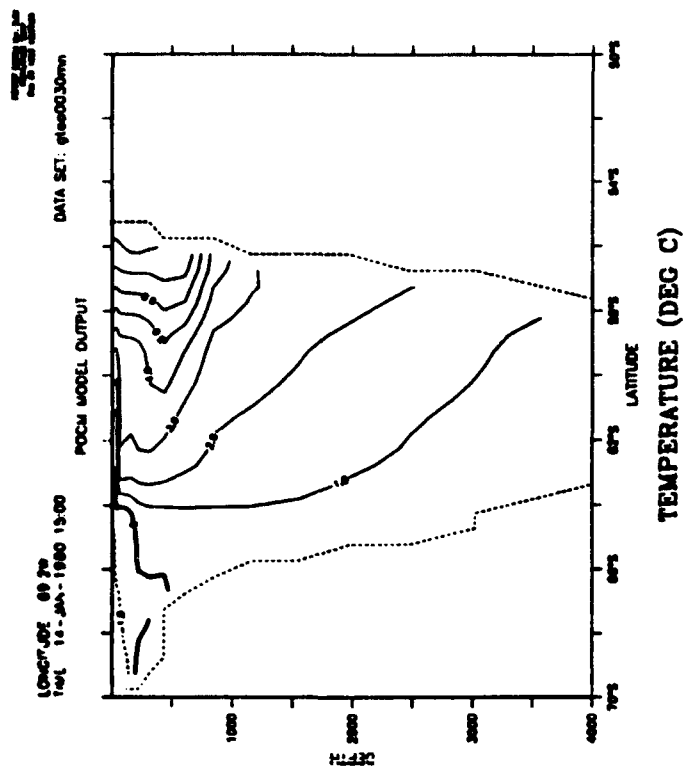
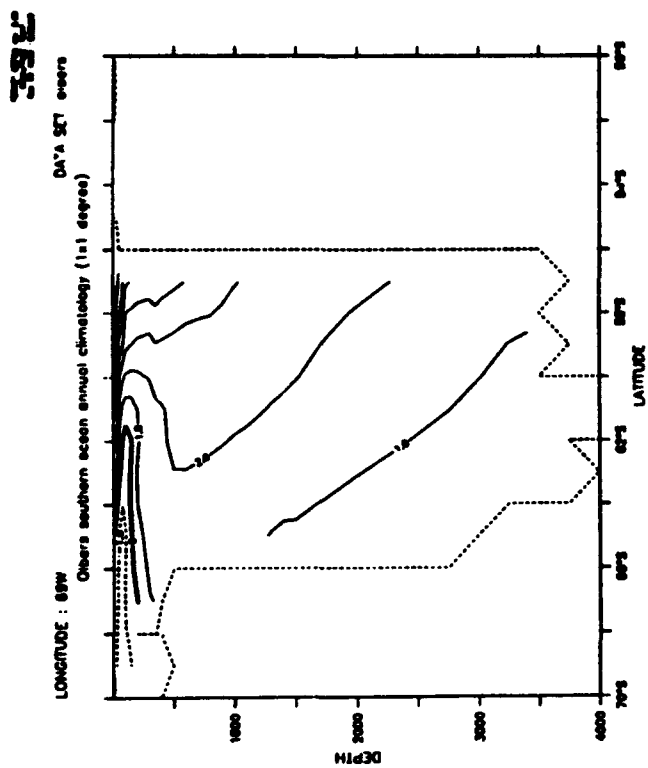


Figure 2.2 100 m Salinity Charts for area 90°W to 30°W
a.) Atlas Data b.) Half Degree Model Solution
c.) Quarter Degree Model Solution

2. Vertical Sections

The Antarctic Circumpolar Current is known to consist of four water mass zones separated by three frontal regions (Whitworth, 1987). From north to south these are the Subantarctic Zone (SAZ), the Subantarctic Front (SAF), the Polar Frontal Zone (PFZ), the Polar Front (PF), the Antarctic Zone, the Continental Water Boundary (CWB), and the Continental Zone. The Subantarctic Front and the Polar Front and the transition zone between them are believed to be circumpolar in extent. A front analogous to the CWB is found in some locations but generally not where the ACC is far from land. These fronts are depicted by the vertical cross section of temperature and salinity in Figures 2.3 and 2.4 a, b and c.

Whitworth and Nowlin (1987, pp 6462) define the SAF and the PF with reference to Antarctic Intermediate Water which is distinguished by a temperature or salinity minimum as follows: "The temperature minimum south of the Polar Front is found at approximately 100 m depth and at the Polar Front this descends rapidly to 300 to 400 m. North of the Polar Front, in the Polar Frontal Zone, the temperature minimum remains distinct and gradually descends to the north until it reached the Subantarctic Front where it undergoes a further rapid descent to 500 to 600 m. North of the Subantarctic Front in the Subantarctic Zone the temperature minimum is weak or absent. In the Polar Frontal Zone a salinity minimum is evident either at the surface or as a weak subsurface expression at about 200 to 300 m, i.e., slightly above the temperature minimum, and the salinity minimum descends rapidly at the Subantarctic Front and to the north forms the pronounced salinity minimum characteristic of Antarctic Intermediate Water."



27

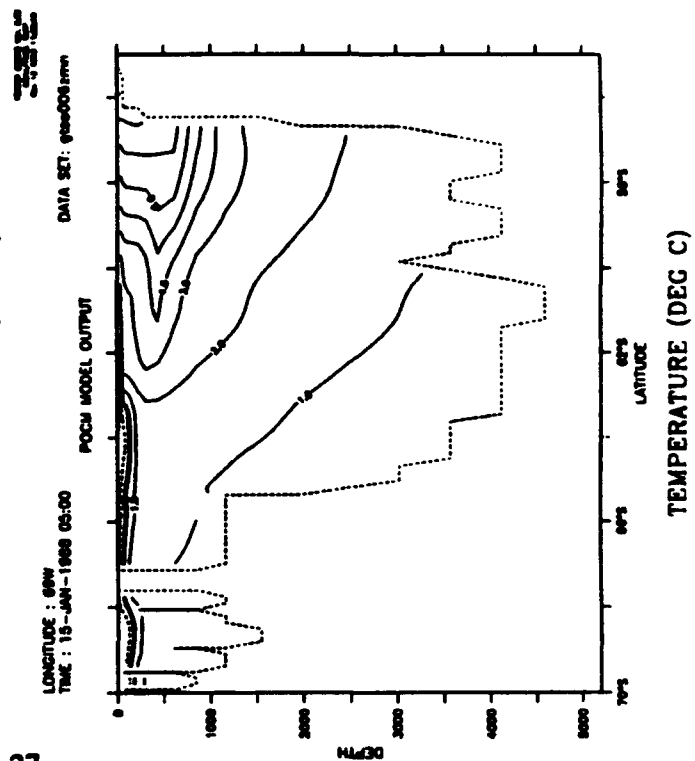
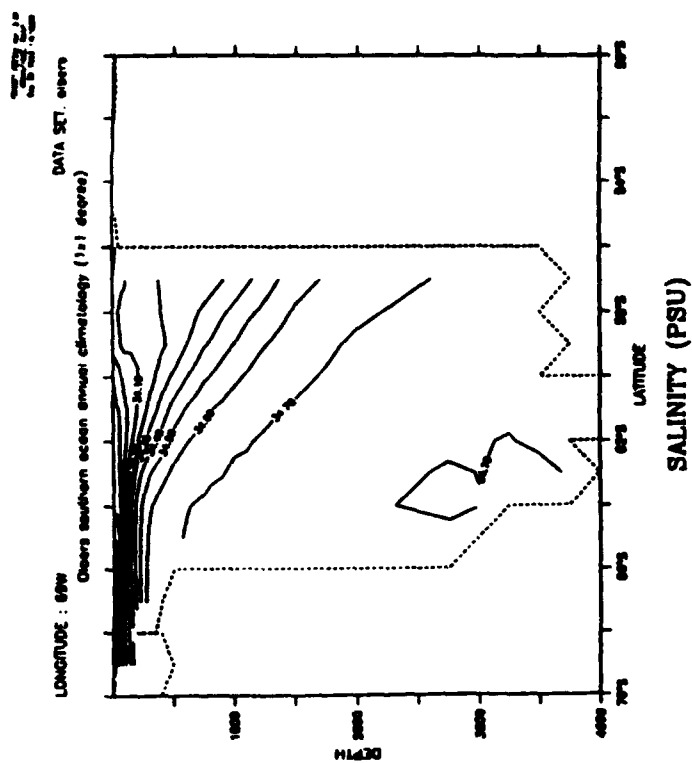


Figure 2.3
Vertical temperature sections along 69°W
a.) Atlas Data b.) Half Degree Model Solution
c.) Quarter Degree Model Solution



28

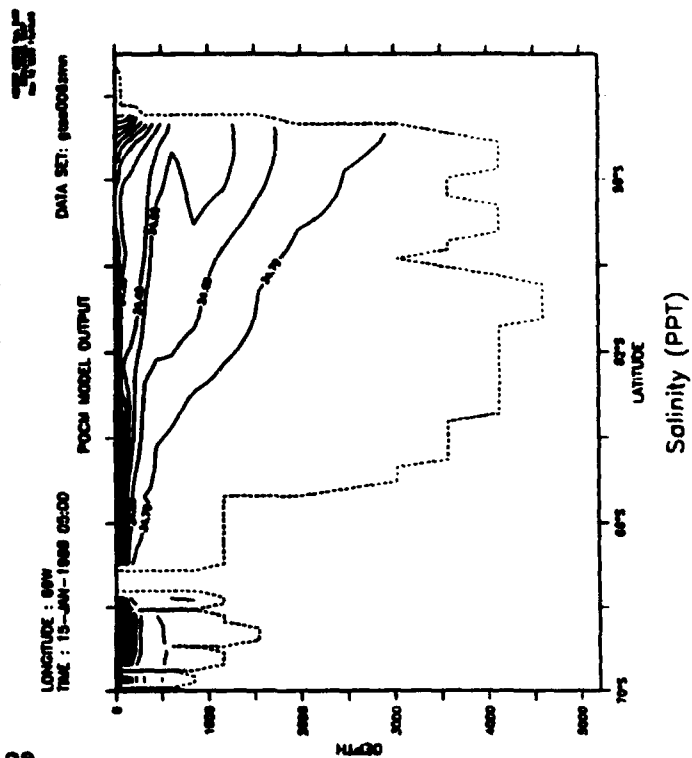


Figure 2.4 Vertical salinity sections along 69°W
a.) Atlas Data b.) Half Degree Model Solution
c.) Quarter Degree Model Solution

a. Temperature Section (along 69W)

There are some noticeable differences between the observed data and the model solutions. Most prominent in the Atlas observations is a tongue of cooler water, as described above associated with Antarctic Intermediate Water, extending from the surface at 68°S to about 300 m at 60S. In the half degree model the 0° isotherm sinks to much greater depth than in the observations, but the tongue that develops at about 300 m is much weaker than the observations. The representation of Antarctic Intermediate Water in this region is especially weak. Additionally, the water in the Subantarctic Frontal Zone to the north of the SAF is represented by an especially deep pool of warm water (temperatures greater than 6 ° C at 800 m) along the coast of South America. In the observations temperatures above 6° C are no deeper than 100 m.

In the quarter degree model the AAIW is better represented. A tongue of cool water descends from the surface and moves northward. The 0°C isotherm is shallower in the quarter degree solution than in the observations. As in the half degree model, the pool of warm water along the coast of South America is much deeper than observed. This also leads to a more vertical temperature gradient in the SAF region than is present in the observations.

b. Salinity Section (along 69°W)

In the salinity sections (Figures 2.4 a, b, and c) the top 300 m of the model and observation plots are in slightly closer agreement. Both have a surface salinity minima in the Polar Frontal Zone and the SAF where the salinity minimum descends. However, the gradient in the half degree model is much stronger in the center of the Drake Passage due to the large salinity maximum in the center of the Passage. In the observations the central peak of the salinity maximum is found much closer to Antarctica (65S) than to

the center. The quarter degree model is in better agreement with the observations but a weak secondary salinity peak in the center of the Passage near 62°S is present which leads to differences in the slope of the gradient from those observed. Another maximum near 58°S is in good agreement with the observations.

Lastly, a salinity minimum associated with the abyssal AABW is present in the observations and lacking in either model solution.

3. Circulation Comparisons

a. Surface Circulation (37.5 m)

Only the model solution charts are presented for the surface and deep circulations because similar resolution and data are not available in the current observations for currents in the Southern Ocean, particularly at depth. The quarter degree model vectors were plotted for every other grid point to give a similar resolution to the half degree model and for legibility. The quarter degree model used a Mercator grid with 0.4° spacing at the equator.

In both the half degree and quarter degree models a cyclonic eddy sets up downstream of the flow through the Drake Passage. Both models show an easterly flow around the Antarctic continent which is consistent with observations and was lacking in previous non-ECMWF runs. The quarter degree eddy is much smaller and weaker than that shown in the half degree model.

Also prominent is the western boundary current in the Weddell Sea along the Antarctic Peninsula. (This will be covered in more detail in the section on the Weddell Sea.) The quarter degree flow is more complex, showing a stronger flow along the continental boundary but a less well defined flow in the interior of the basin.

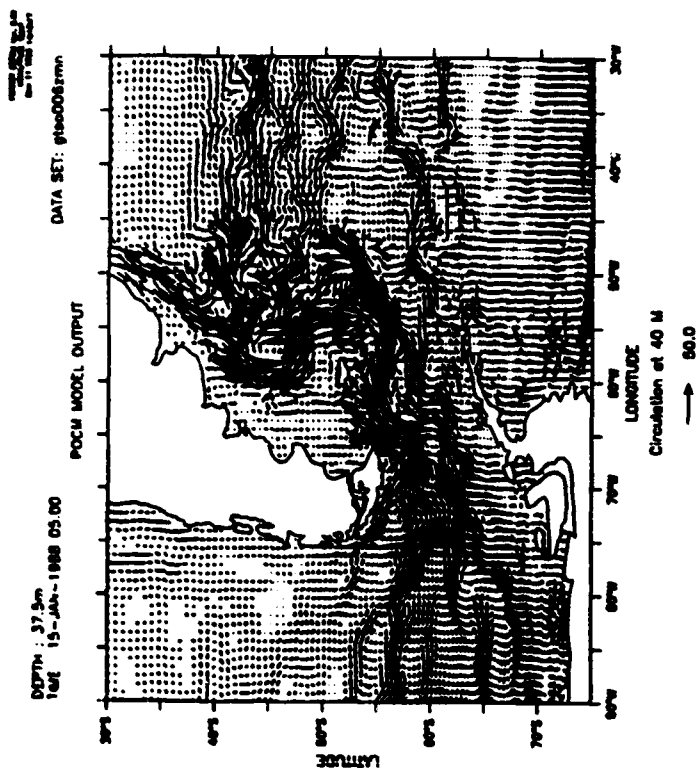
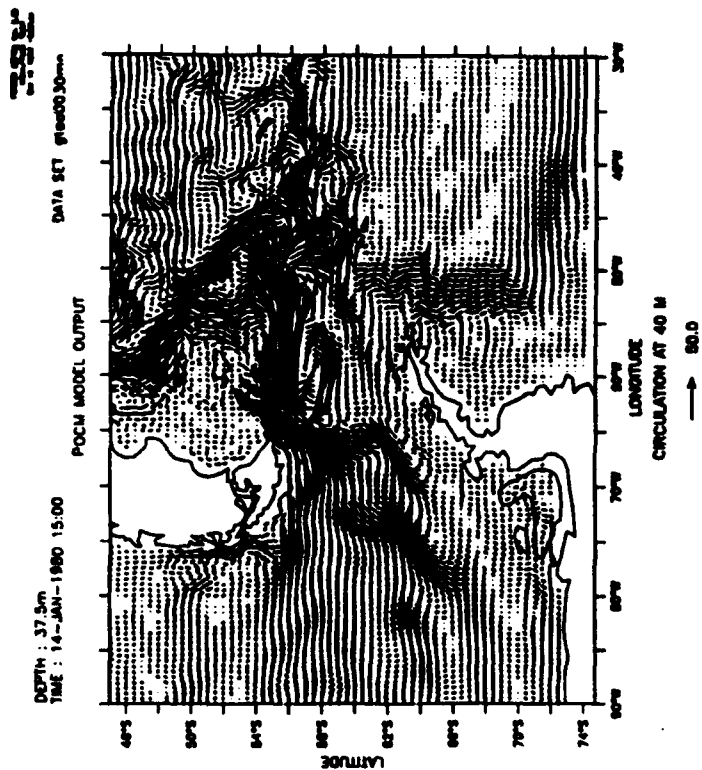


Figure 2.5 Surface Circulation for area 90°W to 30°W
a.) Half Degree Model Solution b.) Quarter Degree Model Solution

Both models show a strong western boundary current in the Argentine Basin, but in the quarter degree model the flow to the north is more direct. In the half degree model it is more northwestward initially and begins its turn toward the north at about 45°W vice 55°W in the quarter degree model.

b. Deep Circulation (3500 m)

In the deep circulation the difference in bathymetry between the quarter degree model and the half degree model plays a major role (see Figures 2.6 a and b). The cyclonic eddy downstream from the Drake Passage is present in the deep circulation in the half degree model. In the quarter degree model the bathymetry shifts the cyclonic circulation almost 10° downstream from the circulation at the surface and as compared to the half degree model. The quarter degree model, as expected, shows the presence of many more eddies than the half degree model. The western boundary current in the Weddell Basin is stronger in the quarter degree model. In the Argentine Basin the western boundary current flows southward along the coast of South America in both models.

4. Potential Vorticity

The potential vorticity for the observations and the models were calculated using FERRET, a software tool developed by the National Oceanic and Atmospheric Administration (NOAA). FERRET is an interactive program designed for use with large, well ordered data sets, allowing the user to work with explicitly stored variables, abstract mathematical functions and mathematical transforms. FERRET was also used to produce most of the plots in this study.

Potential vorticity is a useful measure of how well "ventilated" a layer is. A layer may be poorly ventilated if the Ekman pumping at the surface of the layer is weak or the

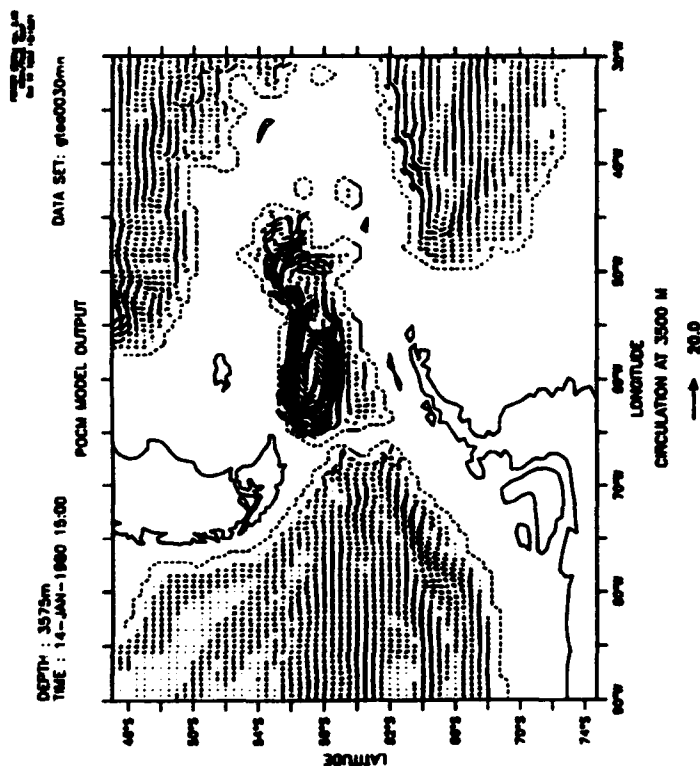
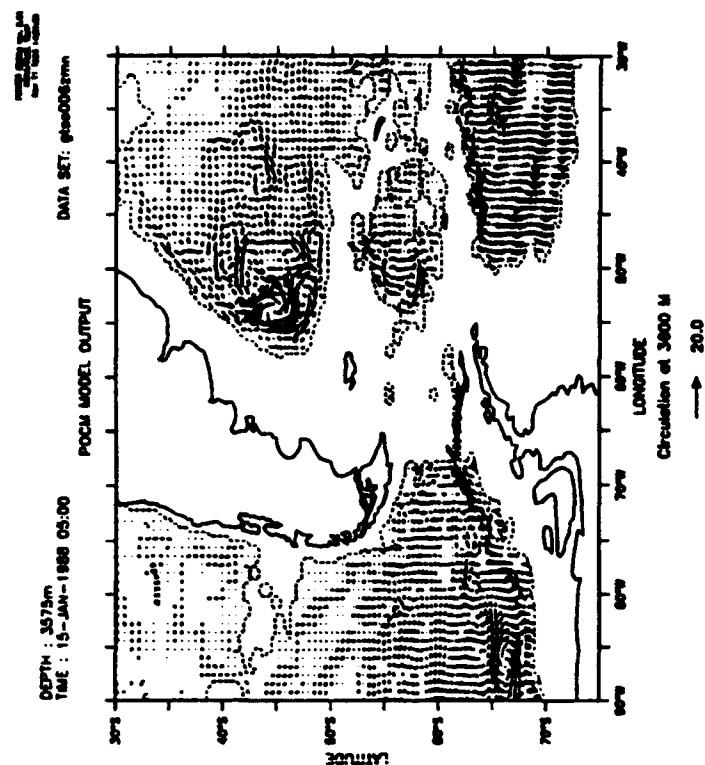
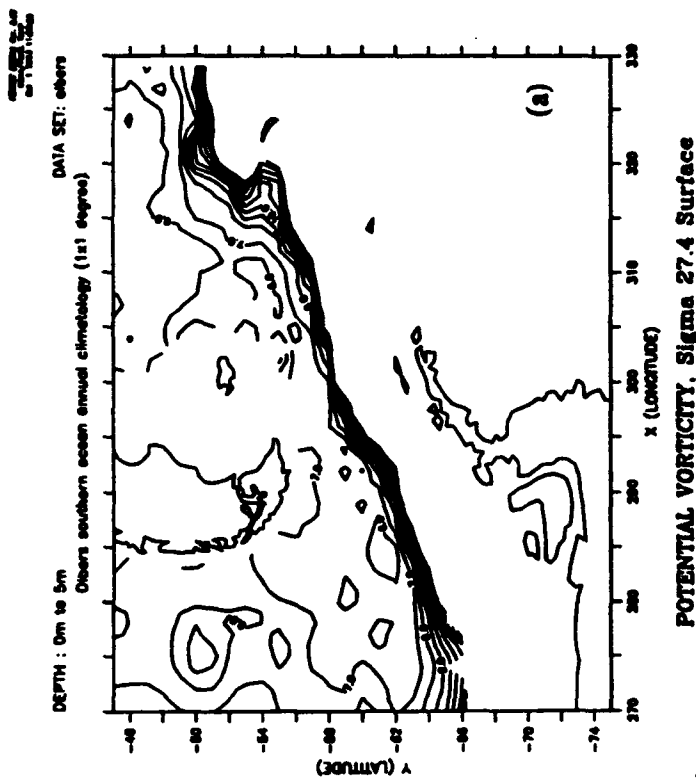


Figure 2.6 Deep Circulation for area 90°W to 30°W
a.) Half Degree Model Solution b.) Quarter Degree Model Solution

dynamics serve to isolate the layer from the boundary conditions. A layer may be considered to be unventilated if the fluid tends to recirculate many times within the layer before having its properties reset at the surface outcrop of isopycnals. (Keffer, 1985)

The observations (Figures 2.7 a,b, and c) show high levels of potential vorticity encircling the Antarctic continent. The quarter degree model shows definite improvement from the half degree model, but still has a long way to go to match the levels found in the observations. The observations and the models are in relatively good agreement as to the position of the maximum potential vorticity. It is possible that the models and the observations would be in better agreement if the models could resolve the higher values of potential vorticity. This difference in resolution could be due to the vertical resolution of the models, 20 levels vice 38 levels found in the observations.



35

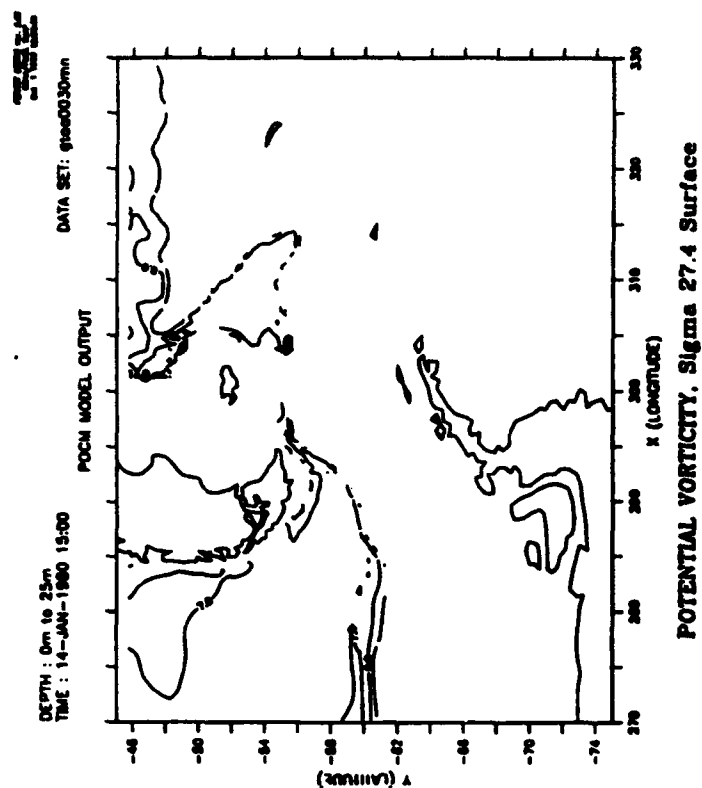
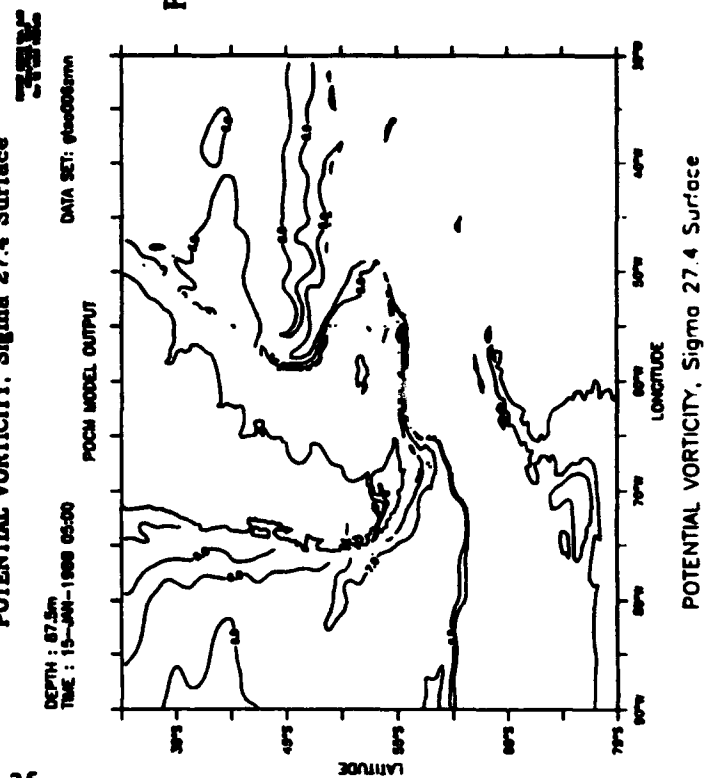


Figure 2.7

Potential Vorticity for area 90°W to 30°W

a.) Atlas Data b.) Half Degree Model Solution c.) Quarter Degree Model Solution

B. CENTRAL ATLANTIC/ AGULHAS CURRENT REGION (30°W - 30°E)

The Central South Atlantic sector is divided by the mid-ocean ridge that splits it into two basins: the Argentine Basin to the west of about 20°W and the Cape Basin to the east (Figure 1.1.) The dominant current flow at the surface appears to be wind driven. In this sector the westerlies dominate the flow between 60°S and 40°S and the ACC flow is unimpeded and relatively zonal with moderate eddy activity. An increase in the eddy activity and a reverse in the westerlies occurs to the northeast in vicinity of the Cape of Good Hope and the Agulhas Current System.

The Agulhas Current System is one of the most energetic regions of the Southern Ocean. The Agulhas Current is the major western boundary current of the South Indian Ocean with volume transports on the same order as the Gulf Stream (Read and Pollard, 1993). It follows the African coastline until it separates from the continental slope at the Agulhas Bank between 20° and 22° E. After separation the current executes a rather abrupt anticyclonic turn, which is referred to as the Agulhas Retroflexion. This current loop regularly intercepts itself and forms warm rings that are the largest and most energetic in the world ocean. As a result, the current shows the highest variability in the Southern Hemisphere (Forbes, 1993).

1. Area Temperature and Salinity (100 m)

a. Temperature

The observations and the model solutions over this region are in remarkably close agreement (Figures 2.8 a,b, and c). The major difference is the tighter temperature gradient south of the Cape of Good Hope which continues into the central Atlantic between 40°S and 45°S found in the half degree model. The models seem to display a much higher level of eddy activity, even over a five year average. The atlas observations are much smoother in general.

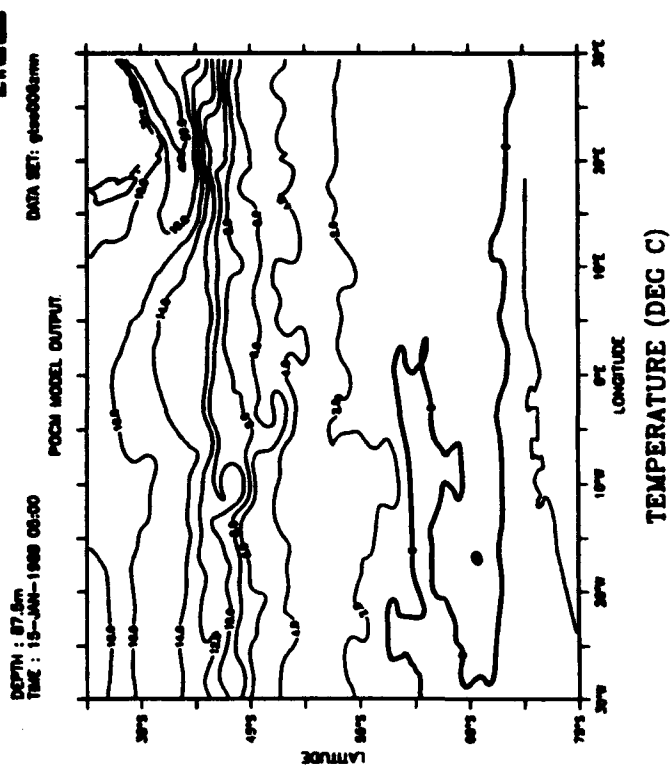
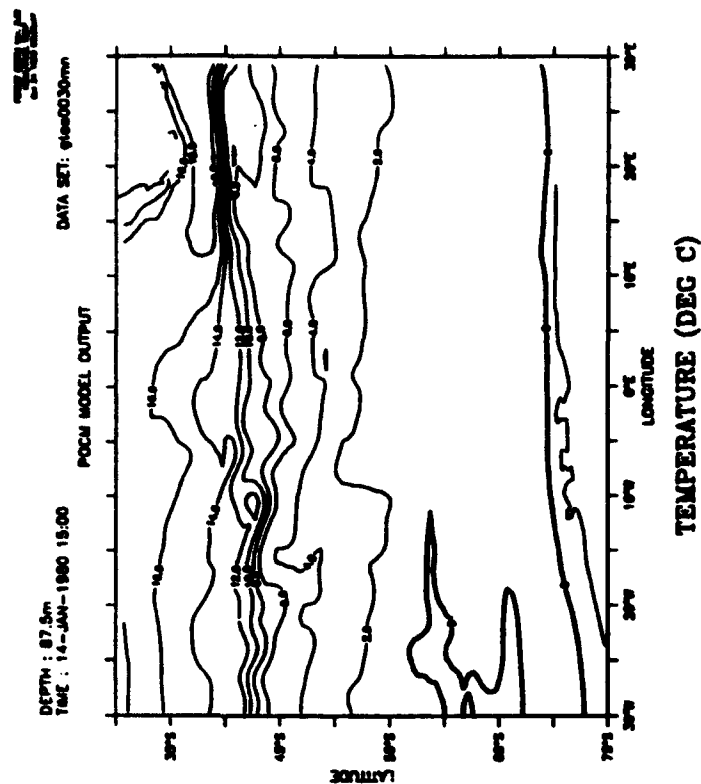
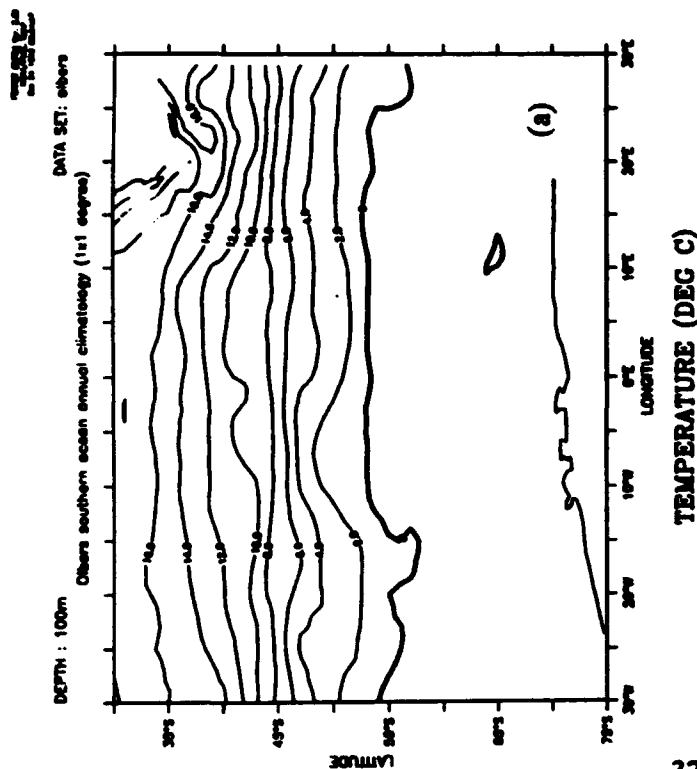


Figure 2.8 100 m Temperature charts for area 30°W to 30°E
a.) Atlas Data b.) Half Degree Model Solution
c.) Quarter Degree Model Solution

The warmer water associated with the Agulhas Current penetrates much farther west in the Atlantic than is shown in the observations. The models also show a semi-permanent warm eddy near 10°W and 45°S. This appears to be related to a wide canyon in the Mid-Atlantic Ridge.

In the half degree model the 0° C isotherm is placed much farther to the south, around 70S but in the quarter degree model the 0° C isotherm covers a greater area as a large tongue of colder water extends eastward from the Weddell Basin.

b. Salinity (100 m)

In general both model solutions have higher overall salinity values (Figures 2.9 a, b, and c). The salinity minimum associated with the ACC is 0.4 ppt higher than the observed values (34.4 ppt vs. 34.0 psu). The minimum is found slightly more to the south in the half degree model than in the observations, but the quarter degree model is closer to the observations. The minimum is found centered around 52°S in the observations, around 48°S in the half degree model and 50°S in the quarter degree model. This could also contribute to the tighter salinity gradient found south of the Cape of Good Hope in the half degree model that is comparable to the tighter gradient found in the temperature data. The salinity maximum found south of 60°S in the observations is in relatively good agreement but again the models are slightly higher in salinity by about .2 ppt (34.6 vs. 34.4 ppt) and greater in extent than is found in the observations.

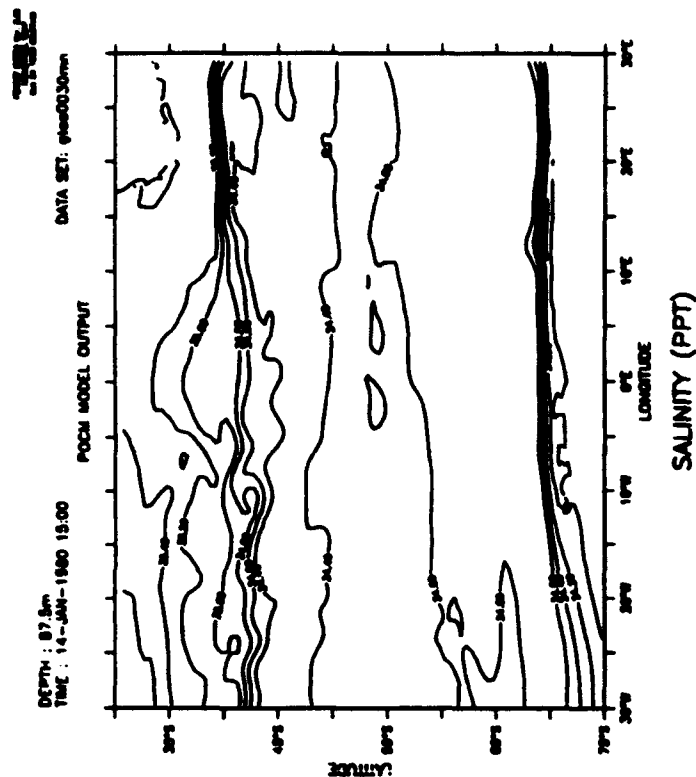
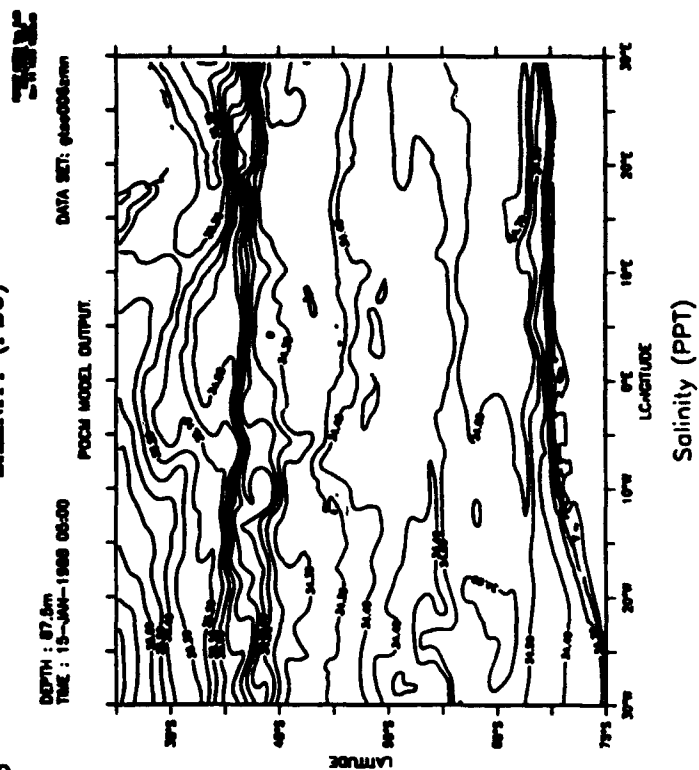
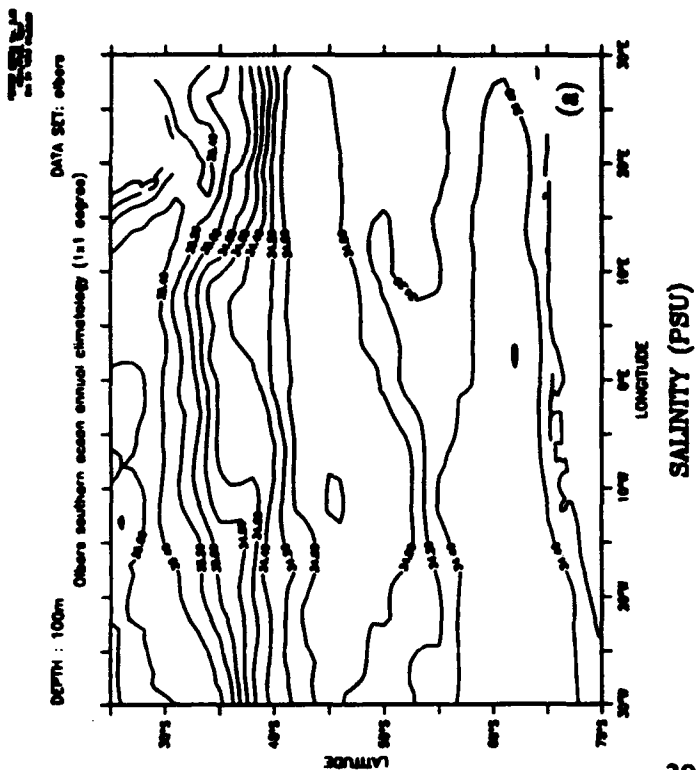


Figure 2.9 100 m Salinity Charts for area 30°W to 30°E
a.) Atlas Data b.) Half Degree Model Solution
c.) Quarter Degree Model Solution

2. Vertical Sections

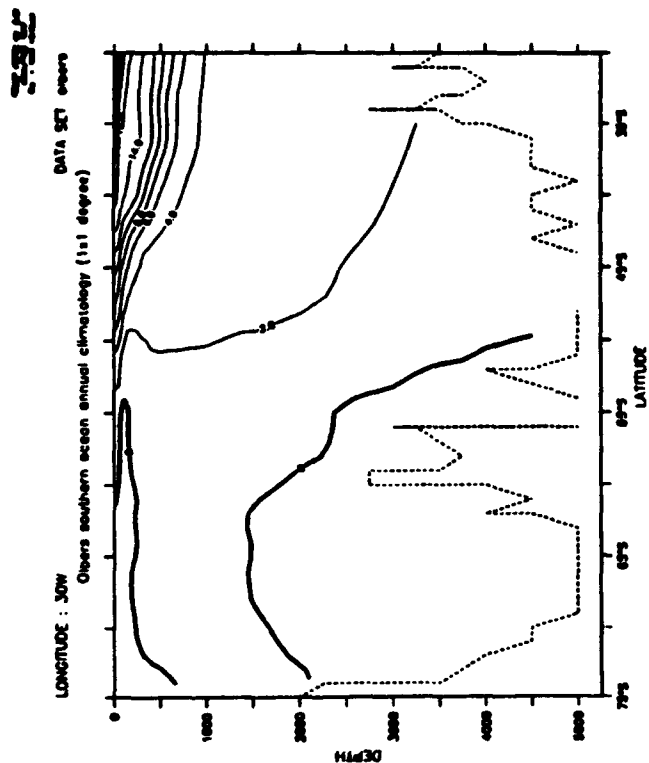
a. Temperature Sections along 30°W

As was found in the temperature sections in the Drake Passage, the models' representation of AAIW is weaker than that found in the observations (Figures 2.10 a, b and c). But, along this section it is much stronger in the half degree model than was previously found in the Drake Passage section.

The surface pool of warmer water at 35°S corresponds fairly well, but again the 16° C isotherm is much deeper in the model than in the observations. Also worth noting is the 0°C isotherm at depth which is present in both models and in the observations; all are in excellent agreement.

b. Salinity Sections along 30°W

The salinity sections along 30W (Figures 2.11 a, b and c) are also in good agreement as the salinity minimum associated with the AAIW in the models and the observations begin their descent from the surface at approximately 43°S. At 30°S the salinity minimum has descended to a depth of 1000 m in both the models and the observations. Once again the models are slightly more saline indicating a salinity minimum of 34.4 ppt vice 34.2 psu. The quarter degree model is slightly more saline than the half degree model. (34.5 ppt vs. 34.4 ppt) A salinity maximum is present in both the atlas observations and the model at 2800 m in vicinity of the Mid-Atlantic Ridge. This is associated with the influx of South Indian Ocean water from the east.



41

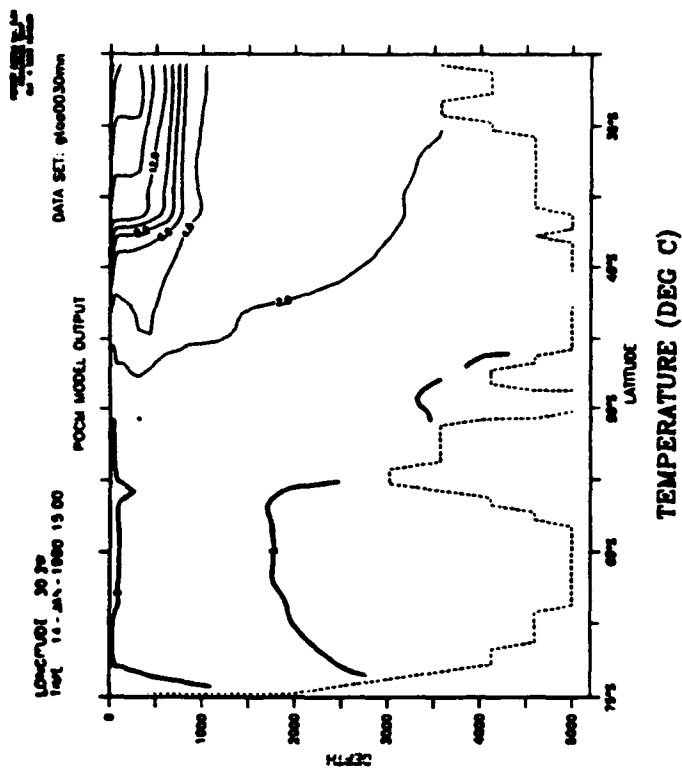
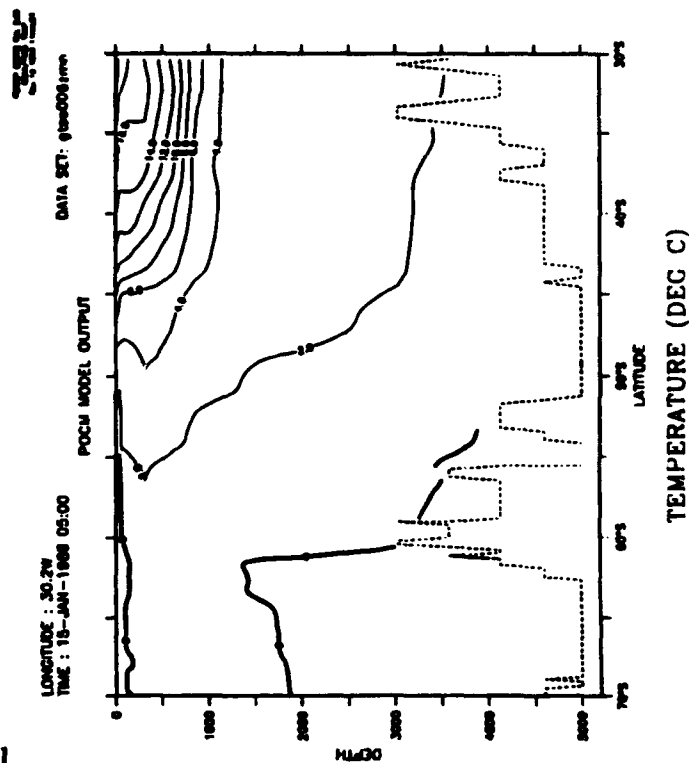


Figure 2.10 Vertical temperature sections along 30°W
a.) Atlas Data b.) Half Degree Model Solution
c.) Quarter Degree Model Solution

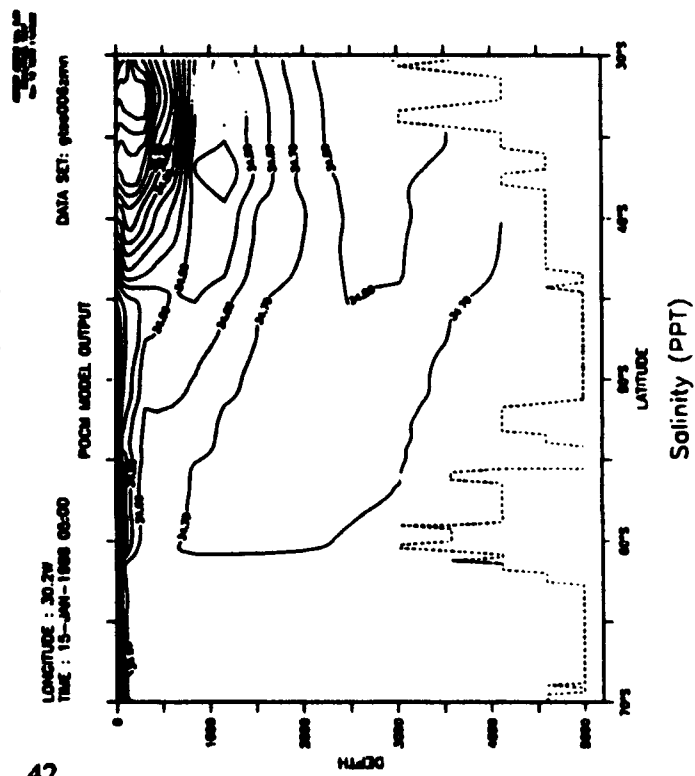
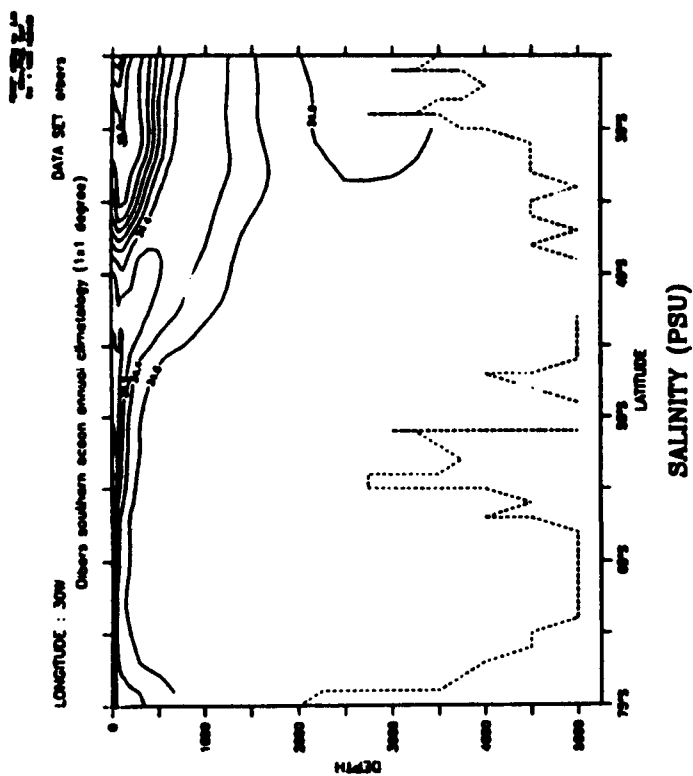


Figure 2.11 Vertical salinity sections along 30°W
a.) Atlas Data b.) Half Degree Model Solution
c.) Quarter Degree Model Solution

c. Temperature Sections along 25°E

The temperature sections along 25°E (Figures 2.12 a, b and c) follow the general trend displayed thus far, relatively weak AAIW in the model and showing some improvement in the quarter degree model. There is good agreement in the lower levels and the pool of warmer water to the north near the continent of Africa is slightly deeper in the model than is found in the observations. Again there is slight improvement in the quarter degree model in that there is not as wide a gap between the 8 °C isotherm and the 12° C isotherm in the quarter degree model as compared to the half degree model.

d. Salinity Sections along 25°E

The salinity sections (Figures 2.13 a, b and c) are in fairly good agreement, the major differences being the very tight gradient displayed in both the quarter and half degree models between 70°S and 55°S in the top 100 m. Equatorward from 55°S to the north the models and the observations are in good agreement.

3. Circulation

a. Surface (37.5 m)

The surface circulation as in most regions of the ACC is dominated by the winds and the topography of the region (Figures 2.14 a and b). The easterlies are well represented along the continental boundary of Antarctica in both the quarter degree and half degree models. The ACC is split into three frontal regions that are well displayed in this section, the Polar Front, the Subantarctic Front and the Subtropical Front. The location of each of these fronts agree well with the observed average position of these fronts. The Agulhas Current System appears to penetrate more directly to the southwest of the Cape of Good Hope in the quarter degree model before beginning its turn to the north (10°E in the quarter degree model and 15°E in the half degree model).

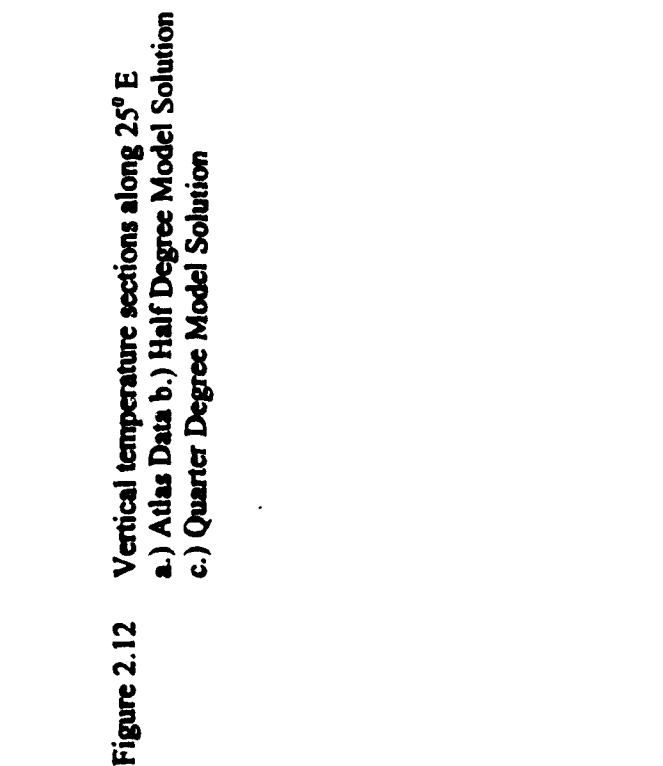
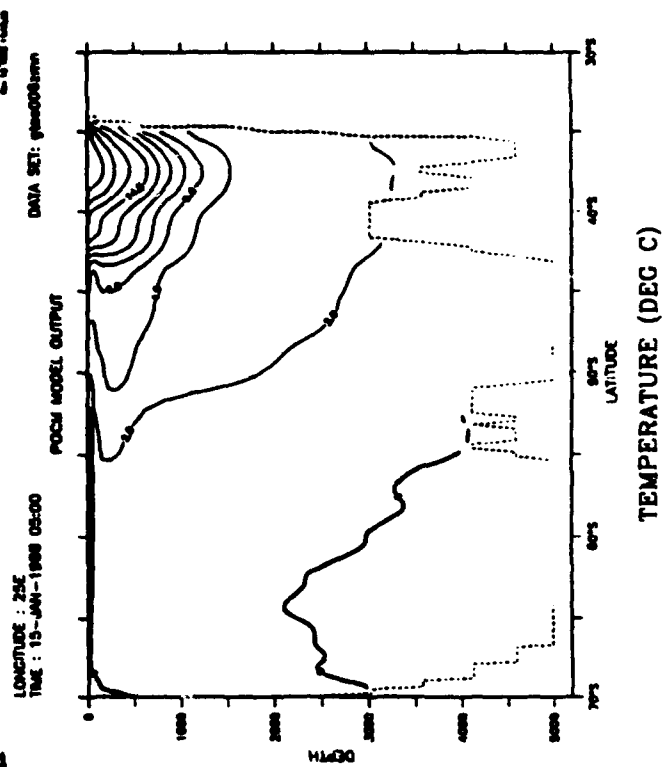
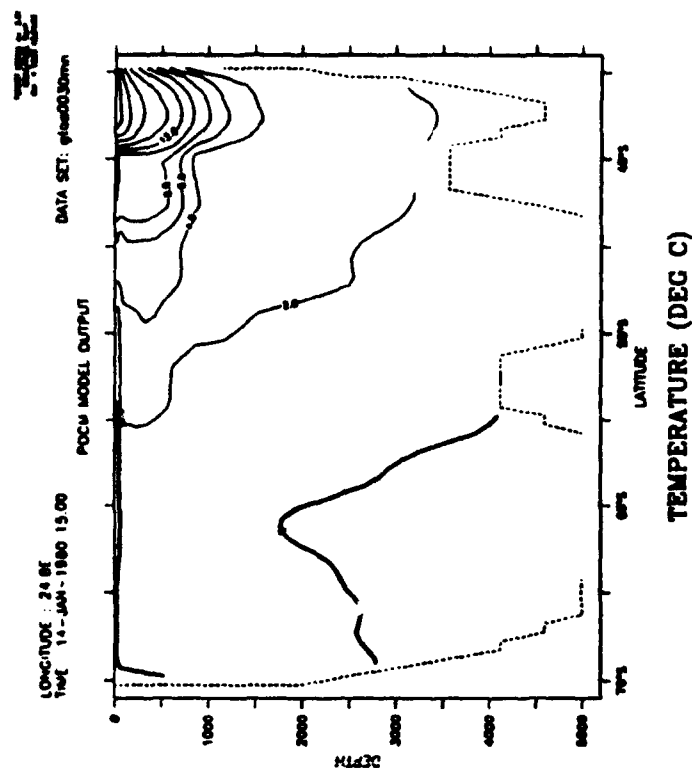
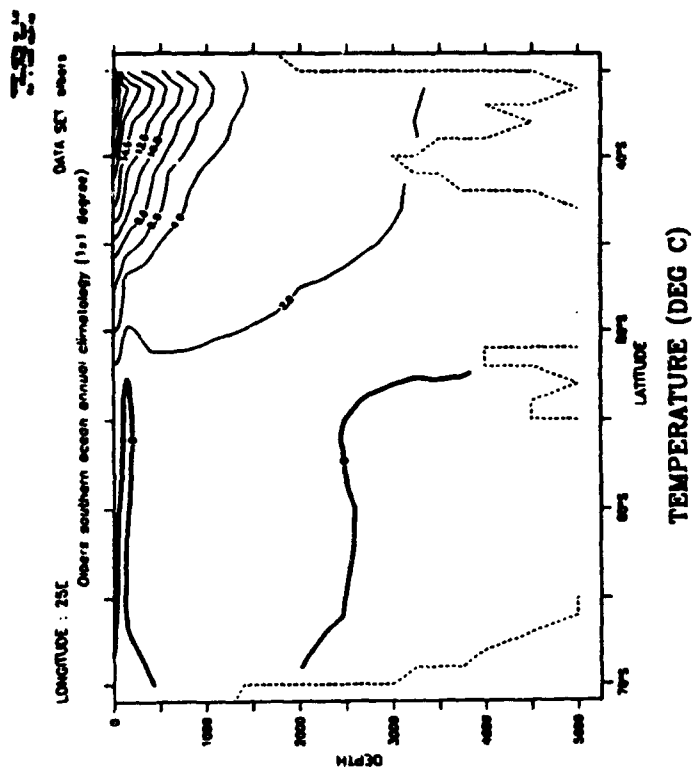
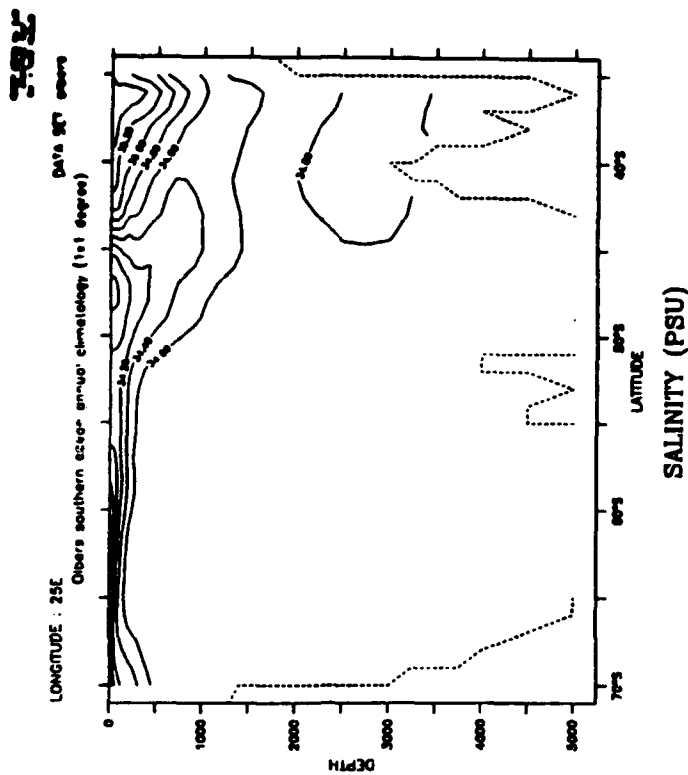


Figure 2.12 Vertical temperature sections along 25° E
a.) Atlas Data b.) Half Degree Model Solution
c.) Quarter Degree Model Solution



45

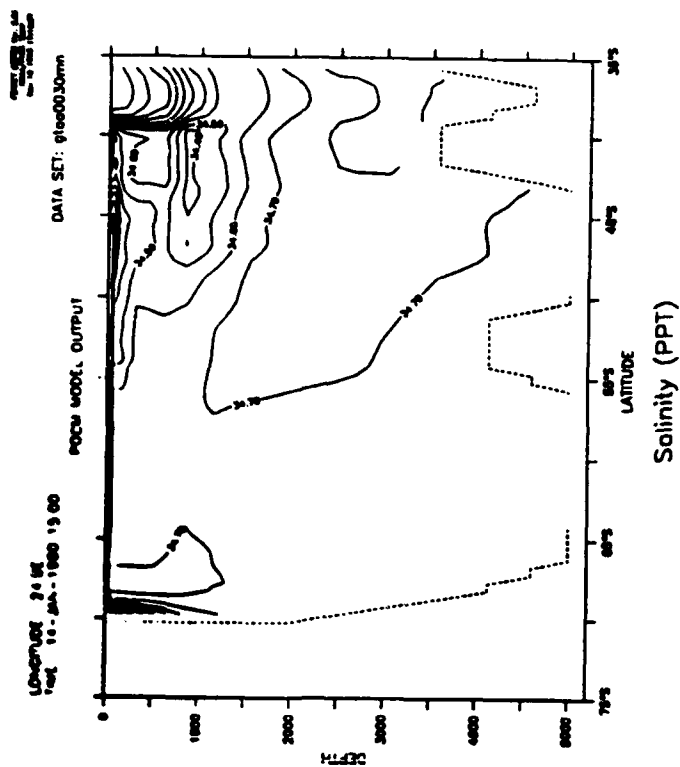
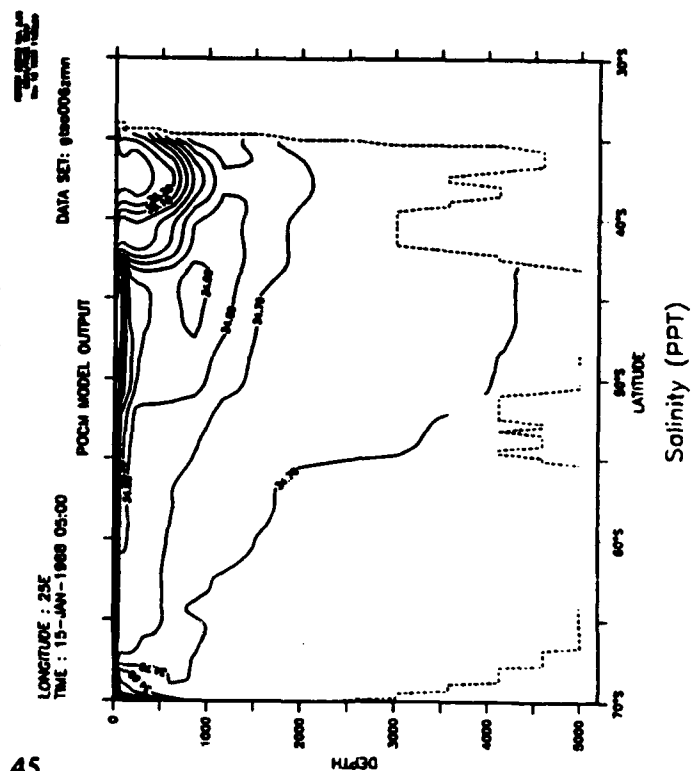


Figure 2.13 Vertical salinity sections along 25°E
a.) Atlas Data b.) Half Degree Model Solution
c.) Quarter Degree Model Solution

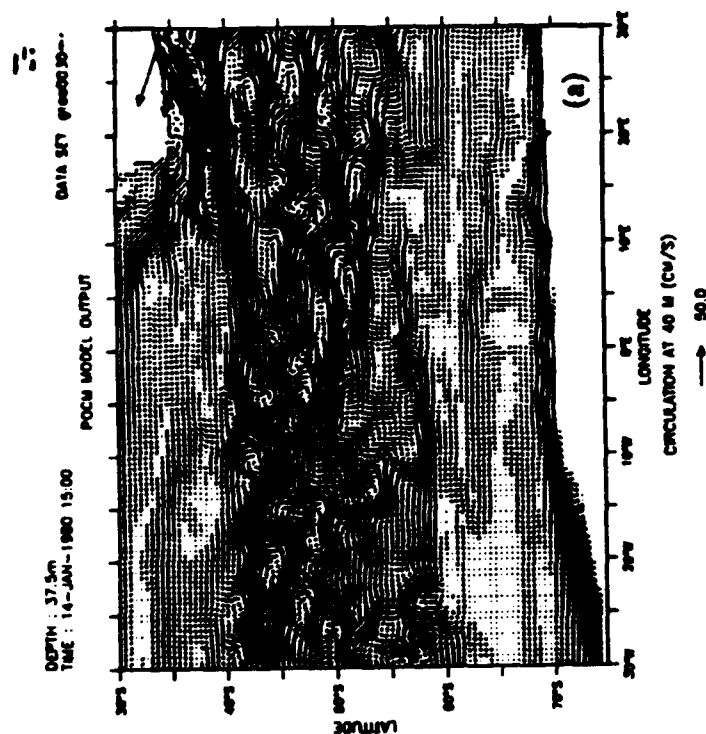
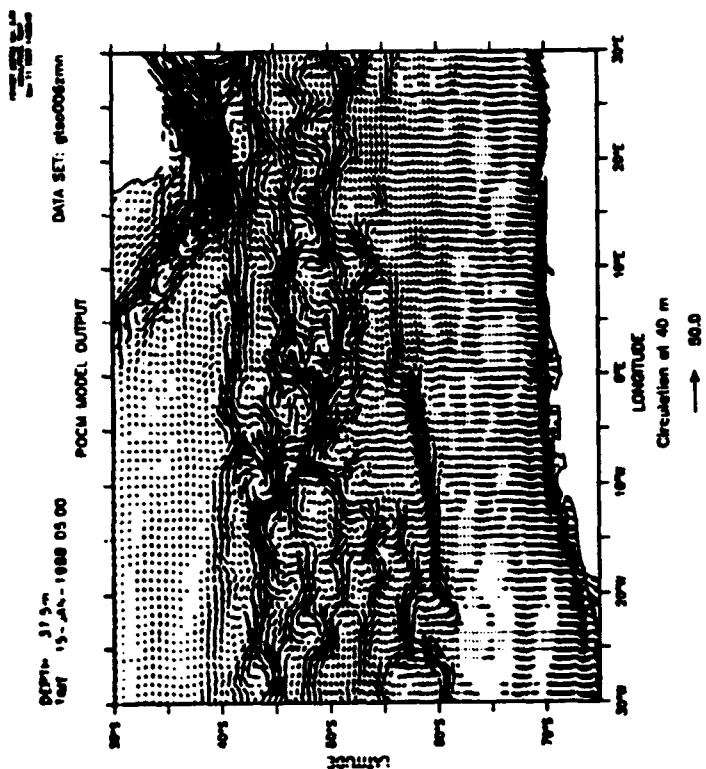


Figure 2.14 Surface Circulation for area 30°W to 30°E
a.) Half Degree Model Solution b.) Quarter Degree Model Solution

b. Deep Circulation (3500 m)

The deep circulation in the Central Atlantic (Figures 2.15 a and b) very dramatically shows the important current interaction with topography and the mixing processes that ensue. This is slightly greater in the quarter degree model but is no less impressive in the half degree model .

The western boundary current in the abyssal flow seem to be stronger in the half degree model both, in the Argentine Basin and in the Cape Basin. The flow to the south of Africa in the half degree model shows the model definitely carries the westward flowing Agulhas Current to the deepest levels. The quarter degree model shows a more northerly flow of the Agulhas Current than the half degree model.

4. Potential Vorticity

The potential vorticity shown in Figures 2.16 a, b, and c shows some improvement in the quarter degree solution as compared to the half degree solution. By the Cape of Good Hope the quarter degree model shows seven units of potential vorticity which is also present in the observations, but which covers a larger area than is shown in the observations. The quarter degree model shows a broader region of six units of potential vorticity extending into the Atlantic associated with the Agulhas Current than is shown in the observations. This might be due more to the use of sections in the observational data than any substantial difference between the model solutions and the observational data. The quarter degree model is in better agreement with the observations than with the half degree model.

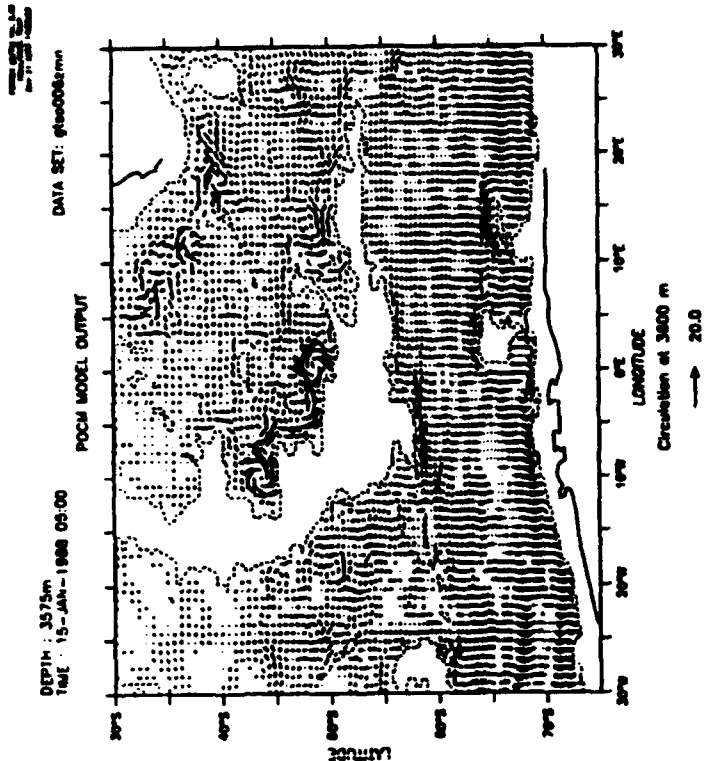
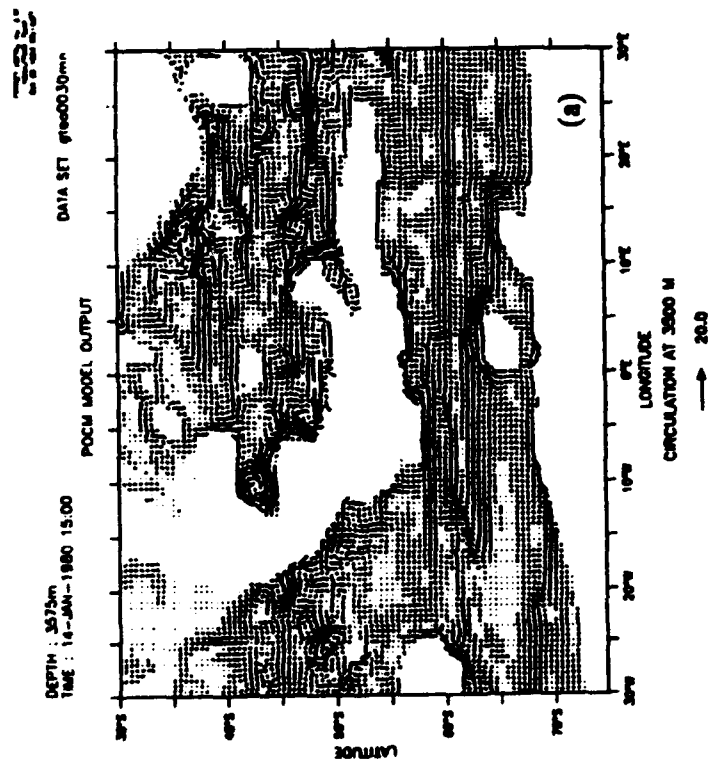
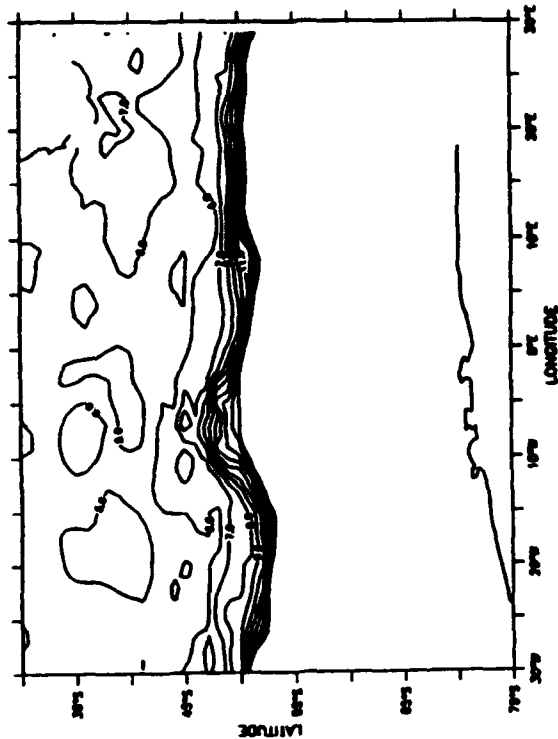


Figure 2.15 Deep Circulation for area 30°W to 30°E
a.) Half Degree Model Solution b.) Quarter Degree Model Solution



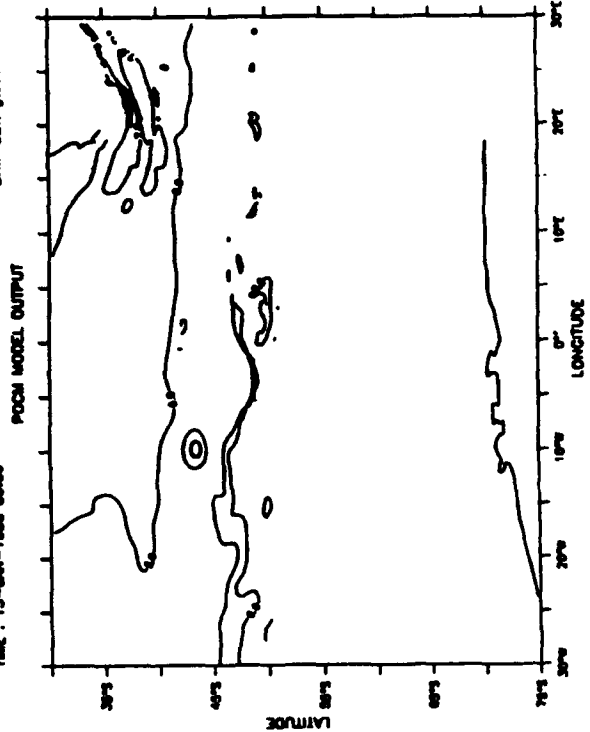
DEPTH : 0m to 5250m
 Others southern ocean annual climatology (1x1 degree)
 DATA SET: others



POTENTIAL VORTICITY, Sigma 27.4 Surface



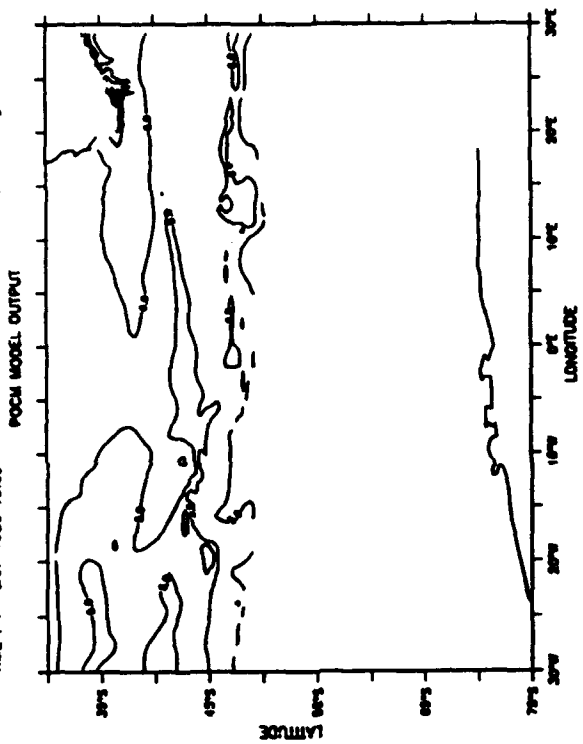
DEPTH : 87.5m
 TIME : 15-JAN-1988 05:00
 DATA SET: gmo0030mm



Potential Vorticity



DEPTH : 0m to 5200m
 TIME : 14-JAN-1988 15:00
 DATA SET: gmo0030mm



POTENTIAL VORTICITY, Sigma 27.4 Surface

Figure 2.16 Potential Vorticity for area 30°W to 30°E
 a.) Atlas Data b.) Half Degree Model Solution
 c.) Quarter Degree Model Solution

C. KERGUELEN PLATEAU/CROZET BASIN AREA

Southwest of Australia, the ACC makes its most northern excursion in the Southern Ocean. This is due to topographic steering by the Crozet and Kerguelen Plateaus. This is also an area rich in eddy activity in the model and observational data. As the turbulent flow of the ACC flows over this topographic region, considerable mixing between the warm South East Indian Ocean waters and the ACC takes place.

1. Area Temperature and Salinity (100 m)

a. Temperature

A strong frontal boundary is found north of the Crozet and Kerguelen Plateaus between 45°S and 40°S. Both the model and the observations are in good agreement about placing this front (Figures 2.17 a, b and c). There is some discrepancy between the models and the observation on the placement of the 0° C isotherm. The models place it quite far south, in the vicinity of the continent. While the observations place it much farther to the north, along 57°S. The model and the atlas are in close agreement north of the front, both showing the effects of the transition between the westerly winds that dominate the ACC and the monsoonal winds that dominate the Indian Ocean.

b. Salinity (100 m)

The salinity isohalines (Figures 2.18 a, b and c) are not in quite as good agreement as the temperatures were. In general as noted before the model has a tendency to be more saline than the observations. The gradient associated with the Subtropical Front is in good agreement in the western portion of the region, and becomes less well defined as the gradient expands once past the Kerguelen Plateau in the observations and in the models. Also to the south near the continental boundary of Antarctica, a relatively tight salinity gradient is present in both models that is not present in the observations.

2. Vertical Sections

a. Temperature sections along 60°E

Once again the model solutions show warmer water at greater depths than the observations to the north (around 35°S) but the model and observational data are in much closer agreement than in the Drake Passage (Figures 2.19 a, b, and c) . A relatively weak portrayal of the AAIW is demonstrated, but it is still better than was represented in the Drake Passage. Another interesting difference in this section is the representation of the 2° C isotherm. The model and observations are in good agreement at lower levels to the north but to the south, the temperatures are much warmer in the 500 m level from 62°S to 50°S. Again this could point to the weak development of AAIW. This discrepancy is slightly improved in the quarter degree model. The 0° C isotherm in both models at depth is in excellent agreement with the observations.

b. Salinity sections along 60°E

In the salinity sections (Figures 2.20 a ,b and c) the model outputs and observations are in good agreement at depth. Both show a well mixed homogenized water mass of 34.7 psu. Both models illustrate a tongue associated with North Indian Ocean Deep Water (NIDW) at about 400 m along the 34.6 ppt isohaline extending from 58° S to 52°S. The observations are not quite as dramatic but indicate a stair step in this region which shows a change in water mass characteristics. As mentioned in previous sections, the salinity gradient at the surface to the south is much greater in the models than that found in the observations.

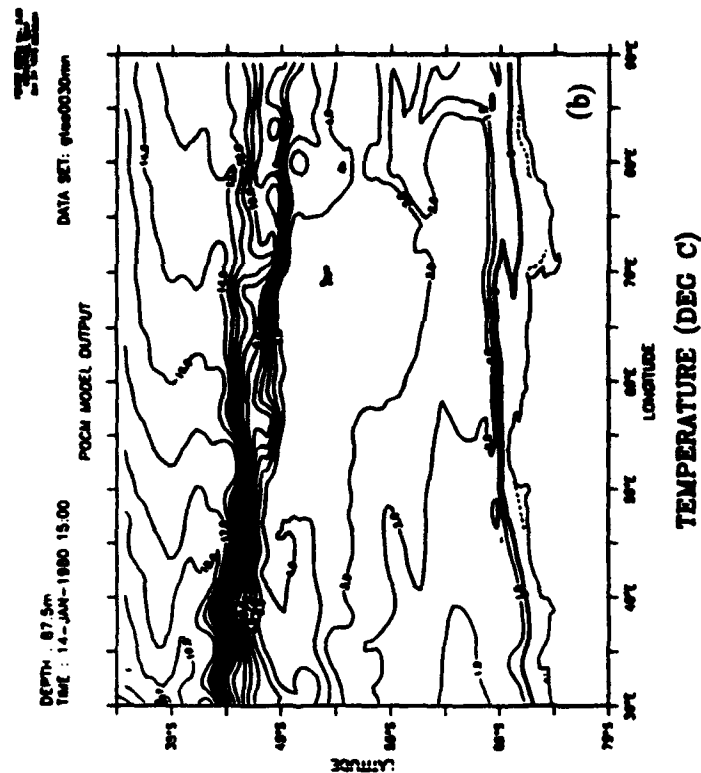
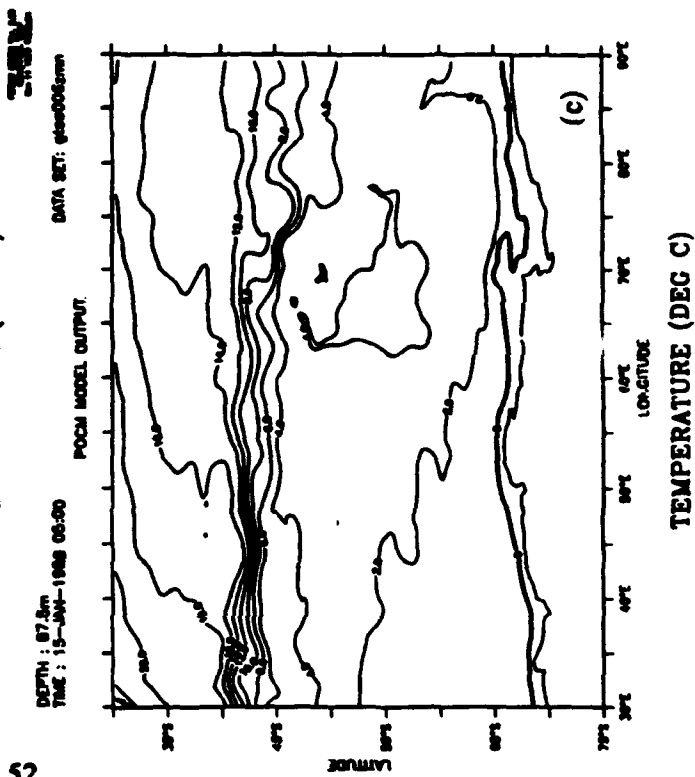
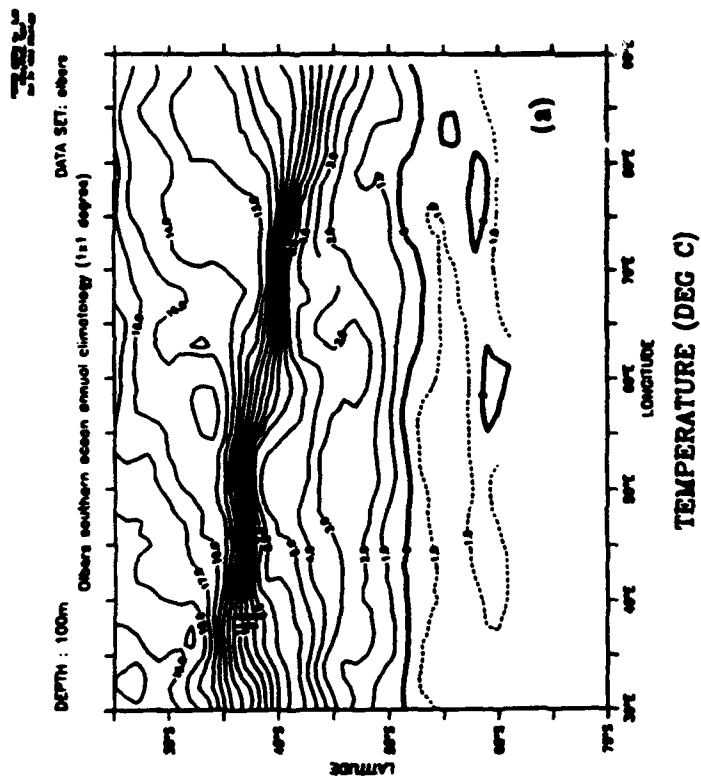
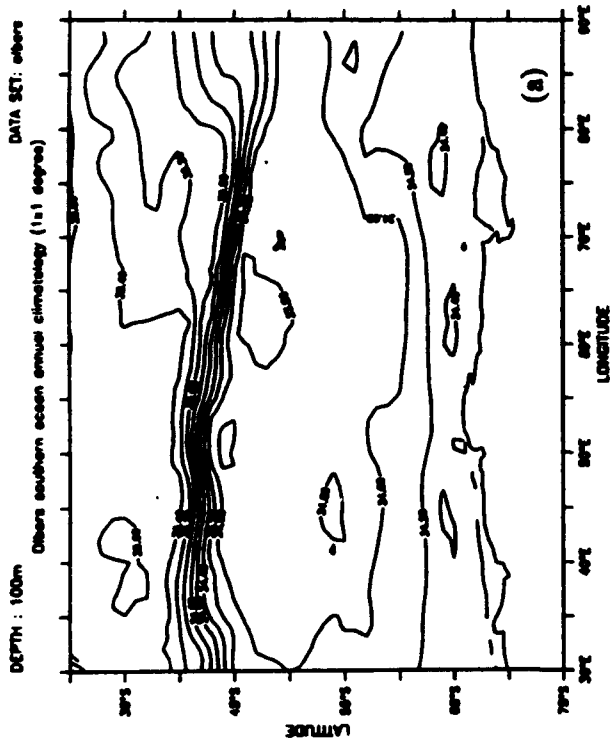


Figure 2.17 100 m Temperature charts for area 30°E to 90°E
a.) Atlas Data b.) Half Degree Model Solution
c.) Quarter Degree Model Solution



53

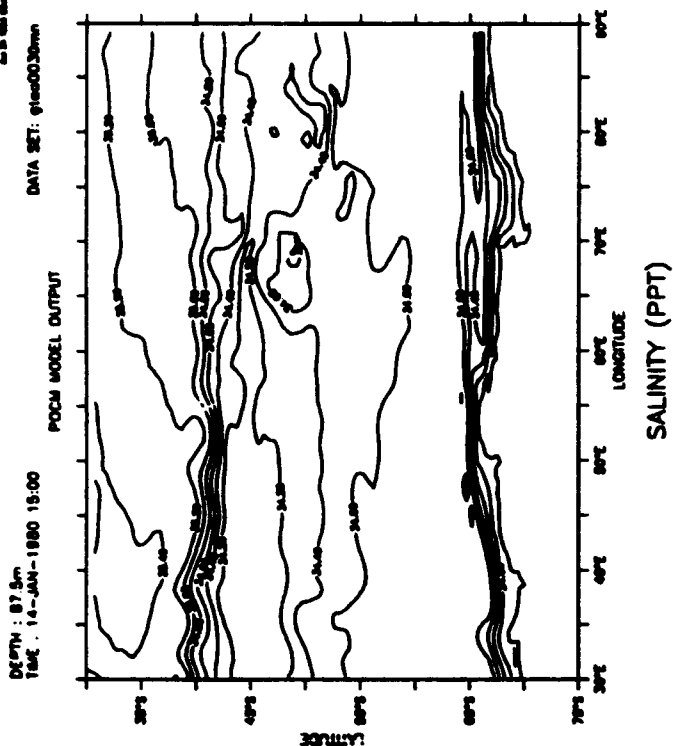
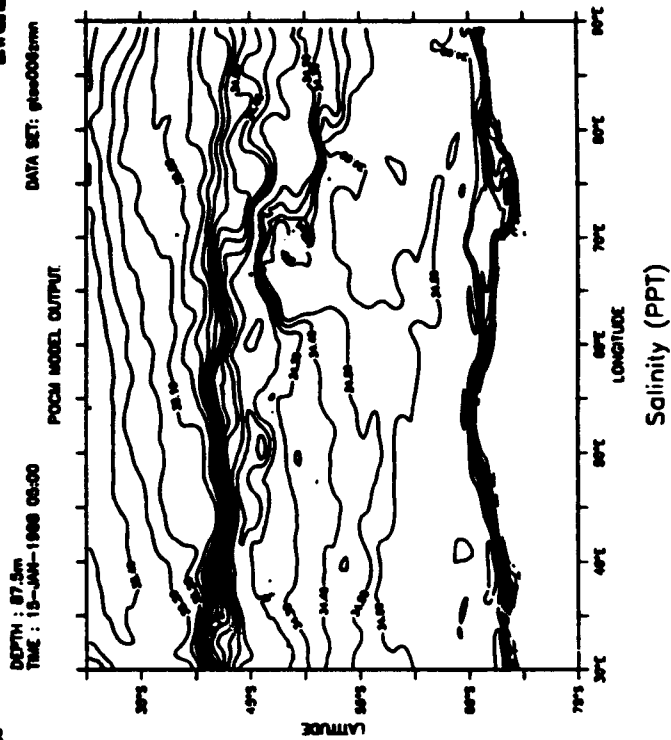
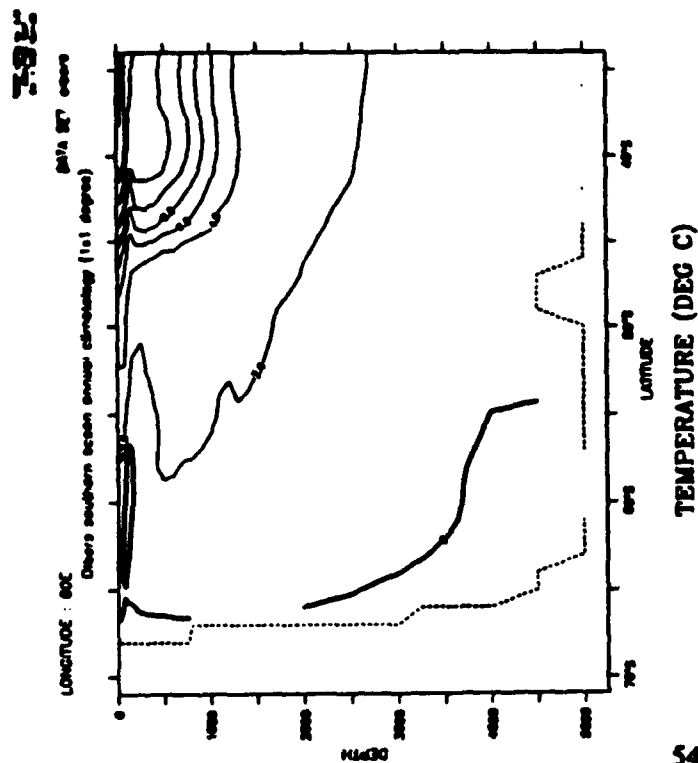


Figure 2.18 100 m Salinity Charts for area 30°E to 90°E
a.) Atlas Data b.) Half Degree Model Solution
c.) Quarter Degree Model Solution



54

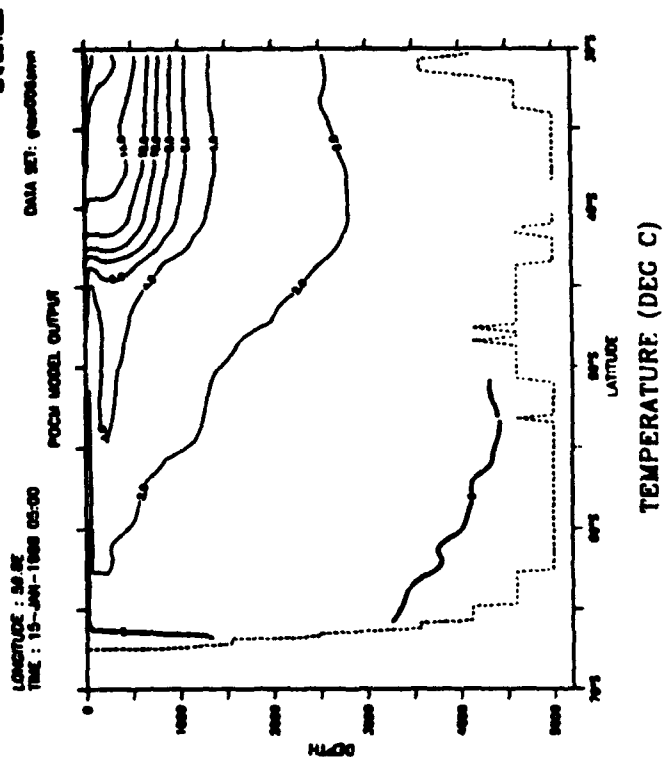


Figure 2.19 Vertical temperature sections along 60°E
a.) Atlas Data b.) Half Degree Model Solution
c.) Quarter Degree Model Solution

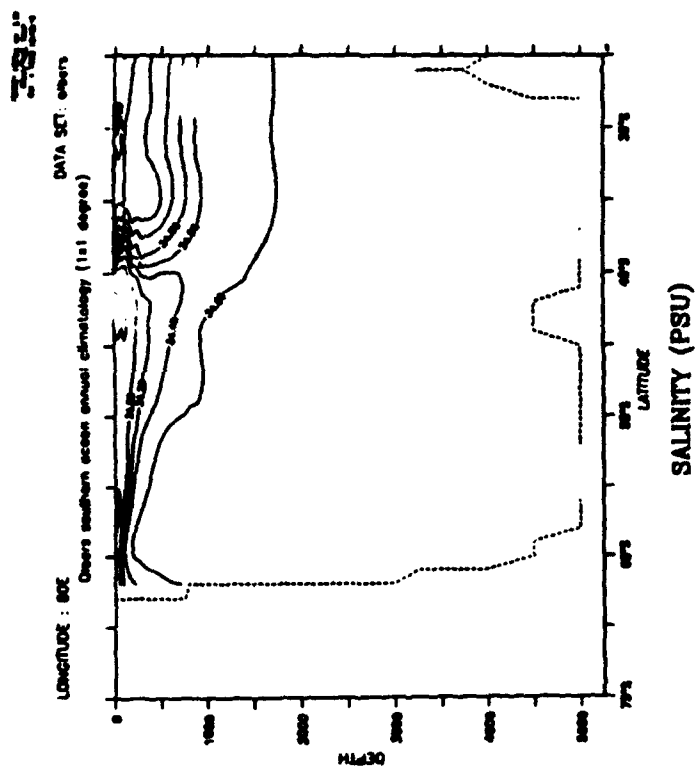
3. Circulation

a. Surface Circulation (37.5 m)

The surface circulation in the Crozet Basin (Figures 2.21 a and b, model only) show the Polar Front propagating to the south of the Kerguelen Plateau and towards the Subantarctic Front and the Subtropical Front north of the plateau. This is in relatively good agreement with circulation pattern presented by Park, Gamberoni and Charriaud (1993) (Figure 2.22). The Agulhas Front is not present in the half degree model solution, but could be said to be present in the quarter degree model. The Polar Front, while south of the Kerguelen Plateau in the observations, is much farther south in the models (60°S vs. 50°S). Also in the quarter degree model the Polar Front appears to split near 72°E into two parts, coming together again at 85°E .

b. Deep Circulation (3500 m)

Once again the improvement in the quarter degree bathymetry is apparent (Figures 2.23 a and b). The eddy activity is still strong down to the lower levels. The interaction between the AABW and the North Indian Deep Water (NIDW) is shown in the southern portion of the Crozet Basin. There appears to be two anti-cyclonic gyres present in the Crozet Basin in both the half and quarter degree models, but the schematic drawn by Park et al. (1993) shown in Figure 2.24 shows a northward flow on the western side of the Crozet Basin. The models show a predominantly southward flow. The eastern portion of the Crozet Basin in the schematic shows a southerly flow of NIDW. The models present a weak northward flow instead. Hence, while some mixing appears to be taking place, the circulation in the model is the reverse of what is shown in the observations.



56

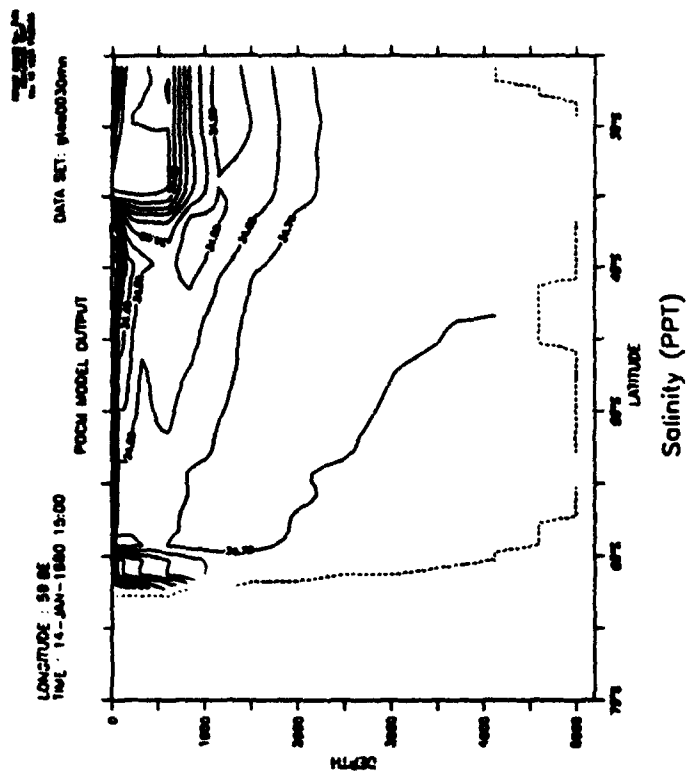
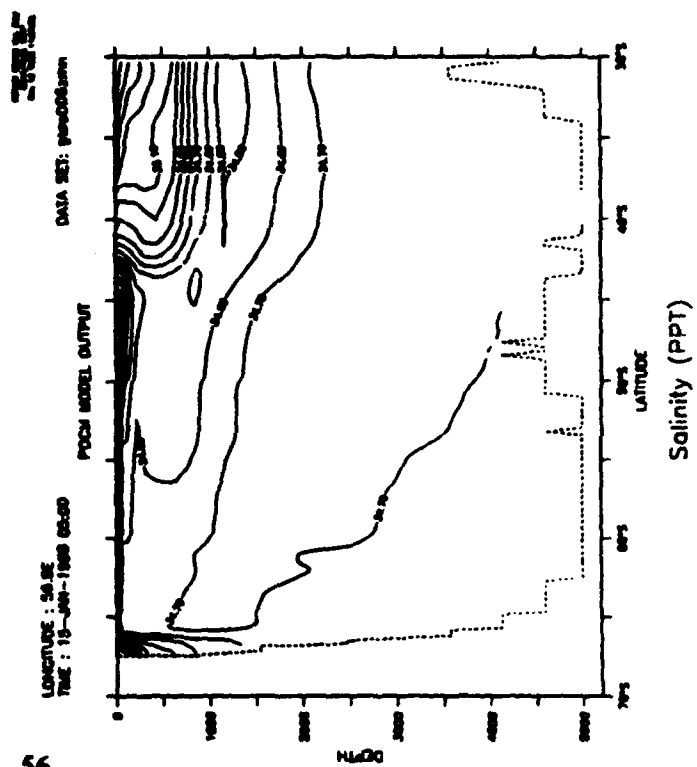


Figure 2.20 Vertical salinity sections along 60°E
a.) Atlas Data b.) Half Degree Model Solution
c.) Quarter Degree Model Solution

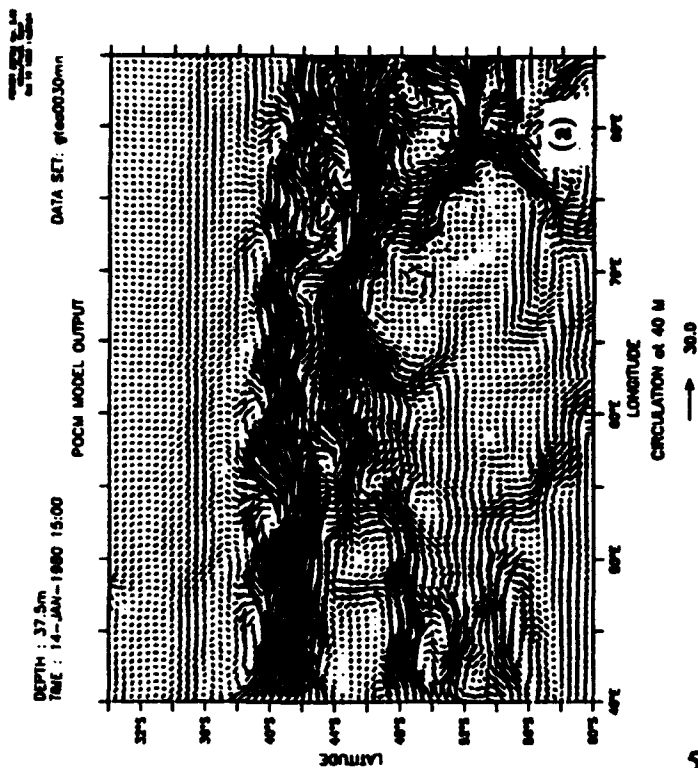
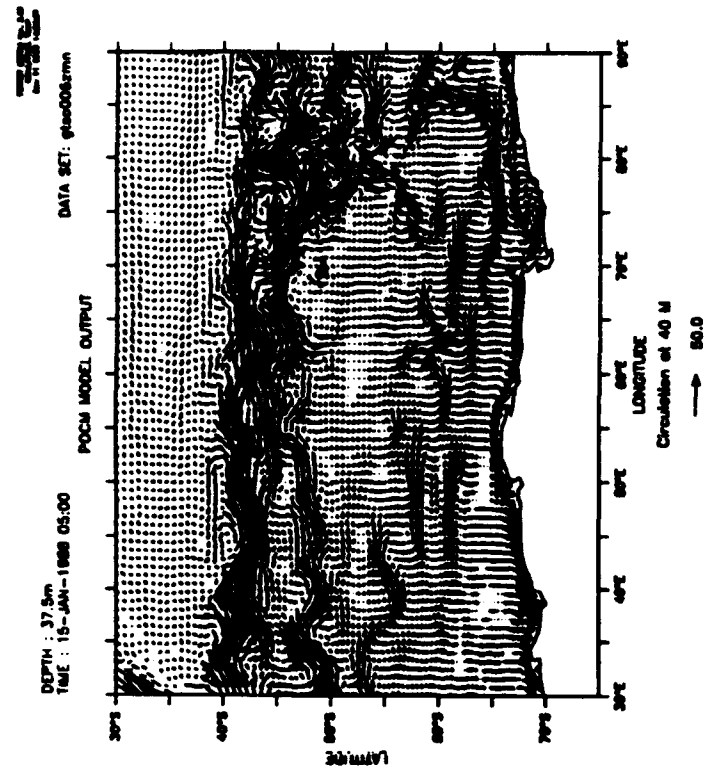


Figure 2.21 Surface Circulation for area 30°E to 90°E
a.) Half Degree Model Solution b.) Quarter Degree Model Solution

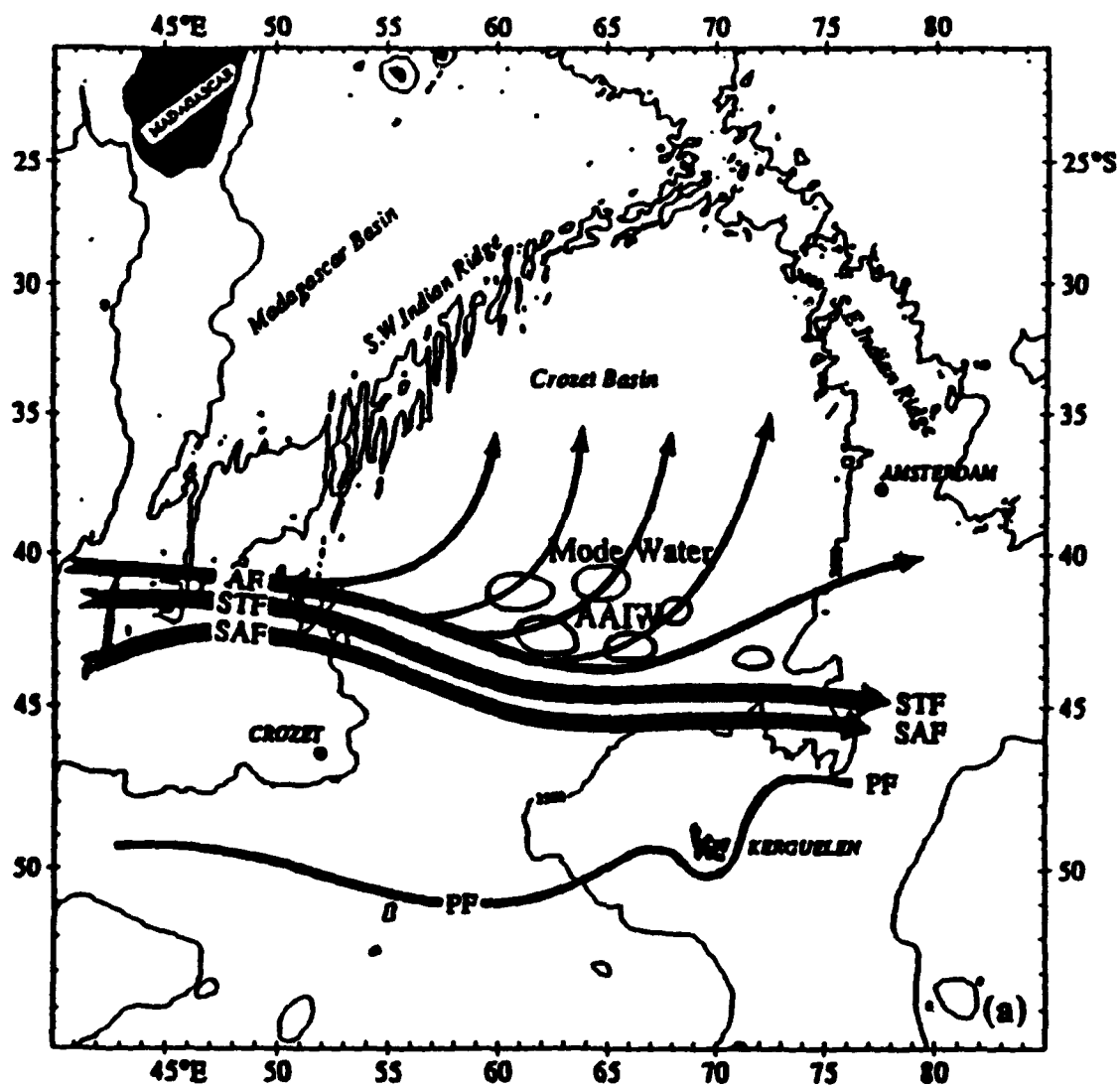


Figure 2.22 Schematic Surface Circulation for area 30°E to 90°E

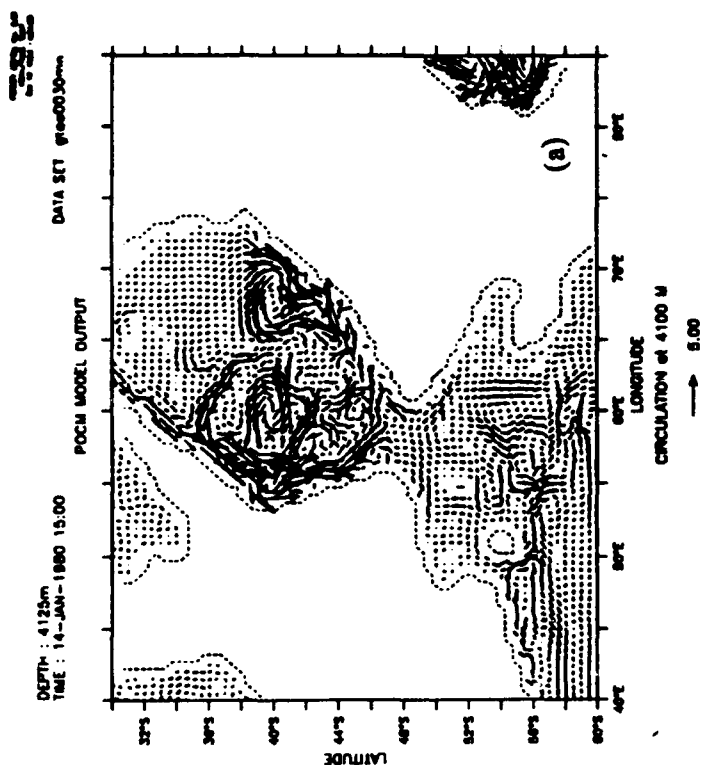
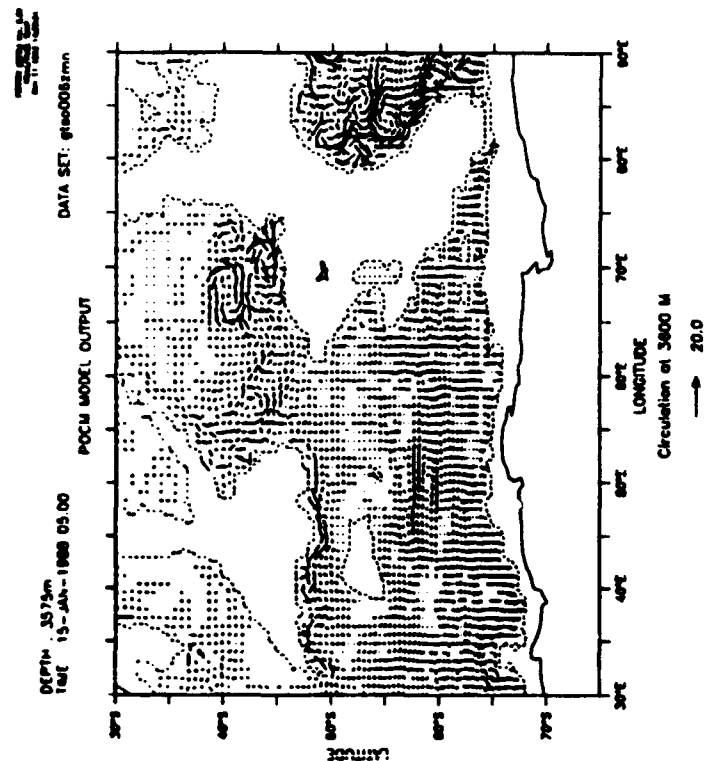


Figure 2.23 Deep Circulation for area 30°E to 90°E
a.) Half Degree Model Solution b.) Quarter Degree Model Solution

4. Potential Vorticity

The potential vorticity in the quarter degree model is a major improvement over the potential vorticity in the half degree model as compared to the observations (Figures 2.25 a,b, and c). The major ventilation effect occurring in the vicinity of the Kerguelen Plateau is vividly represented in both the observations and the quarter degree model.

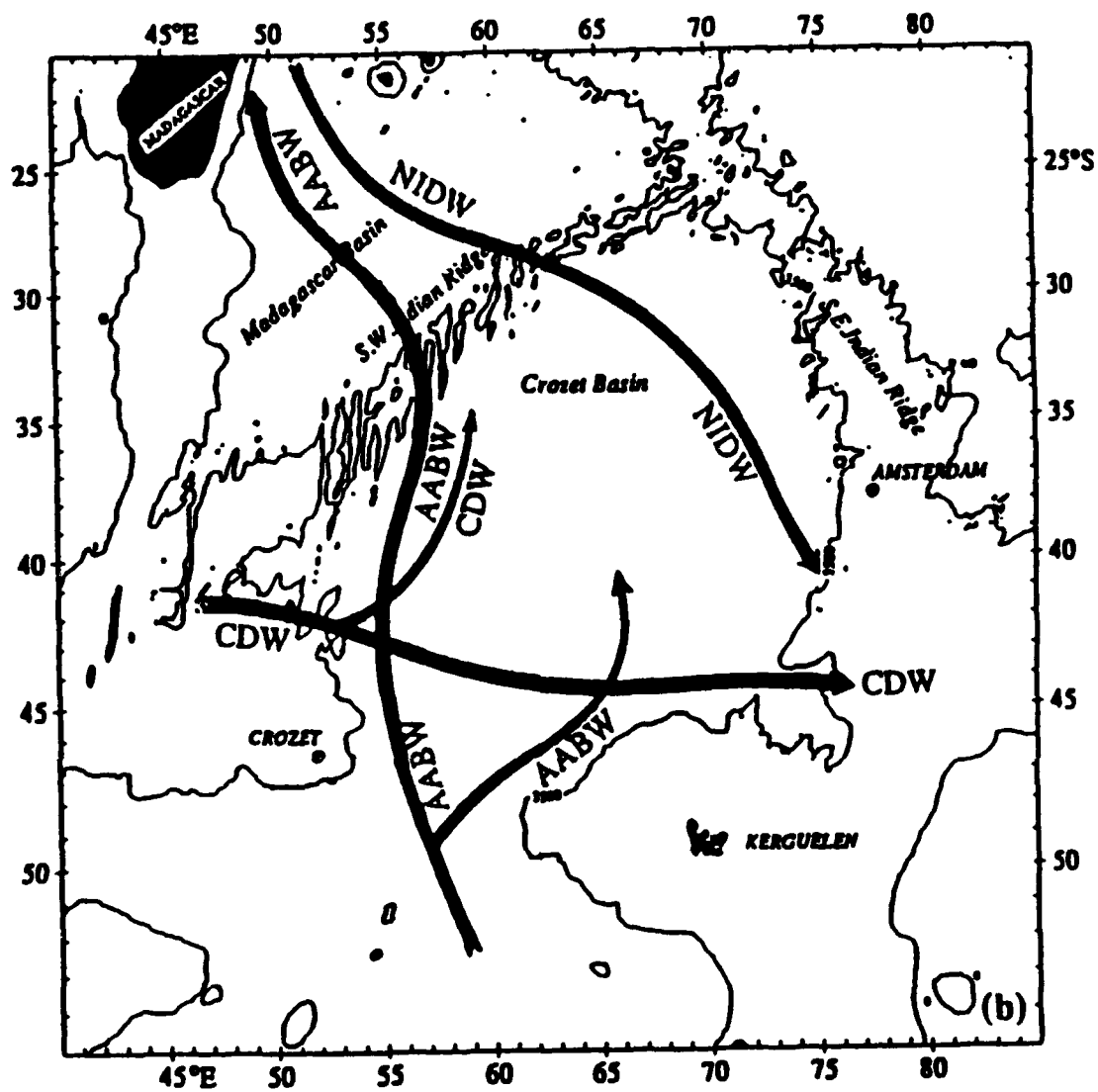
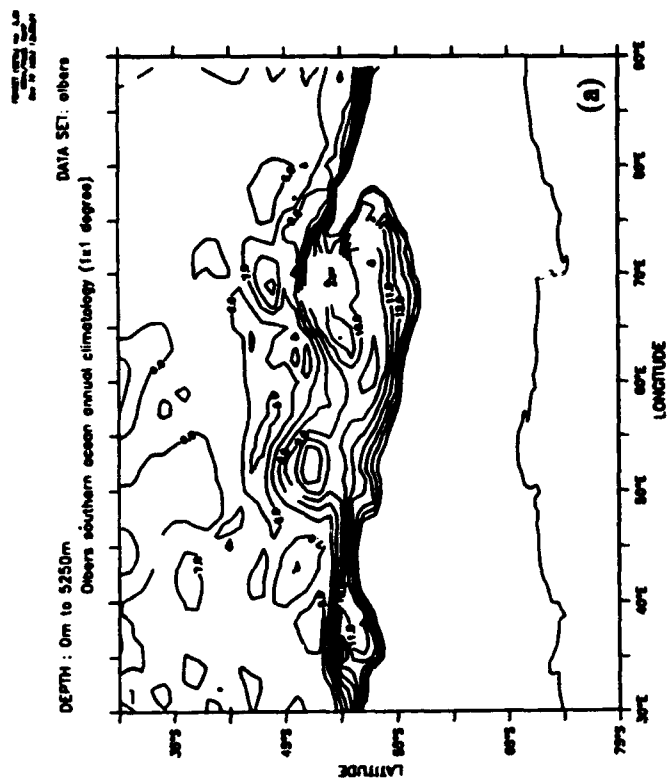


Figure 2.24 Schematic Deep Circulation for area 30°E to 90°E



62

POTENTIAL VORTICITY, Sigma 27.4 Surface

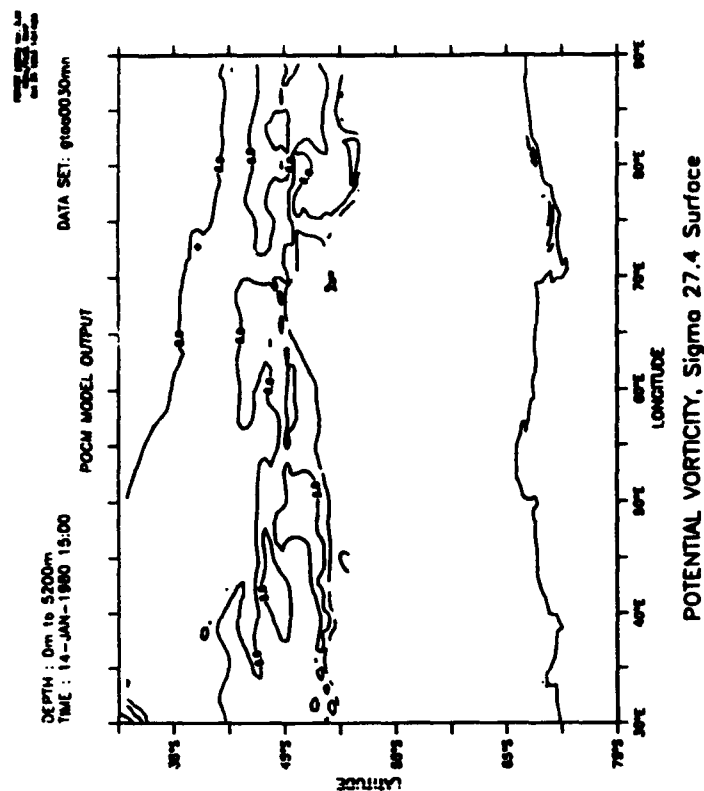
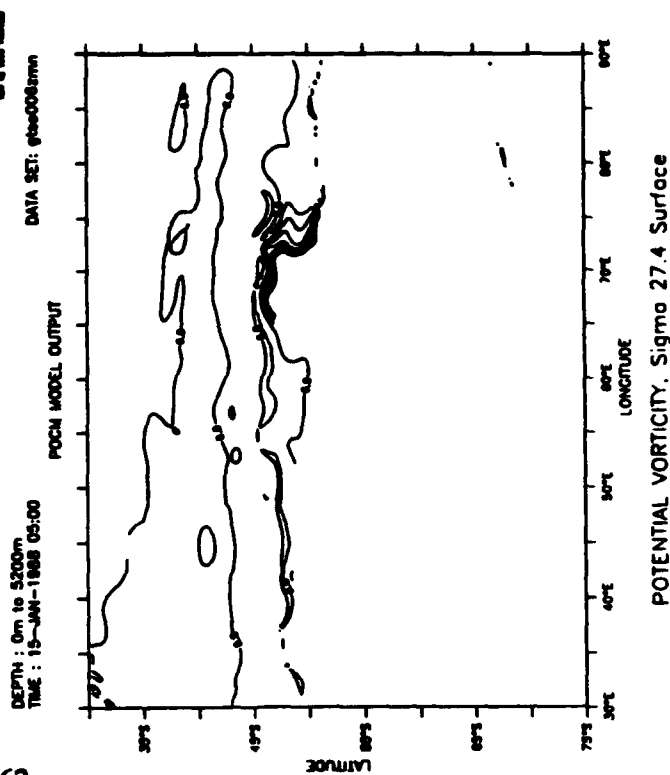


Figure 2.25 Potential Vorticity for area 30°E to 90°E
a.) Atlas Data b.) Half Degree Model Solution
c.) Quarter Degree Model Solution

D. ACC SOUTH OF AUSTRALIA (90°E - 150°E)

The basins to the south of Australia are divided nearly in two by the Mid-Ocean Ridge, which separates the South Indian Basin to the south and the Australian Basin to the north (Figure 1.1). This is shown in the circulation patterns, with the bulk of the ACC passing to the south of the Mid-Ocean Ridge. Strong eddy activity is noted in the vicinity of the mid-ocean ridge as the ACC interacts with this topographical feature.

1. Area Temperature and Salinity (100 m)

a. Temperature

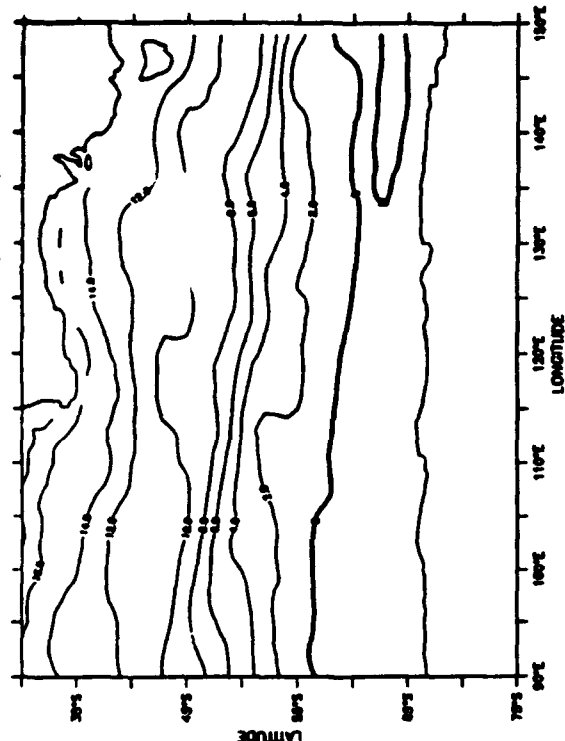
The area temperatures for the model and the solutions are in fairly good agreement (Figures 2.26 a, b and c). The 0° C isotherm of the models is much closer to Antarctica than the observations, the 2° C isotherm is also located much farther to the south than in the models. The observations indicate that the 2° C isotherm in the western portion of the region appears to follow the southern boundary of the Mid-Ocean Ridge, then dropping southward in the vicinity of the Antarctic Discordance (a break in the mid-ocean ridge) near 118°E. The 10°C isotherm seems also to be affected as some of the cooler water moves northward through the Antarctic Discordance. This mixing, shown in the observations, is barely hinted at in the model solutions. The remainder of the area temperatures appear to be in relatively good agreement.

b. Salinity

The regional salinity charts (Figures 2.27 a, b, and c) are in good agreement to the north but the salinity minimum associated with the AAIW is more saline in the model than in the observations (34.00 psu vs. 34.30 ppt). In the half degree model solution the extent of the salinity minimum is smaller, narrowing to just about two degrees of longitude between 140°E and 150°E. The salinity minimum in the observations, by

7.9.1

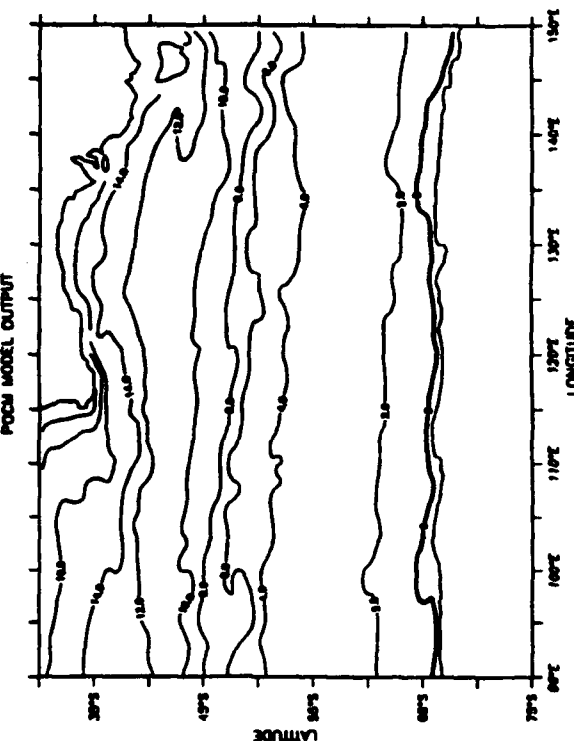
DEPTH : 100m Others southern ocean annual climatology (1st output)



TEMPERATURE (DEG C)

7.9.2

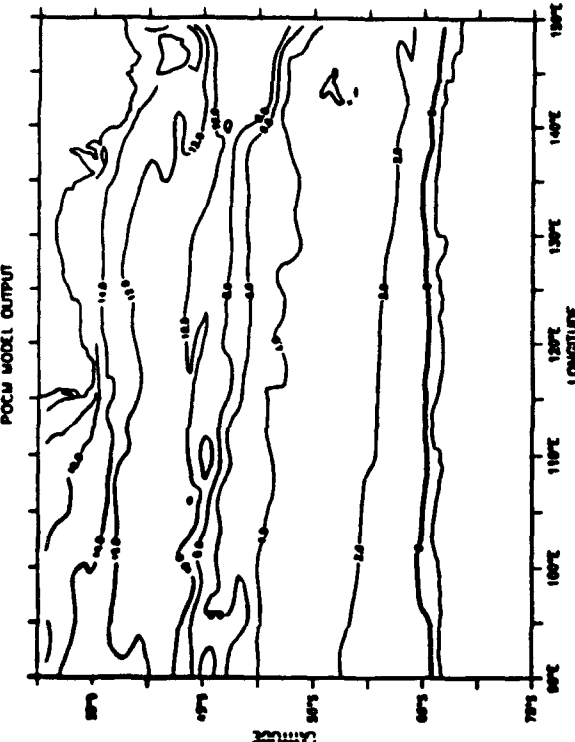
DEPTH : 87.5m TIME : 15-JAN-1988 05:00 DATA SET: gsea0030m



TEMPERATURE (DEG C)

7.9.3

DEPTH : 87.5m TIME : 15-JAN-1988 15:00 DATA SET: gsea0030m

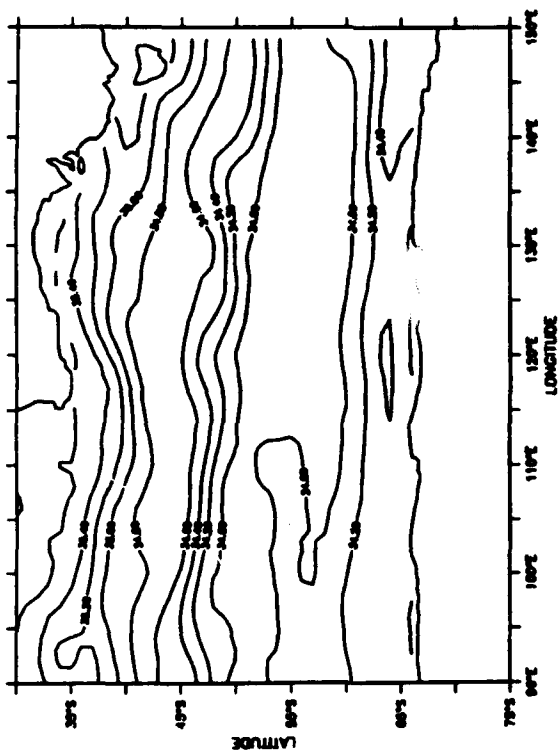


TEMPERATURE (DEG C)

Figure 2.26 100 m Temperature charts for area 90°E to 150°E
a.) Atlas Data b.) Half Degree Model Solution
c.) Quarter Degree Model Solution



DEPTH : 100m
Others south: an ocean annual climatology (1st degree)
DATA SET: others

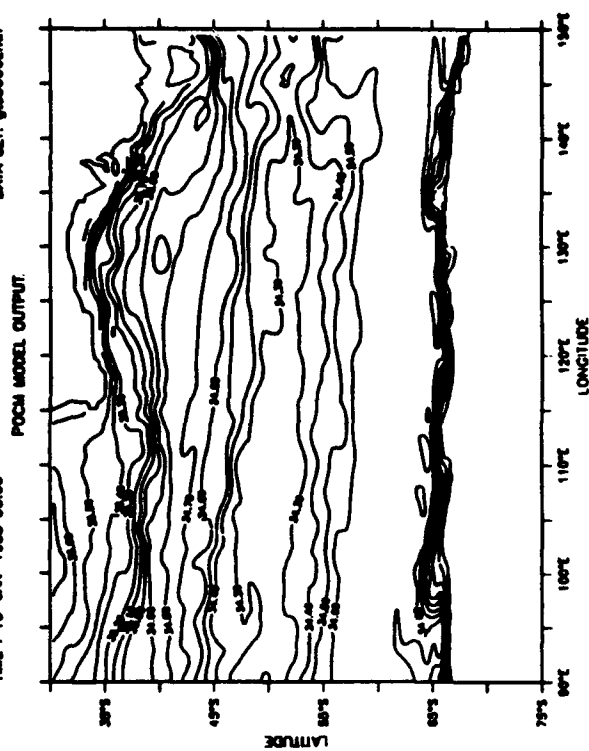


SALINITY (PSU)

65



DEPTH : 87.5m
TIME : 15-JAN-1980 05:00
DATA SET: gls0003mm

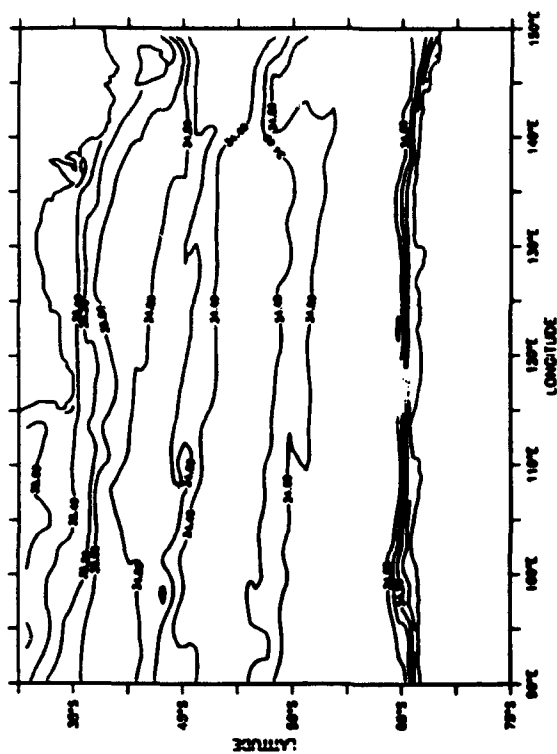


Salinity (PPT)



DEPTH : 87.5m
TIME : 14-JAN-1980 15:00
DATA SET: gls0003mm

POCM MODEL OUTPUT



SALINITY (PPT)

Figure 2.27 100 m Salinity Charts for area 90°E to 150°E
a.) Atlas Data b.) Half Degree Model Solution
c.) Quarter Degree Model Solution

contrast, is broader and in particular is about 5 degrees wide between 140°E and 150°E. The quarter degree model splits the difference between the observations and the half degree model, but places the minimum axis at 53°S vs. 55°S in the observations and the half degree model. Once north of the salinity minimum, the model solutions and the observations come into much closer agreement.

2. Vertical Sections

a. Temperature sections along 130°E

The temperature sections along 130°E (Figures 2.28 a, b and c) begin to display the modification of the AAIW that has taken place upstream. The 0° C isotherm is much smaller than in the previous sections along 60°E (Figure 2.19) in both the model solutions and the observations. The model solutions are still slightly weaker in displaying the penetration of the AAIW to the north but the quarter degree model shows some improvement in this area. The model solutions are in fairly good agreement with the observations but at about 500 m along 40°S the water is 2°C warmer than is indicated in the observations.

b. Salinity sections along 130°E

The salinity minimum representative of the AAIW is much more weakly represented in the models than in the observations (Figures 2.29 a, b and c) but definite minimum at approximately 1000 m is present. The 34.6 isohaline in the model and observations to the north is in very good agreement but the surface gradient south of 55°S is too extreme. This is a continuing problem of the salinity represented in the models being greater than the observations in the regions south of 55°S.

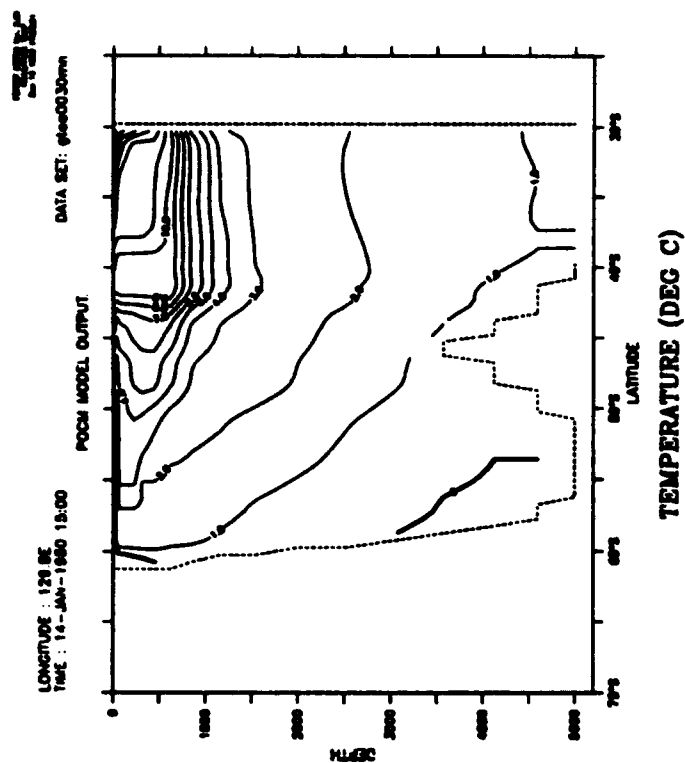
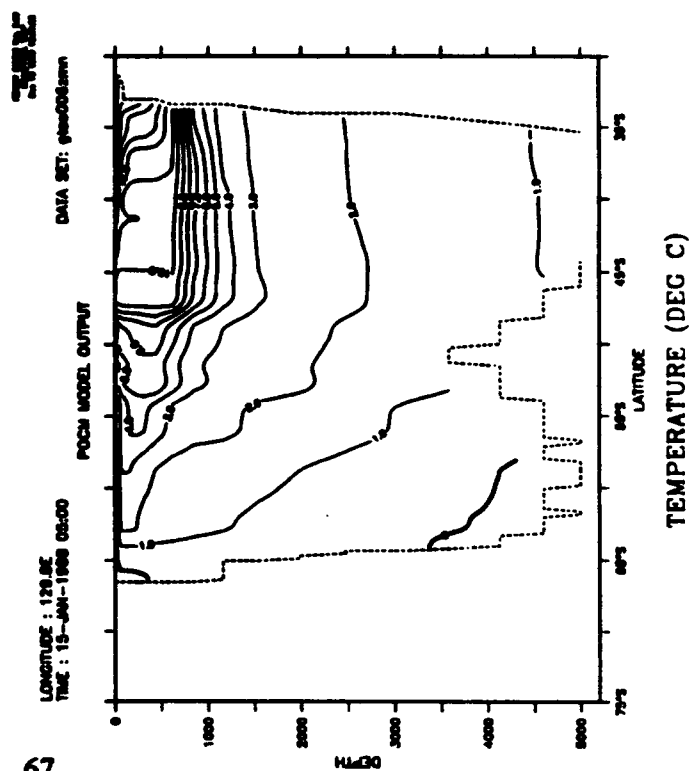
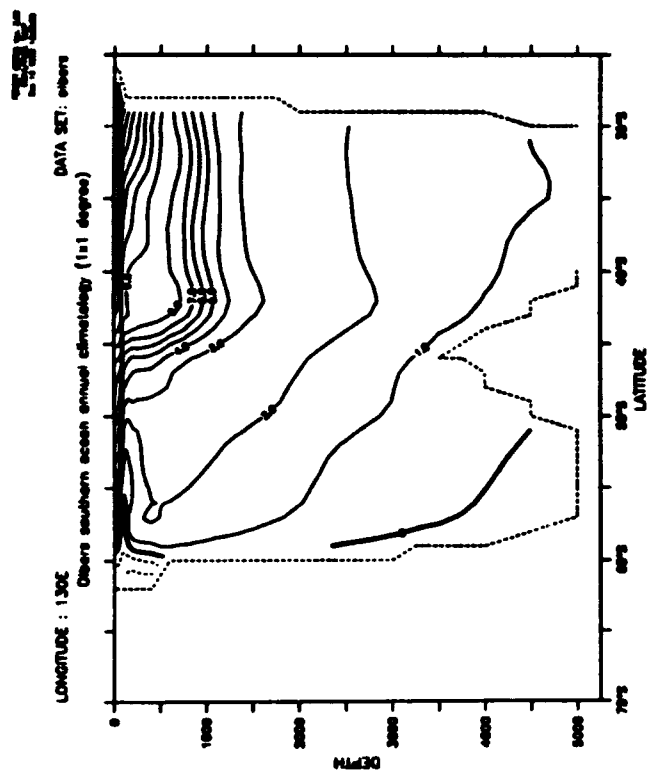


Figure 2.28 Vertical temperature sections along 130°E
a.) Atlas Data b.) Half Degree Model Solution
c.) Quarter Degree Model Solution

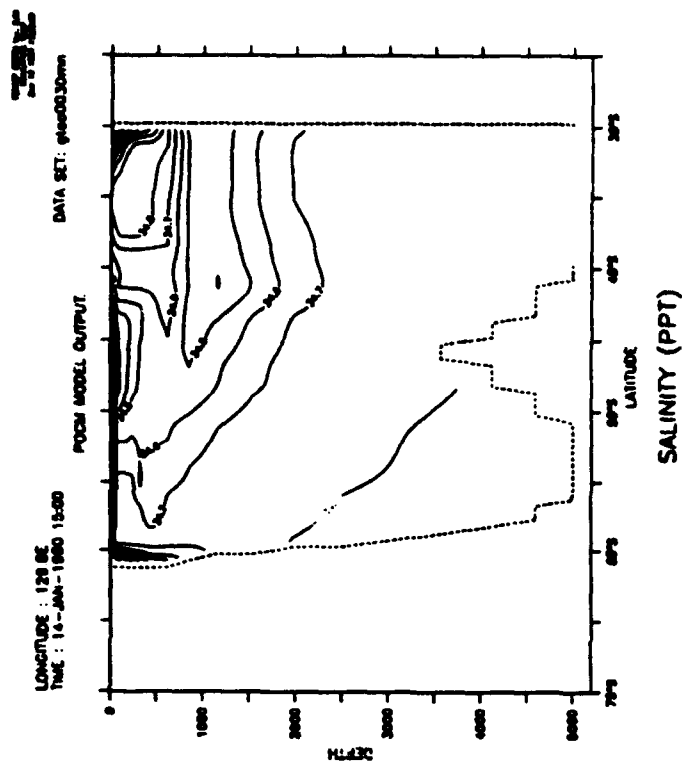
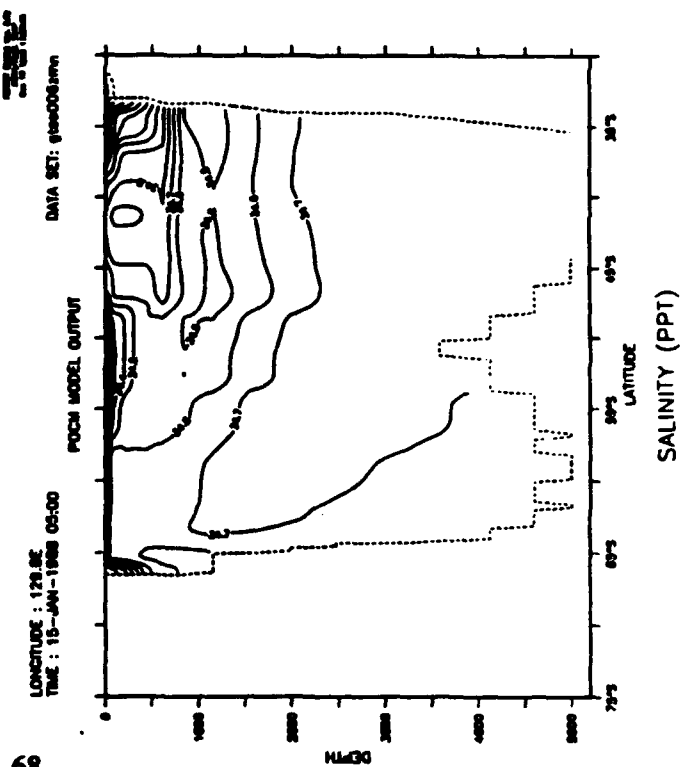
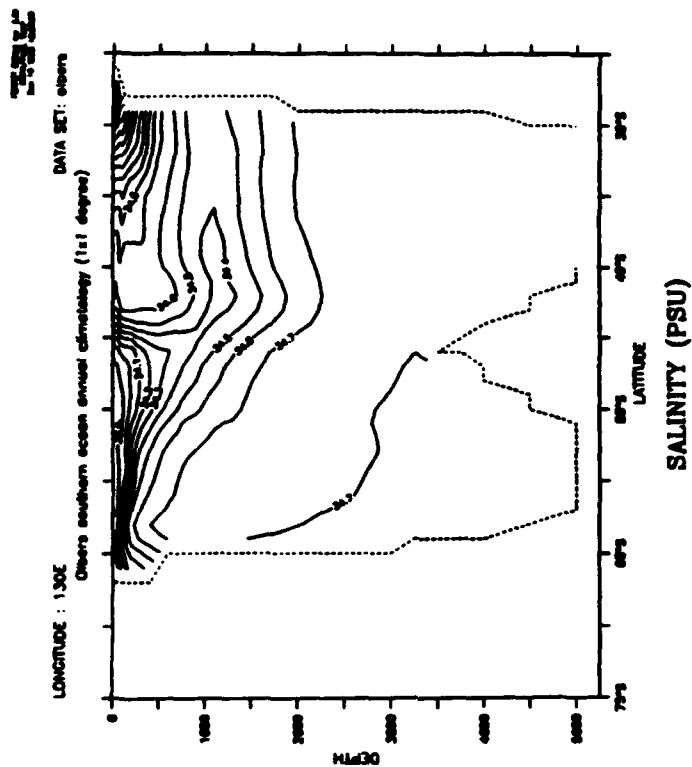


Figure 2.29 Vertical salinity sections along 130°E
a.) (as Data b.) Half Degree Model Solution
c.) Quarter Degree Model Solution

3. Circulation

a. Surface Circulation (37.5 m)

Eddy activity is closely related to the topography of the Mid-Ocean Ridge, even showing a substantial drop-off in the vicinity of the Antarctic Discordance in the half degree model and picking up again as the bathymetry becomes rough again. In the western part of the region the Polar Front, Subantarctic Front and the Subtropical Front are all easily discernible, but past the Antarctic Discordance the fronts seem to come together and are very difficult to separate.

The flow north of the ridge is much weaker as the easterly winds start to take effect north of 45°S. The poleward Leeuwin Current west of Australia is also well represented.

b. Deep Circulation (3500 m)

Eddy activity is much stronger in the quarter degree model than the half degree model especially to the south of the Mid-Ocean Ridge (Figures 2.31 a and b). The western boundary current is reversed along the northern slope of the ridge system, flowing to the southeast and assisting in the formation of two distinct eddies in the Australian Basin in the half degree model. The flow in the quarter degree model show similar eddies along the northern slope, but the flow is northward.

4. Potential Vorticity

The half degree model solution has slightly higher values to the south which corresponds better to the observations. However, the quarter degree model is closer to the general trend of the observations showing a region of lower potential vorticity between maxima to the north and south. The quarter degree model also shows higher values in vicinity of Tasmania than the observations.

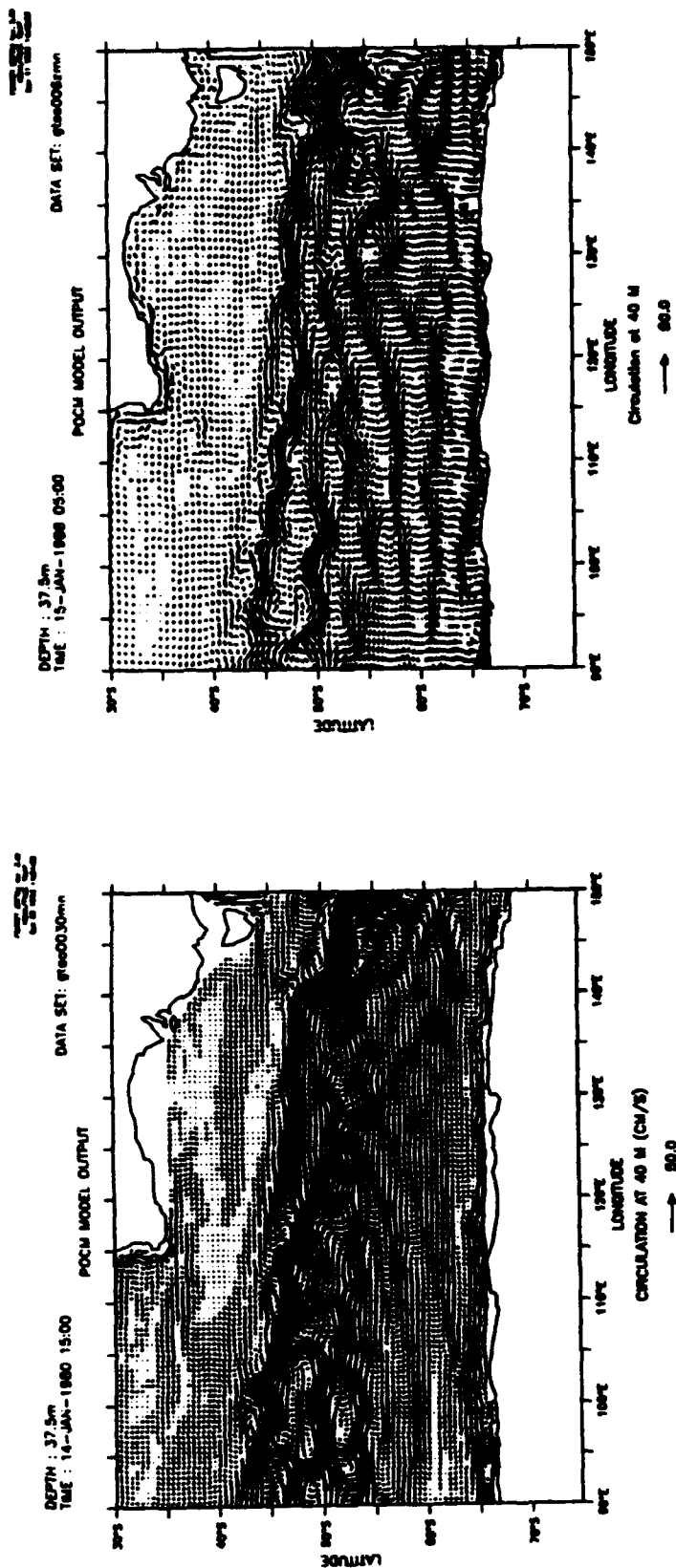


Figure 2.30 Surface Circulation for area 90°E to 150°E
a.) Half Degree Model Solution b.) Quarter Degree Model Solution

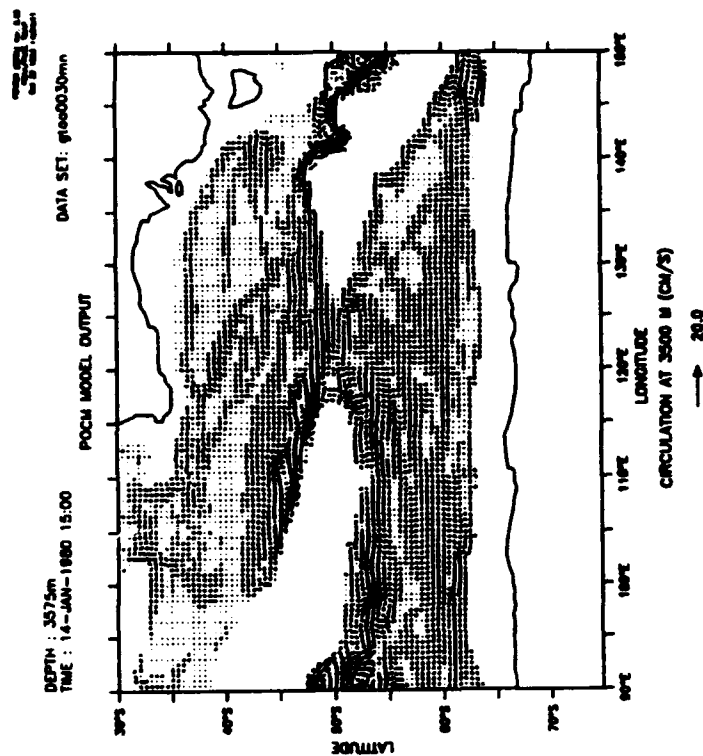
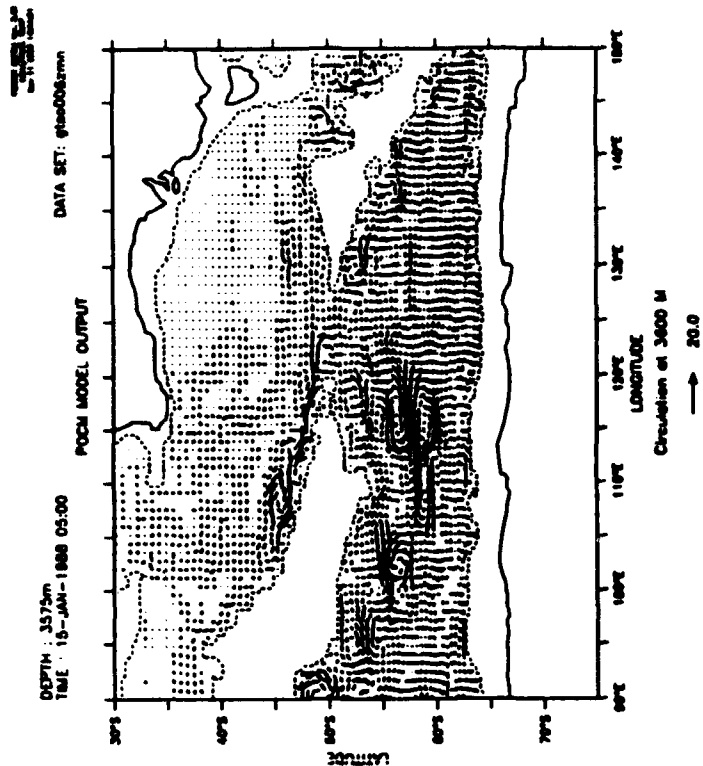
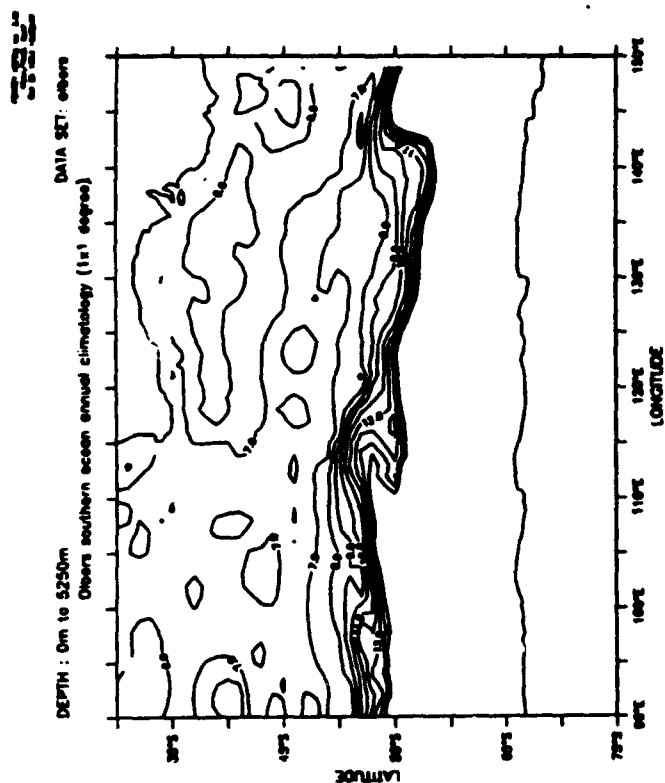


Figure 2.31 Deep Circulation for area 90°E to 150 °E
a.) Half Degree Model Solution b.) Quarter Degree Model Solution



72

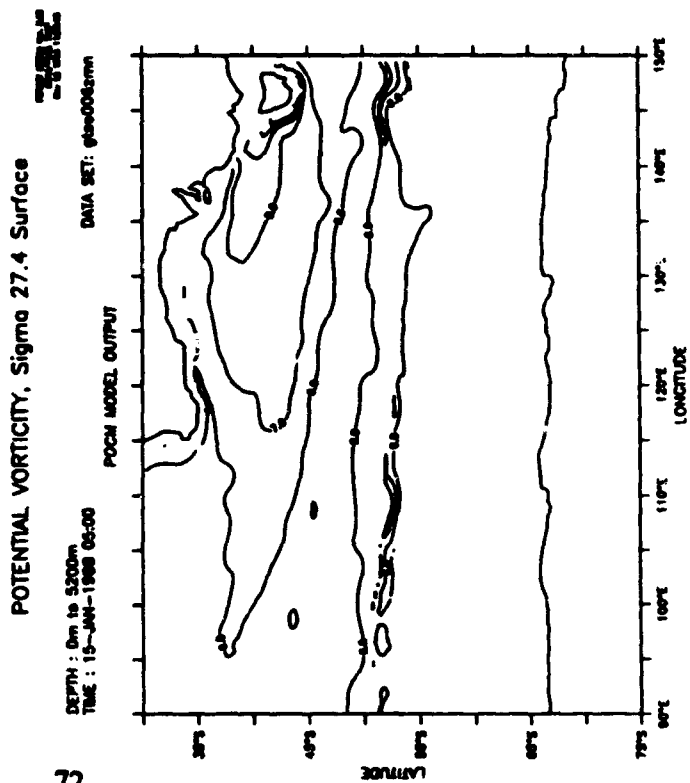


Figure 2.32 Potential Vorticity for area 90°E to 150°E
a.) Atlas Data b.) Half Degree Model Solution
c.) Quarter Degree Model Solution

E. MACQUARIE RIDGE/ROSS SEA (150°E - 150°W)

The Macquarie Ridge juts out from the Mid-Ocean Ridge system towards the Tasman Basin. The Macquarie Ridge system is rich in eddy activity as the barotropic flow is forced against the ridge system and the varying topography spawns eddies. The Ross Sea south of the Mid-Ocean Ridge is a secondary site for the production of Antarctic Bottom Water but is less dense due to its warmer, saltier water than the Weddell Sea produced AABW.

1. Area Temperature and Salinity (100 m)

a. Temperature

The temperature charts for this sector are in relatively good agreement (Figures 2.33 a, b and c). A discrepancy exists between the models and the observations on the placement of the 0° C isotherm but there is excellent agreement on positioning the subtropical temperatures to the north of New Zealand and the Campbell Plateau. Both the models and the observations show a northward meander of the ACC along 175°E. Some discrepancies occur between the models and the observations in the western portion of the area as the half degree model places the 10° C isotherm much farther to the north than the observations (42°S versus 47°S). The quarter degree model is slightly closer to the observations, placing this isotherm near 46°S.

b. Salinity

The salinity charts show good agreement (Figures 2.34 a , b and c). Both the models and the observations show the northward excursion of lower salinity water along 175°E. As has been present in previous areas discussed, a much stronger gradient is present along the coast in the models than in the observations and the models are more saline just

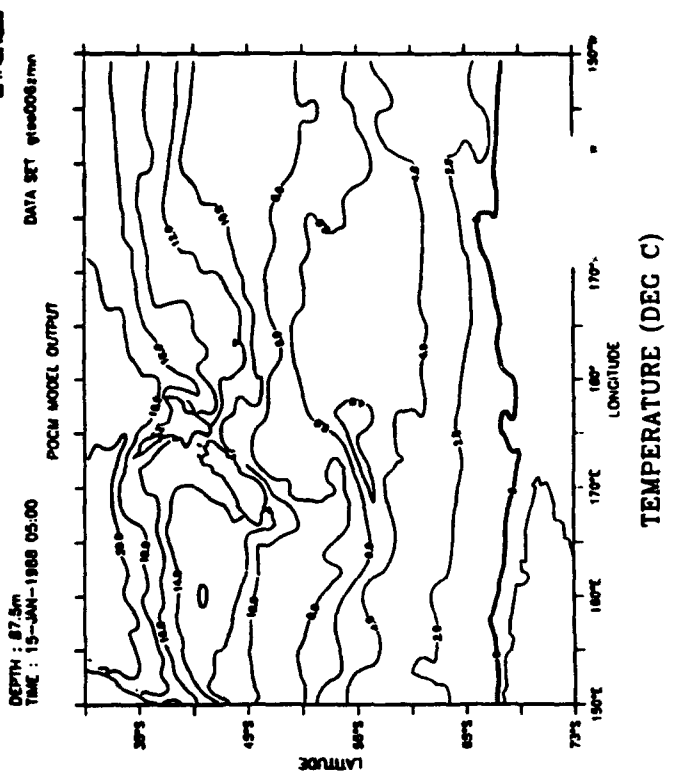
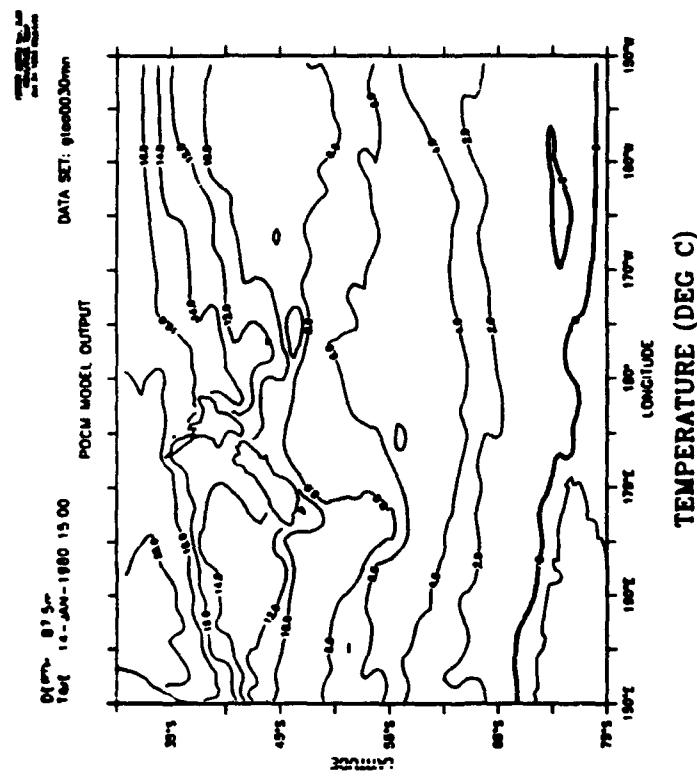
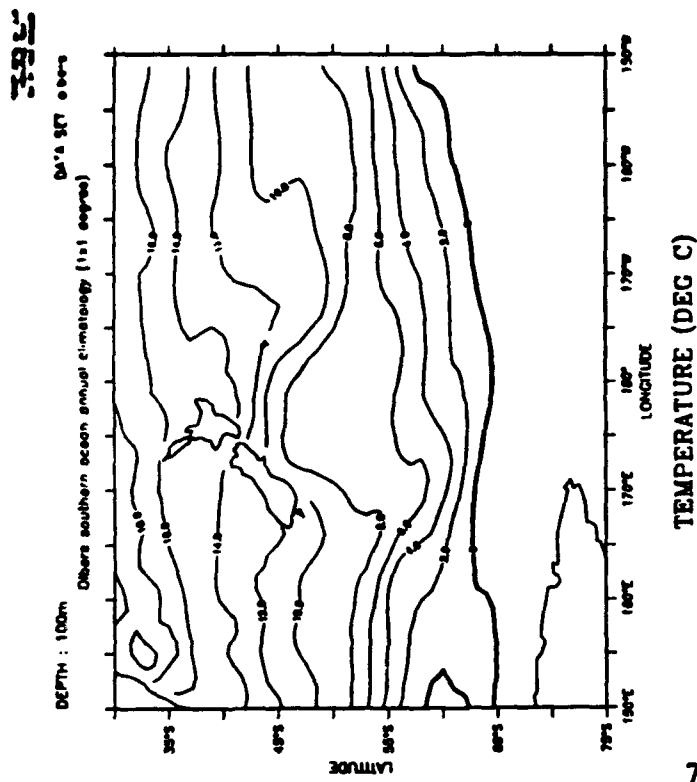
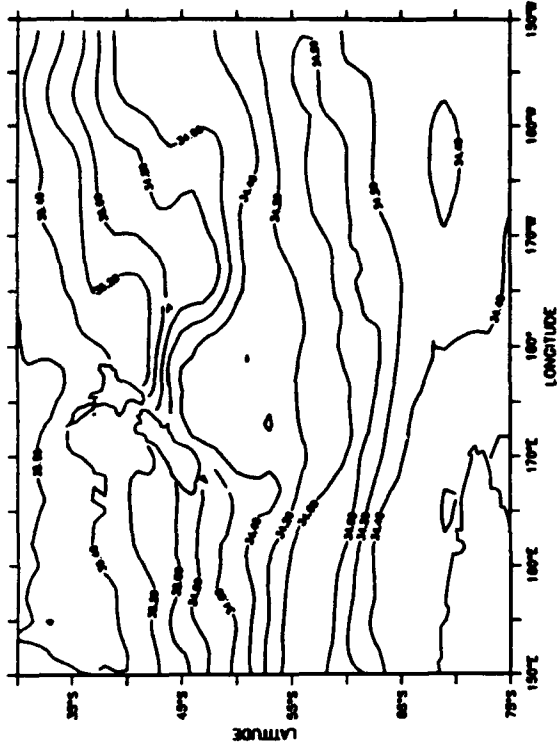


Figure 2.33 100 m Temperature charts for area 150°E to 150°W
a.) Atlas Data b.) Half Degree Model Solution
c.) Quarter Degree Model Solution

NOAA

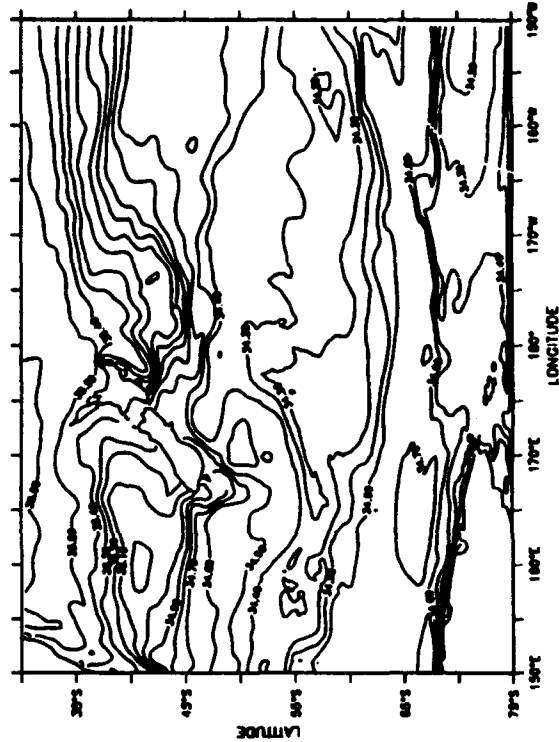
DEPTH : 100m
Obsers southern ocean annual climatology (1st degree)
DATA SET: g1ee001mm



SALINITY (PSU)

NOAA

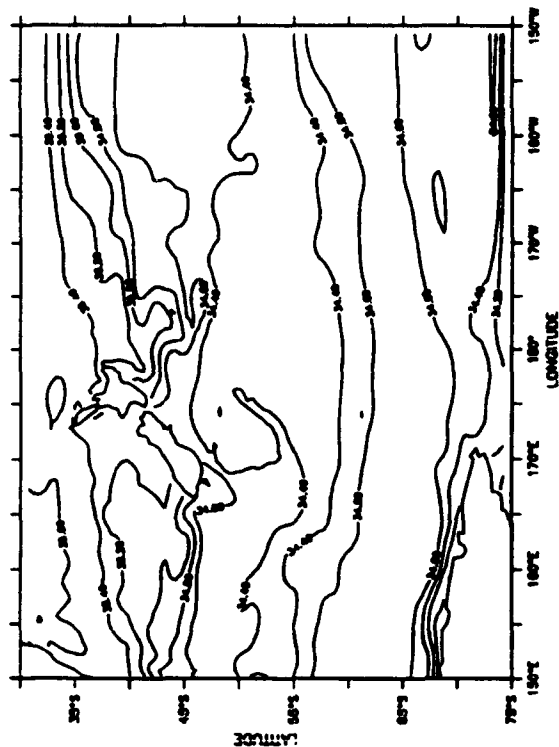
DEPTH : 87.5m
TIME : 15-JAN-1988 05:00
POCM MODEL OUTPUT
DATA SET: g1ee001mm



Salinity (PPT)

NOAA

DEPTH : 87.5m
TIME : 14-JAN-1988 19:00
POCM MODEL OUTPUT
DATA SET: g1ee0030mm



SALINITY (PPT)

Figure 2.34 100 m Salinity Charts for area 150°E to 150°W
a.) Atlas Data b.) Half Degree Model Solution
c.) Quarter Degree Model Solution

north of the coast of Antarctica (\pm 0.6 ppt in this case) along 60°S. The models and the observations become closer in agreement in the northern section of the region.

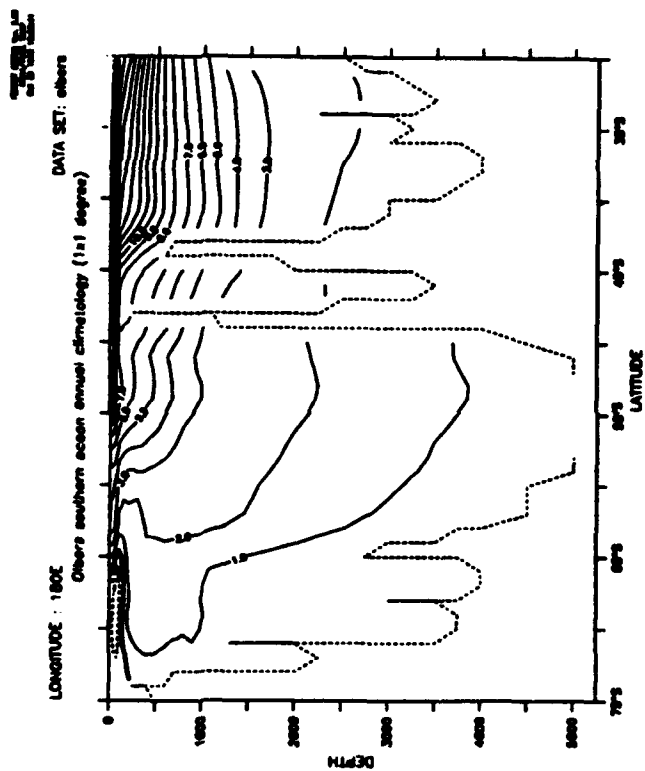
2. Vertical Sections

a. Temperature along 180°E

The vertical temperature section along 180°E extends from the Ross Sea , past the Chatham Plateau to the Southwest Pacific Basin. The sections in the models and the observations are in good agreement (Figures 2.35 a, b and c). All indicate a more northward extension of cooler water than the previous section, a consequence of the wind-driven Ekman transport by the northerly winds which flow off the Antarctic continent in this region (Figure 1.2). Temperatures in the lower depths are in excellent agreement . The upper waters show the continued weak representation of AAIW in the model solutions. The model solutions also depict two cold water eddies above the two peaks temperature peaks near 45°S.

b. Salinity section along 180E

The salinity sections (Figures 2.36 a, b and c) are also in excellent agreement and the representation of the salinity minimum associated with the AAIW is in closer agreement. The model salinities do not exceed that of the observations which is an improvement over previous sections. The salinity maximum in the southern regions (around 65°S) is over predicted in the model resulting in a gradient which is too tight in the upper 100 m. The quarter degree model, however, shows great improvement in this area. The observations also show a salinity minimum at depth which is absent in the half degree model solution but is present in the quarter degree model.



77

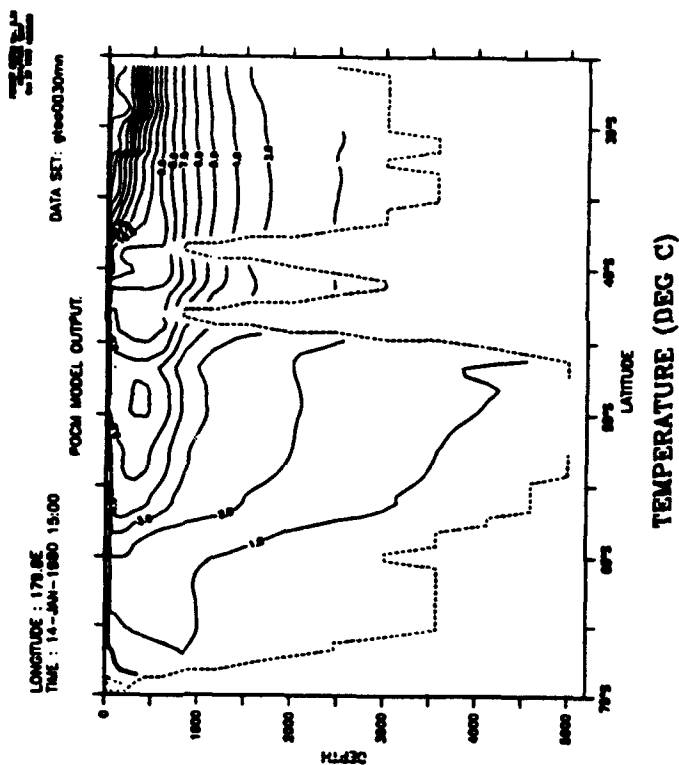
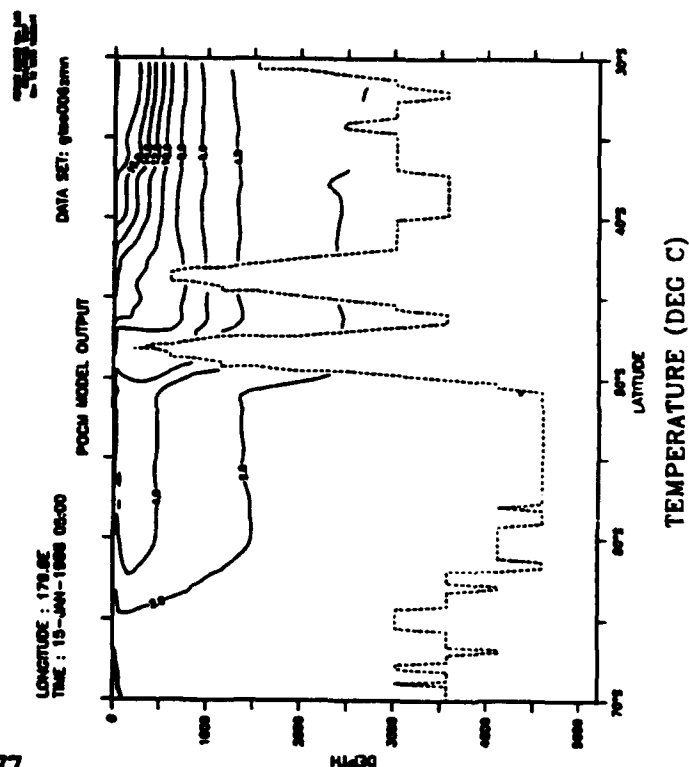
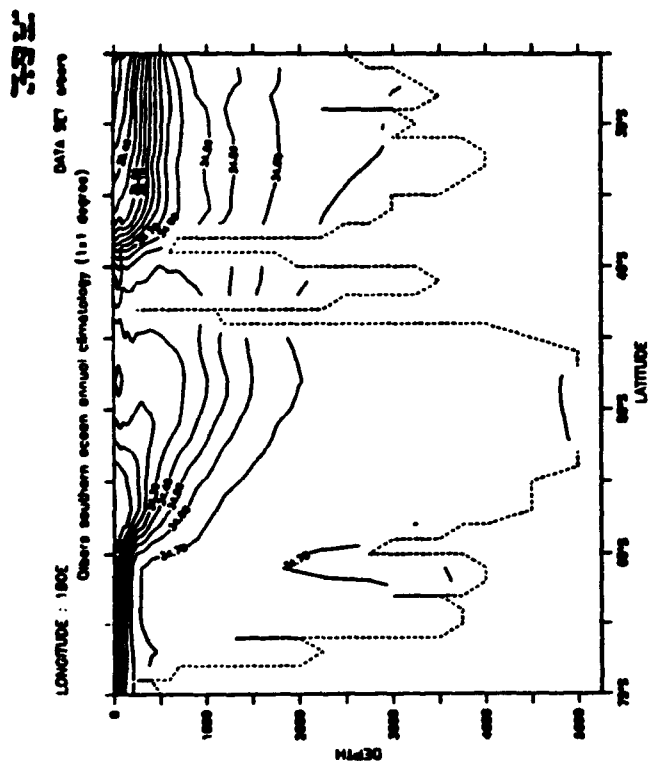
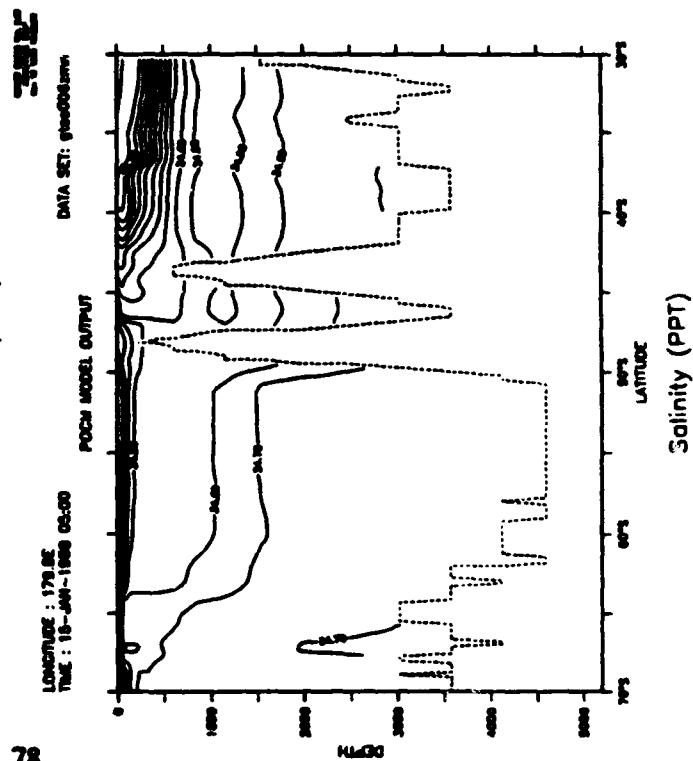


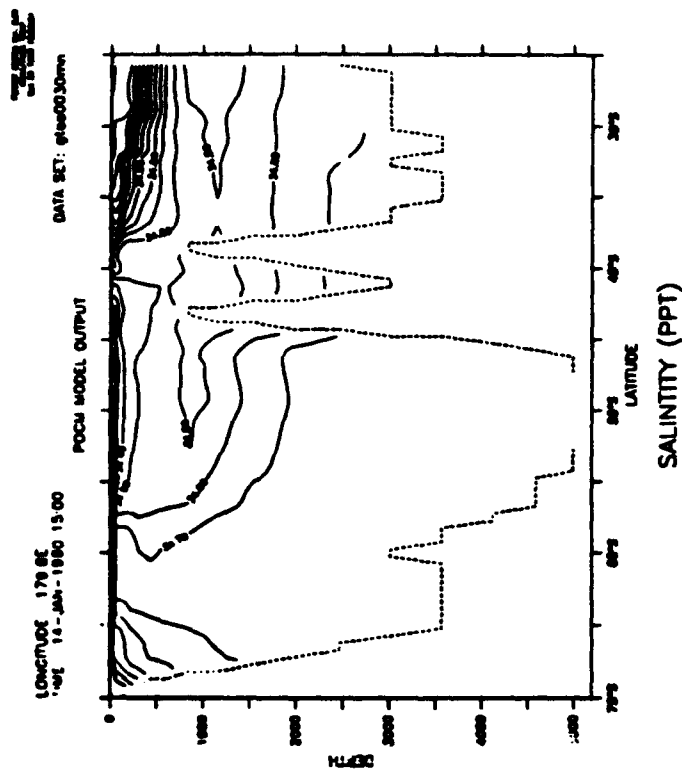
Figure 2.35 Vertical temperature sections along 180°E
a.) Atlas Data b.) Half Degree Model Solution
c.) Quarter Degree Model Solution



SALINITY (PSU)



SALINITY (PPT)



SALINITY (PPT)

Figure 2.36 Vertical salinity sections along 180°E
a.) Atlas Data b.) Half Degree Model Solution
c.) Quarter Degree Model Solution

3. Circulation

a. Surface (37.5 m)

The Subtropical, Subantarctic and the Polar Fronts, which had all begun to merge together at the western edge of the previous region now begin to diverge in this section (Figures 2.37 a and b). The Subtropical Front moves north to 45°S. The Subantarctic Front takes a little longer to assert itself but becomes fairly evident along 55°S, 170°W. The Polar Front along 65°S is fairly continuous and strong throughout the region. The easterlies also cause a consistent westward flow in the vicinity of the Antarctic continent. The quarter degree model and the half degree model are fairly consistent with each other. There is a poleward flow along 180°E between 50°S and 65°S in the quarter degree model that is not present in the half degree model.

b. Deep Circulation (100 m)

Flow over the Macquarie Ridge and through the pass between the Mid-Ocean Ridge and the Campbell Plateau is chaotic and strong (Figures 2.38 a and b). The western boundary current strengthens as it rounds the Campbell Plateau and continues in a northerly direction along the Chatham Plateau into the Southwest Pacific Basin. The western boundary current is also evident south of the Mid-Ocean Ridge in the Southeastern Pacific Basin.

4. Potential Vorticity

The quarter degree model shows excellent agreement with the observations (Figures 2.39 a,b and c). Downstream from the Campbell Plateau both show a narrow band of higher potential vorticity. The levels to the south are, as usual, lower than those in the observations but overall, the contours are in excellent agreement.

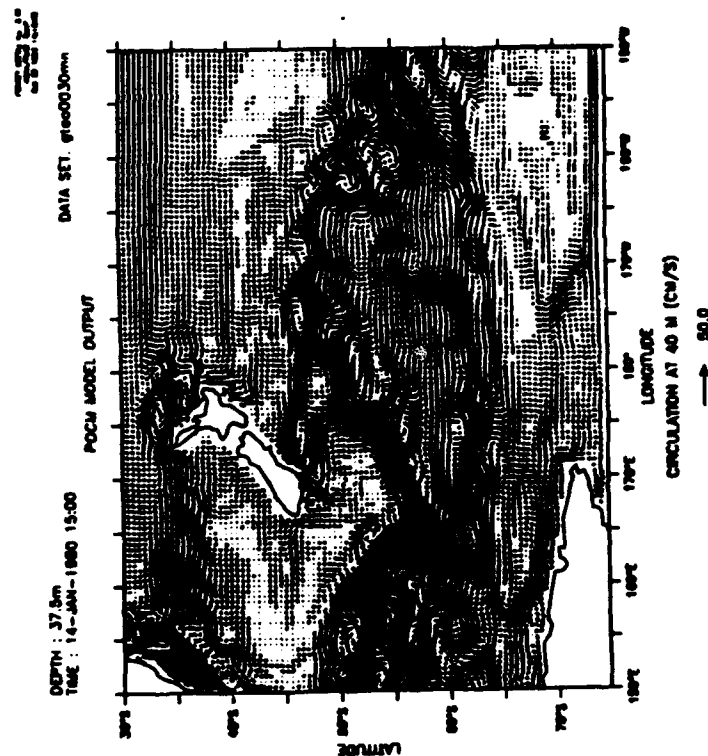
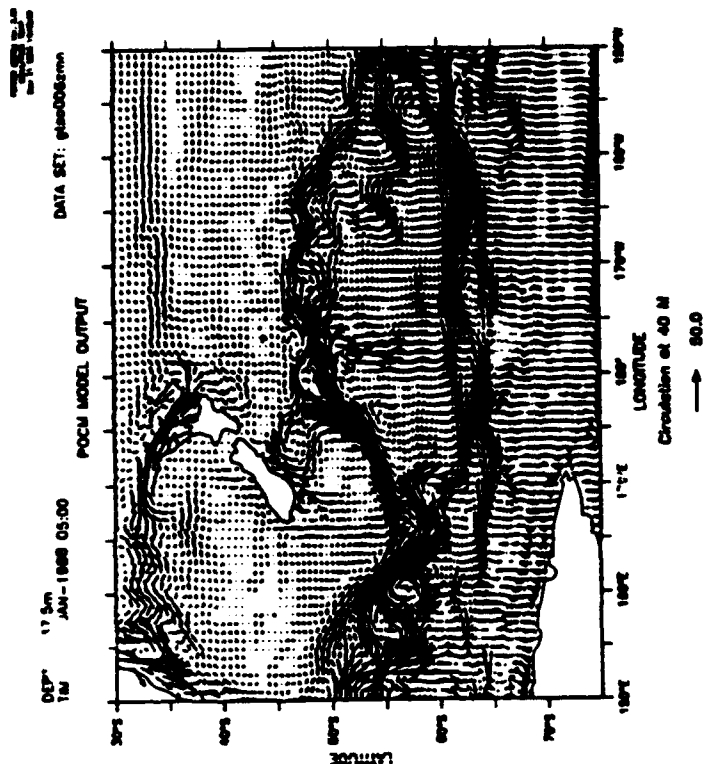


Figure 2.37 Surface Circulation for area 150°E to 150°W
a.) Half Degree Model Solution b.) Quarter Degree Model Solution

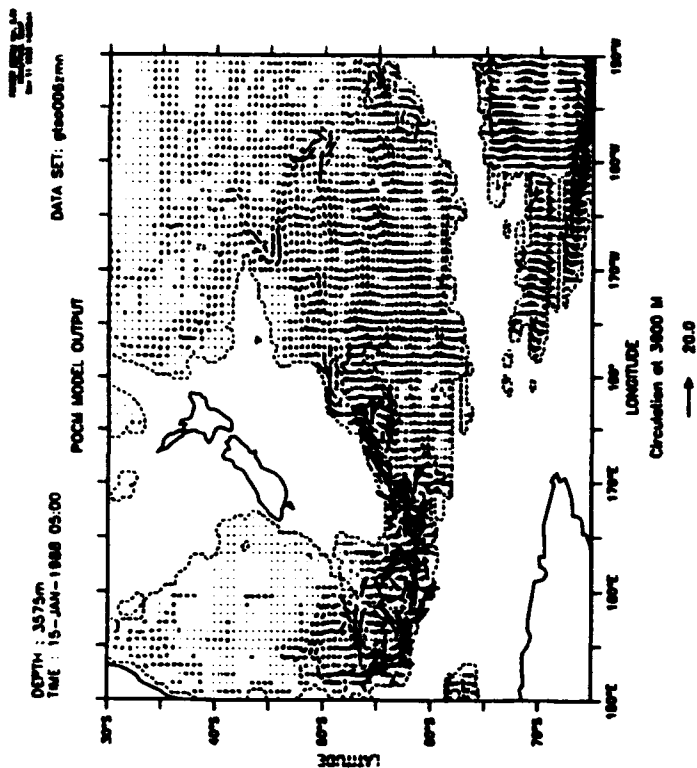
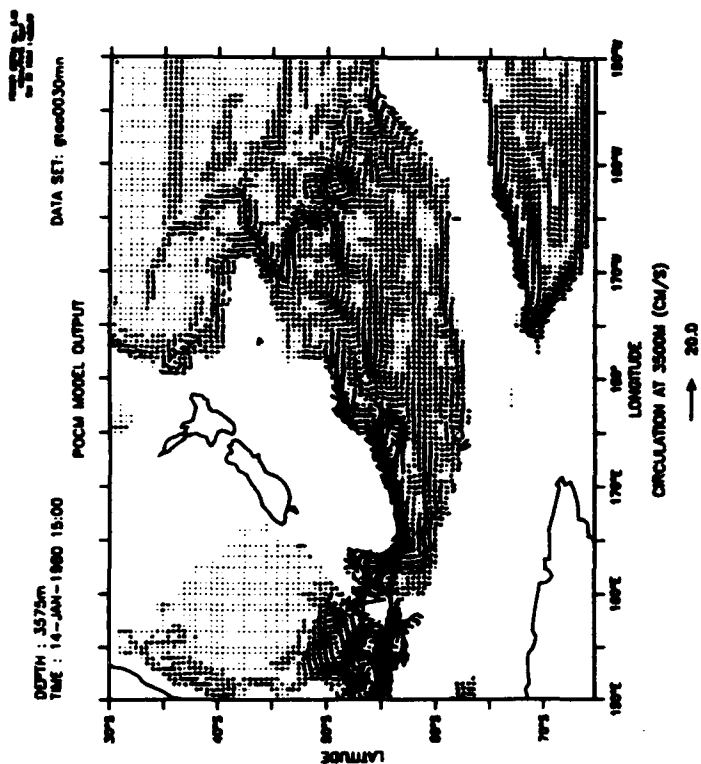
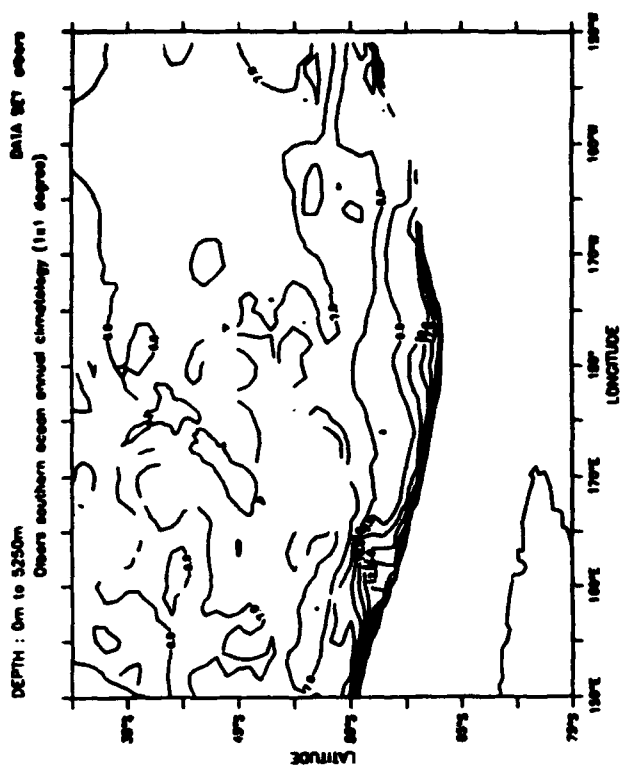


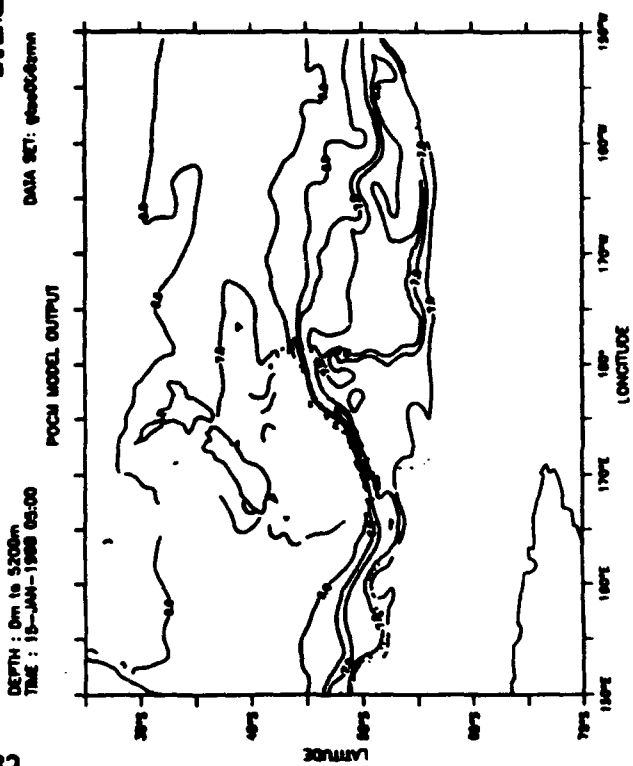
Figure 2.38 Deep Circulation for area 150°E to 150°W
 a.) Half Degree Model Solution b.) Quarter Degree Model Solution

7.3.3



82

7.3.4



7.3.5

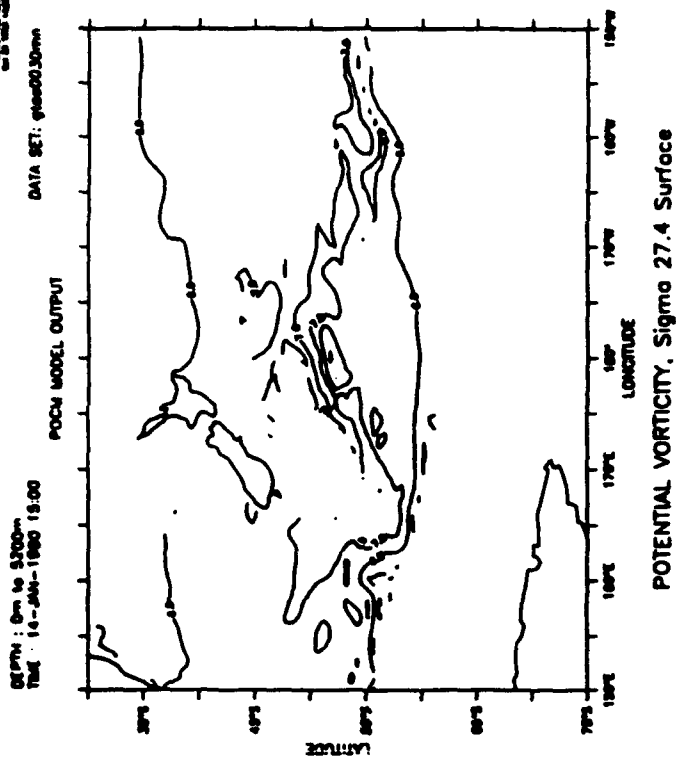


Figure 2.39 Potential Vorticity for area 150°E to 150°W
 a.) Atlas Data b.) Half Degree Model Solution
 c.) Quarter Degree Model Solution

F. CENTRAL PACIFIC (150°W - 90°W)

This is the region with the least topographic interaction; the Mid-Ocean Ridge takes a left turn along 110°W, leaving a relatively clear path for the ACC to flow through the Southeast Pacific Basin to the Drake Passage and the western coast of South America.

See Figure 1.1.

1. Area Temperature and Salinity Charts (100 m)

a. Temperature

The temperature pattern here becomes rather zonal north of 45°S (Figures 2.40 a, b, and c) and the models and the observations are in excellent agreement. The models again continue to place the 0° C isotherm closer to the continent (between 75°S and 70°S in the half degree model and along 70°S in the quarter degree model) while the observations place the 0° C isotherm between 65°S and 70°S. The half degree model also displays an interesting oscillation in the 6° C isotherm near 120°W which is suggested by the observations but is not as pronounced.

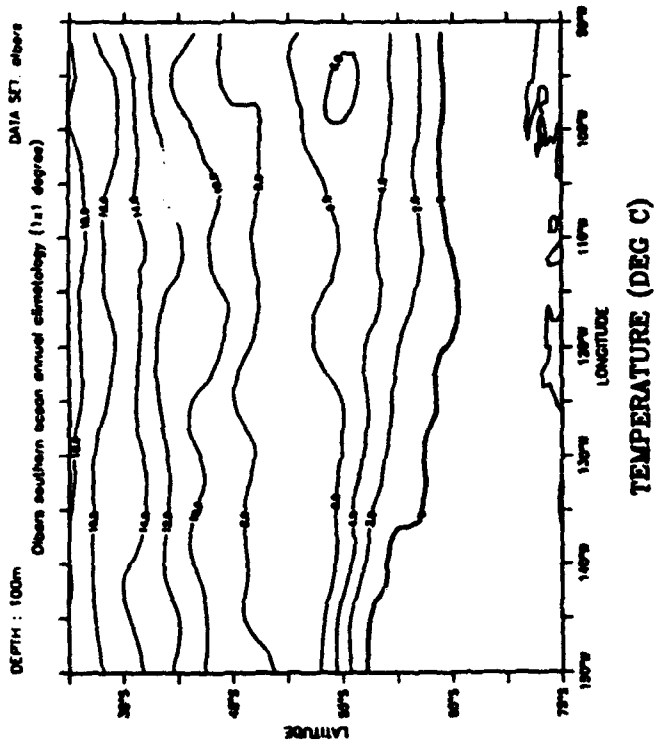
b. Salinity

The salinity minimum in the model and the observations broadens in this region to extend between 65°S and 35°S by the western boundary (Figures 2.41 a, b, and c). The gradient along the coast of Antarctica is much stronger than that represented in the observations.

2. Vertical Sections

a. Temperature along 120°W

The models and the observations are in good agreement in this region (see Figures 2.42 a, b and c). The observations show a deeper penetration of the 0°C isotherm; it is much weaker and shallower in the models. In contrast, a large cold tongue of water at 500 m above a deeper warmer layer near 50°S in the models is not



84

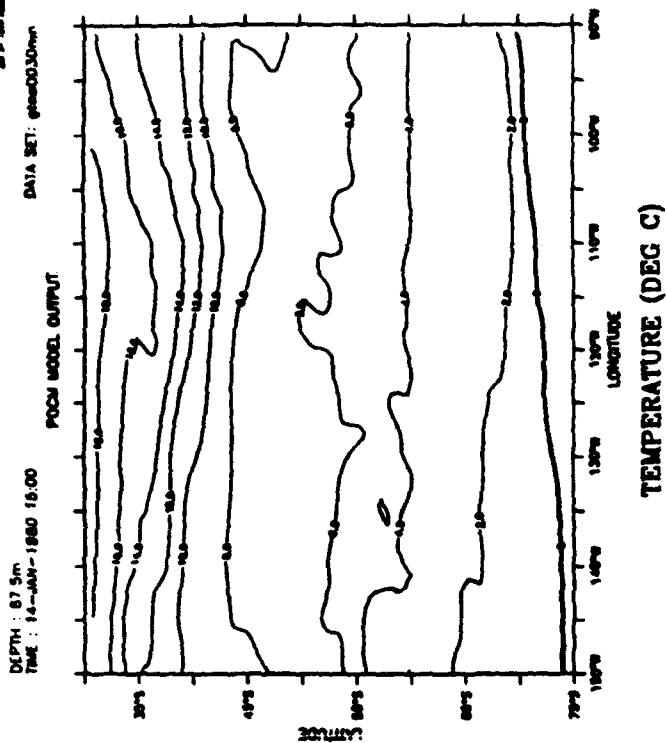
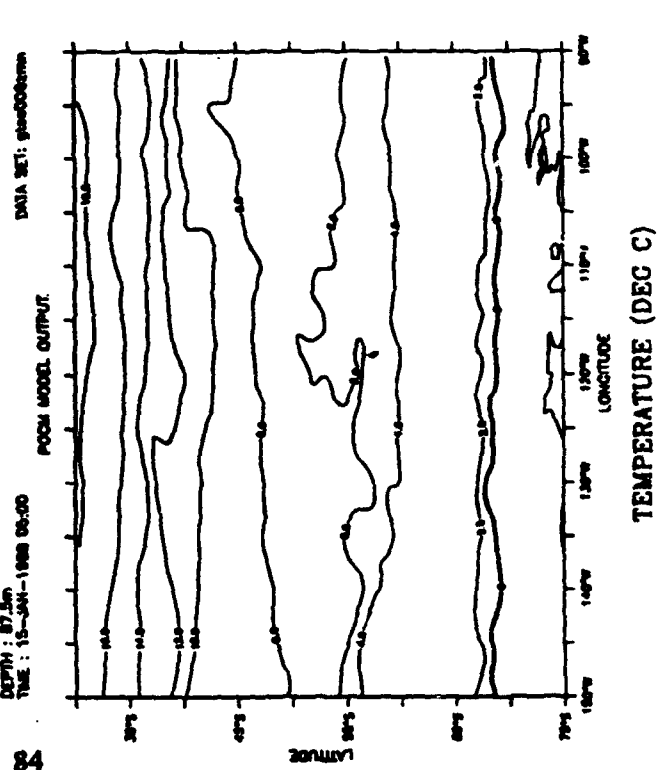
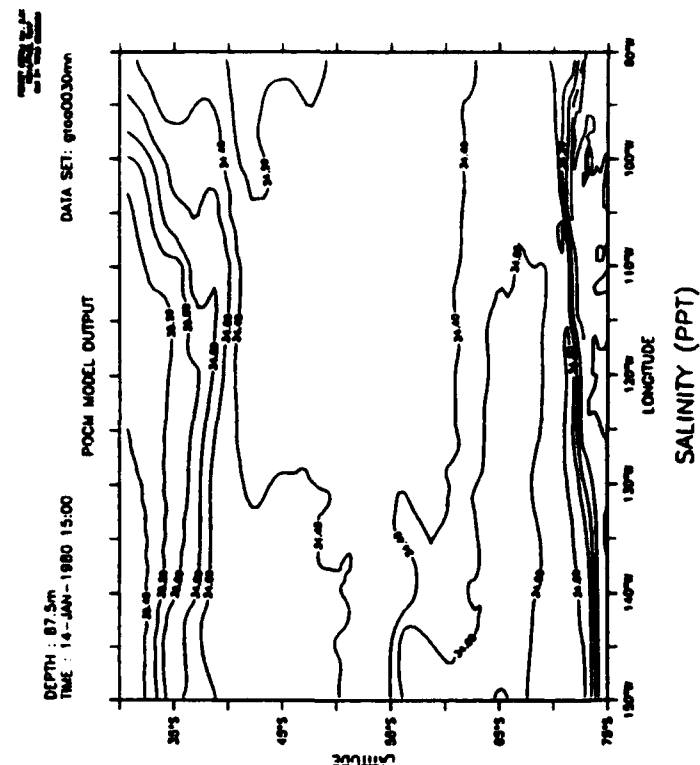
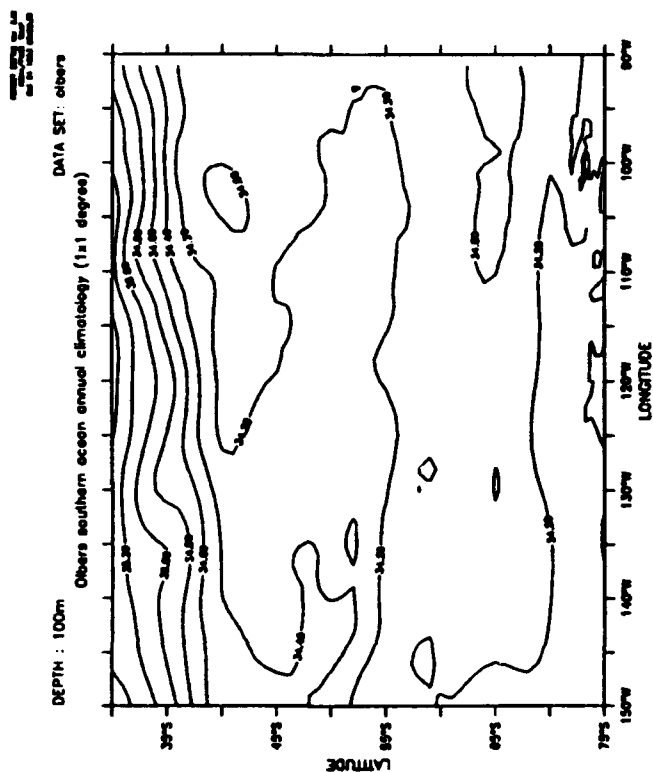


Figure 2.40 100 m Temperature charts for area 150°W to 90°W
a.) Atlas Data b.) Half Degree Model Solution
c.) Quarter Degree Model Solution



85

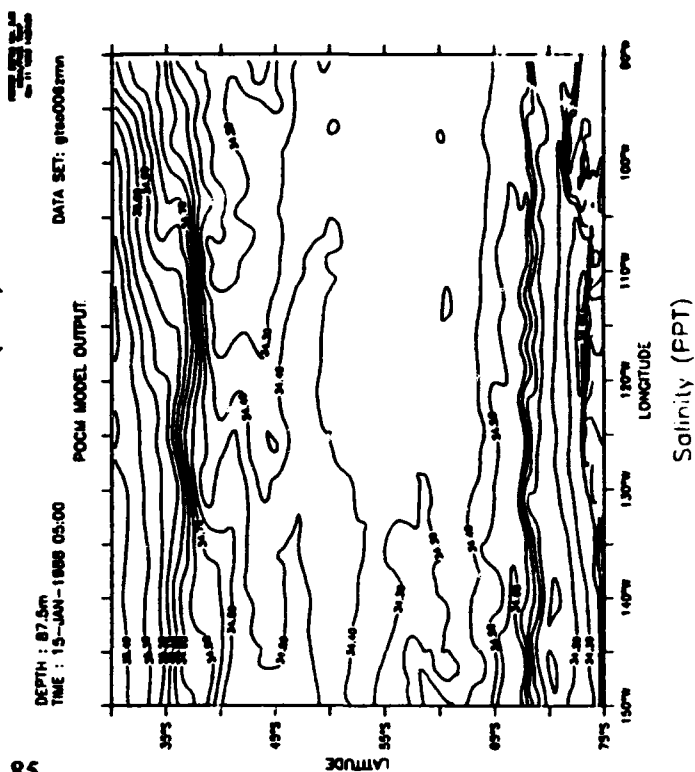
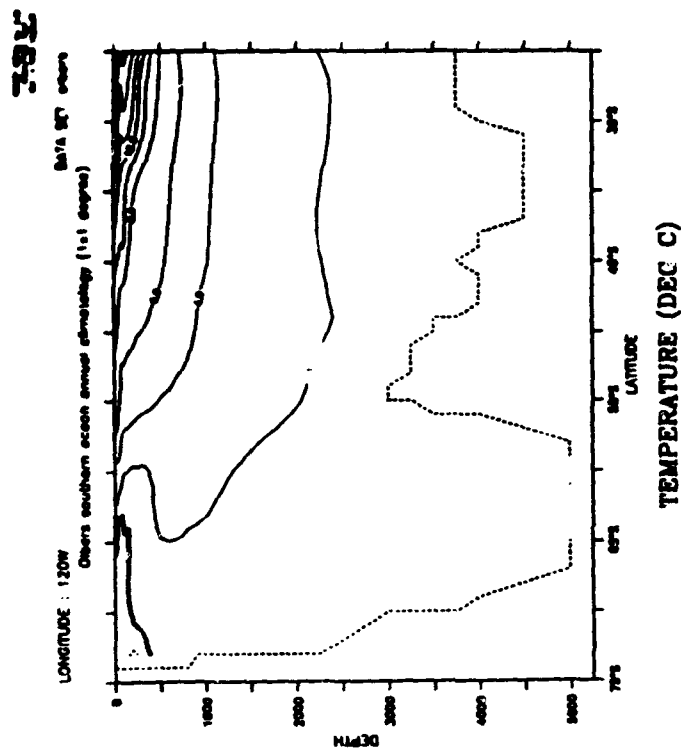


Figure 2.41 100 m Salinity Charts for area 150°W to 90°W
a.) Atlas Data b.) Half Degree Model Solution
c.) Quarter Degree Model Solution



86

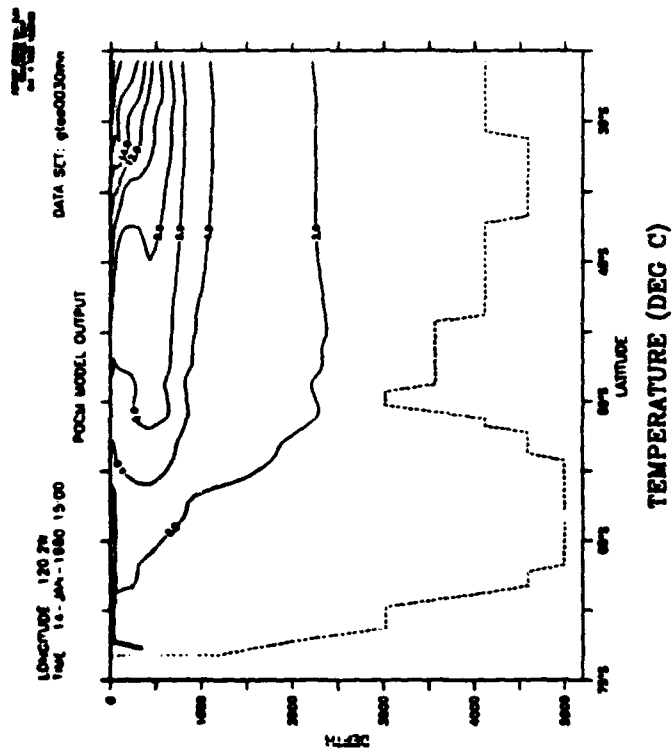
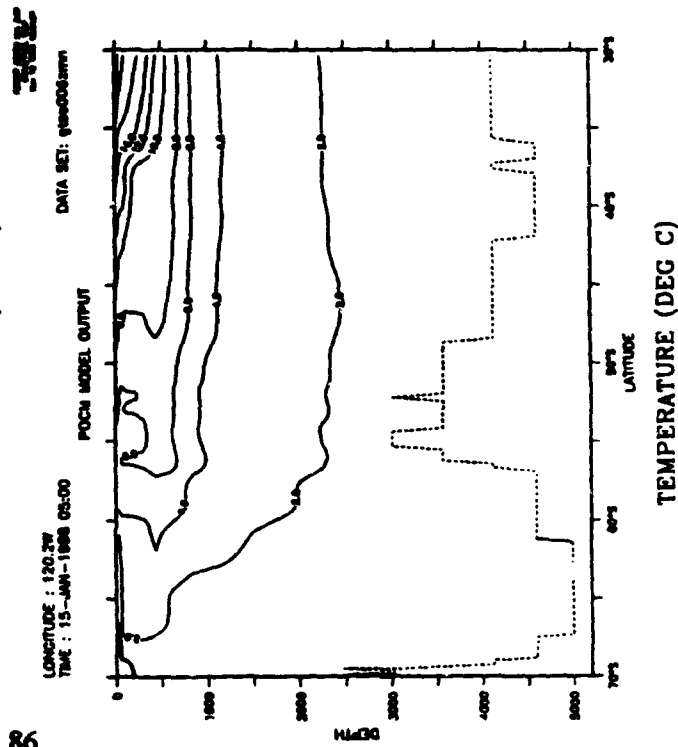


Figure 2.42 Vertical temperature sections along 120°W
a.) Atlas Data b.) Half Degree Model Solution
c.) Quarter Degree Model Solution

represented in the observations. This appears to be a feature brought about by the forcing of the half degree model to Levitus observations below 700 m on a three year time scale. The quarter degree model appears to be in the process of diminishing this feature so that given time, the quarter degree model would come closer to the observations.

b. Salinity Sections along 120°W

The models exhibit the continuing problem of too large a salinity maximum to the south resulting in the gradient in the first 200 m being too strong north of 63°S (Figures 2.43 a, b, and c). As in the last section, the quarter degree model shows marked improvement. The major difference in this section between the models and the observations is the slightly more saline pool of water to the north which extends to nearly 800 m in depth and southward to 50°S. The same water in the observations reaches only to 600 m in depth and extends southward to 40°S.

3. Circulation

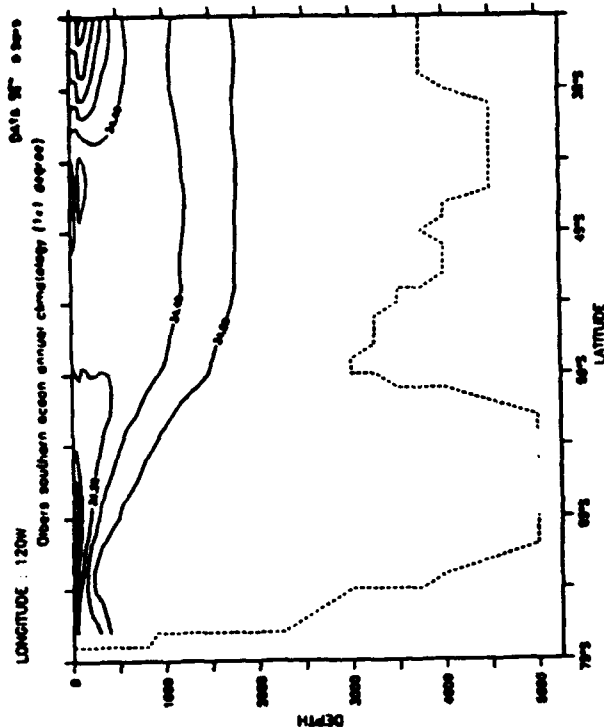
a. Surface Circulation (37.5 m)

The surface circulation is strong and with many eddies evident south of 50°S. At 120°W the number of eddies and the strength of the fronts drop fairly noticeably (Figures 2.44 a, and b). The flow north of 50°S is relatively slow moving and zonal. The flow of the quarter degree model is even slower than the half degree model. The westward flow due to the easterly winds close to the continent is also present in both models.

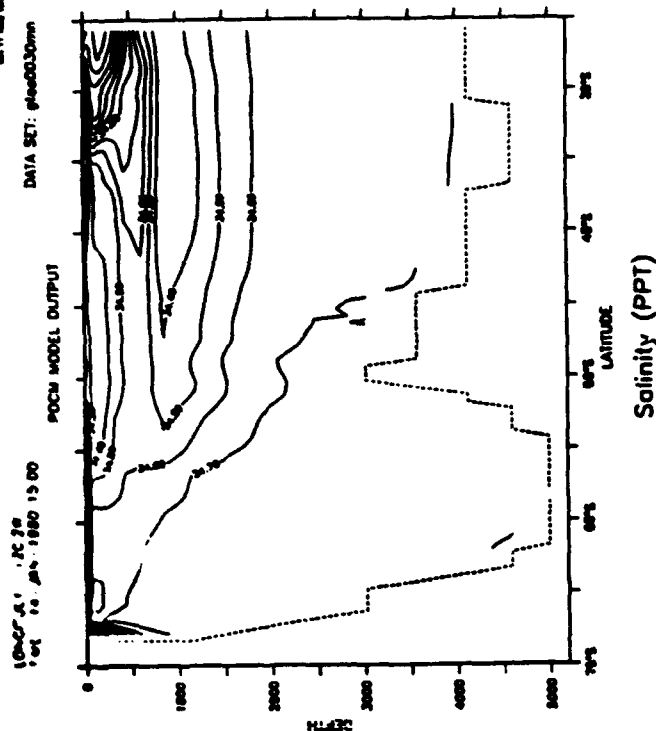
b. Deep Circulation (3500 m)

The zonal eastward flow in the Southeast Basin persists to the lower levels. The western boundary current along the Mid-Ocean Ridge is primarily southward, becoming northerly north of the Chile Ridge. The quarter degree model, as expected, has a higher

2.83



2.84



2.85

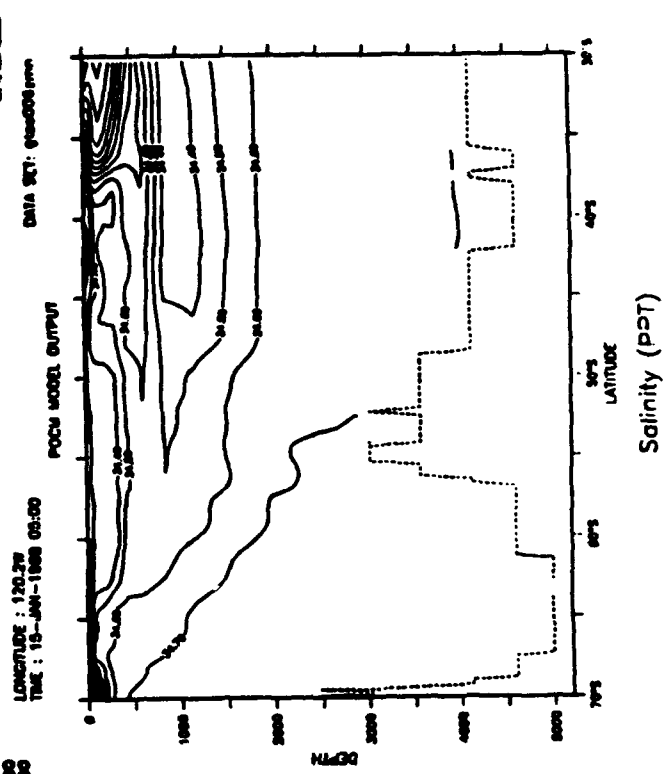


Figure 2.43 Vertical salinity sections along 120°W
a.) Atlas Data b.) Half Degree Model Solution
c.) Quarter Degree Model Solution

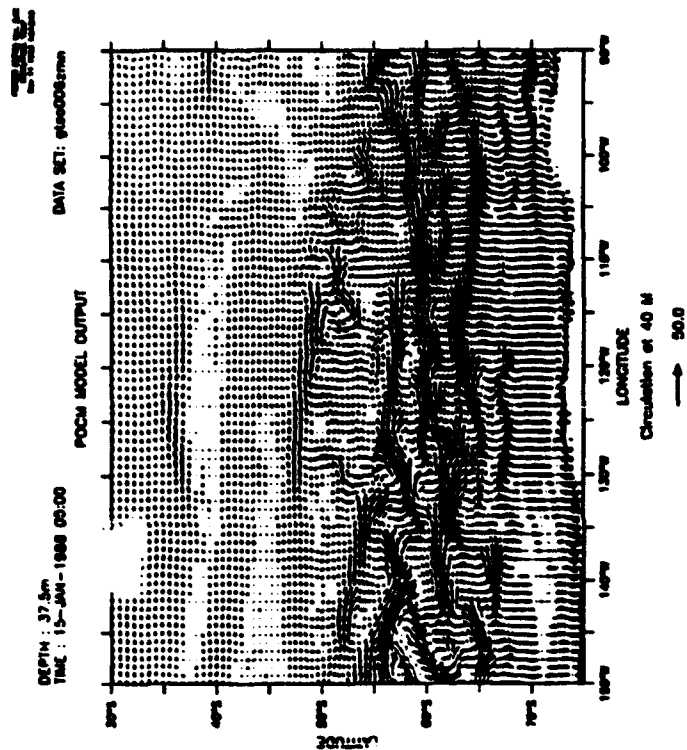
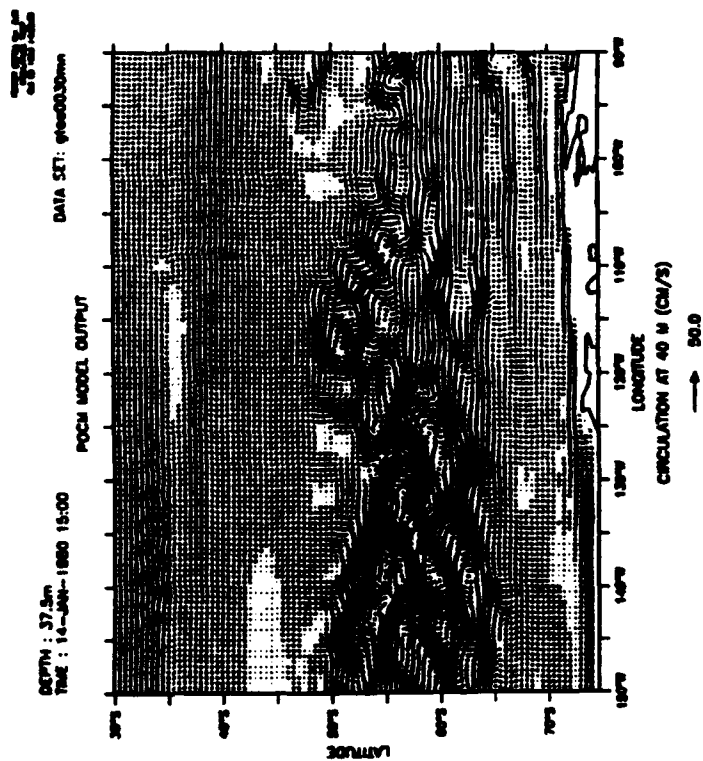


Figure 2.44 Surface Circulation for area 150°W to 90°W
a.) Half Degree Model Solution b.) Quarter Degree Model Solution

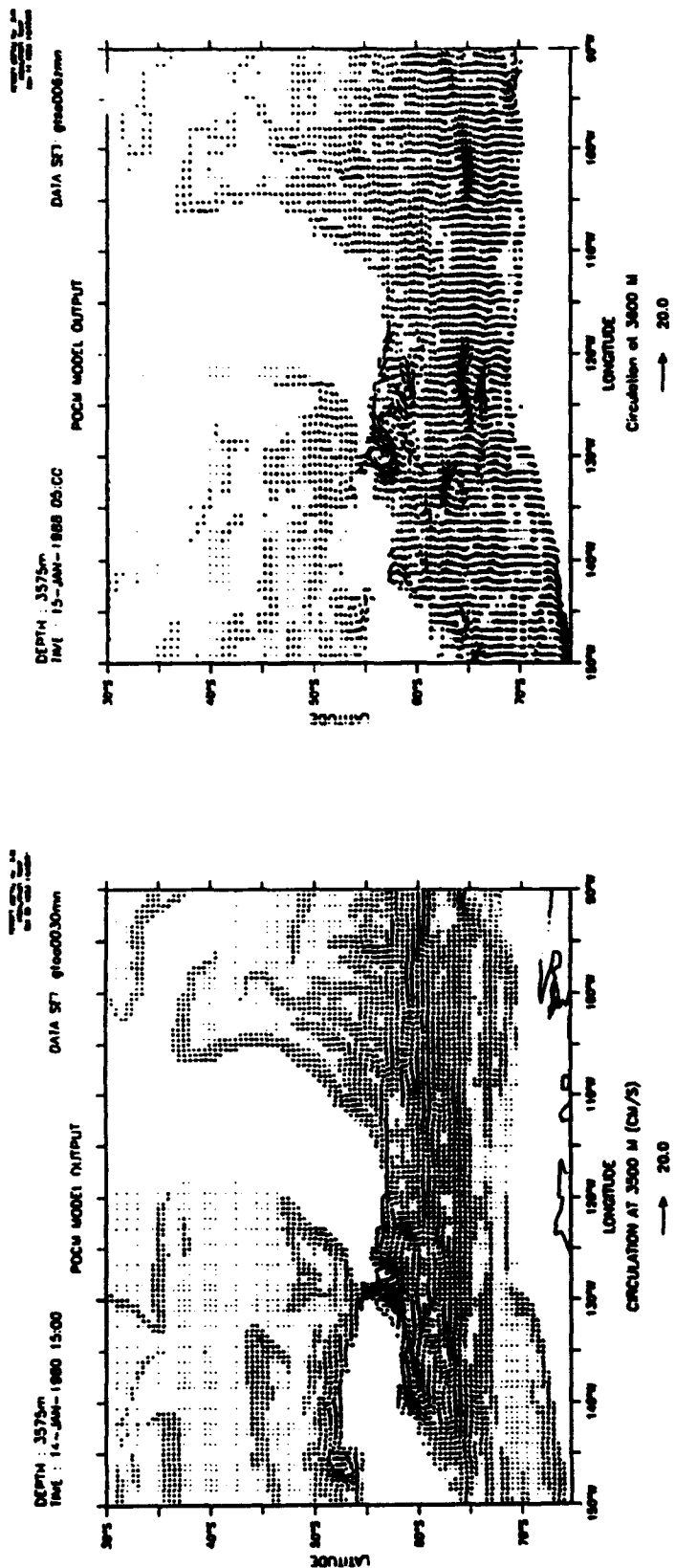


Figure 2.45 Deep Circulation for area 150°W to 90°W
a.) Half Degree Model Solution b.) Quarter Degree Model Solution

level of eddy activity over all and both models show a broad diffuse flow in the Southwest Pacific Basin, north of the mid-ocean ridge.

4. Potential Vorticity

The potential vorticity levels in the observations are much higher and complex than those in the models. Neither model shows the larger values shown in the center of the basin, and as usual, the values to the south around the Antarctic continent are much weaker .

This is one of the more data sparse regions of the ACC so the observational values of potential vorticity may or may not be correct.

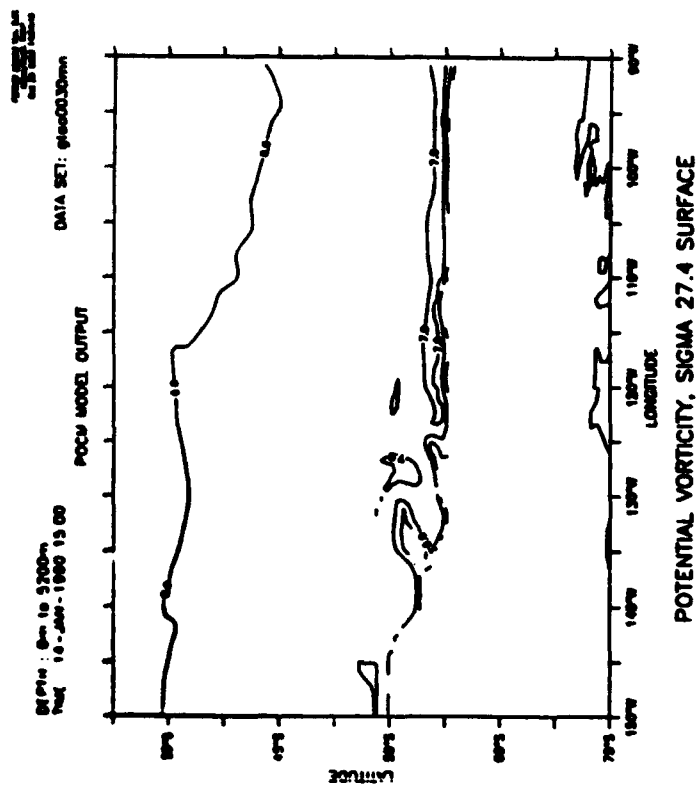
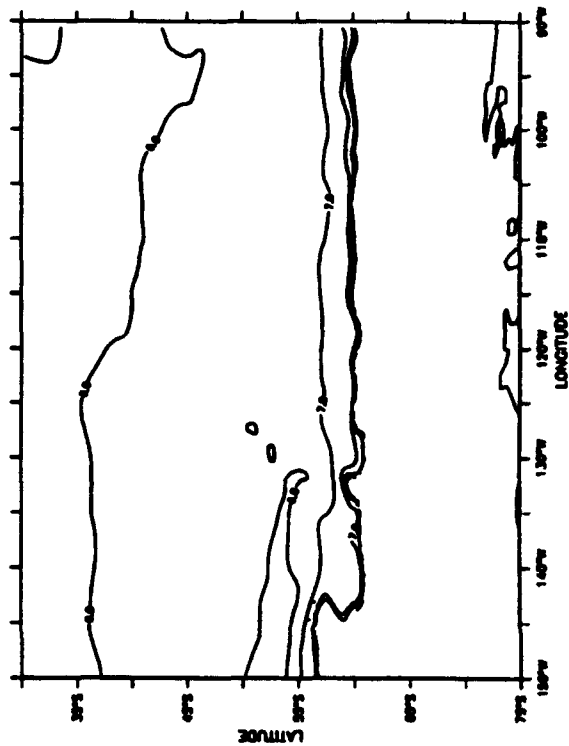
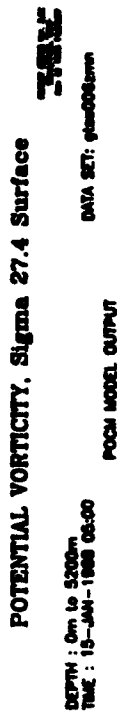
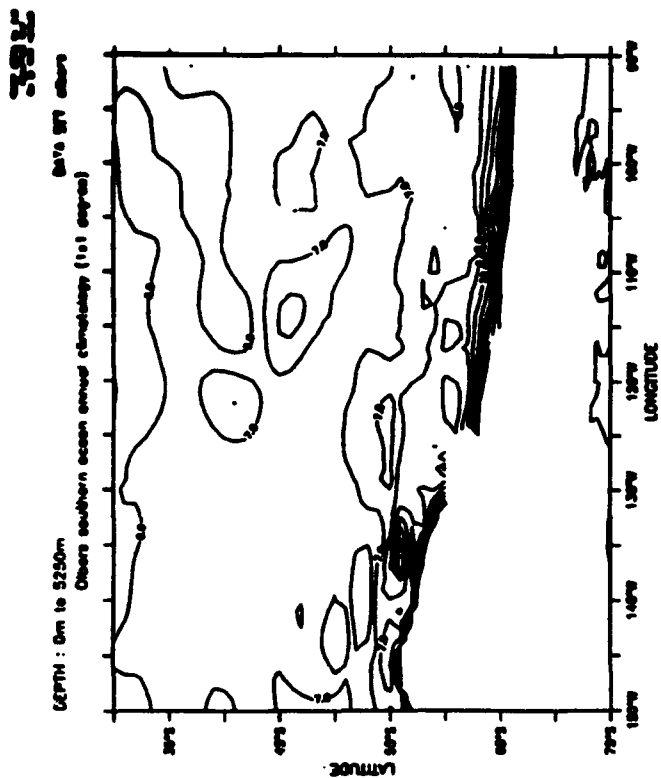


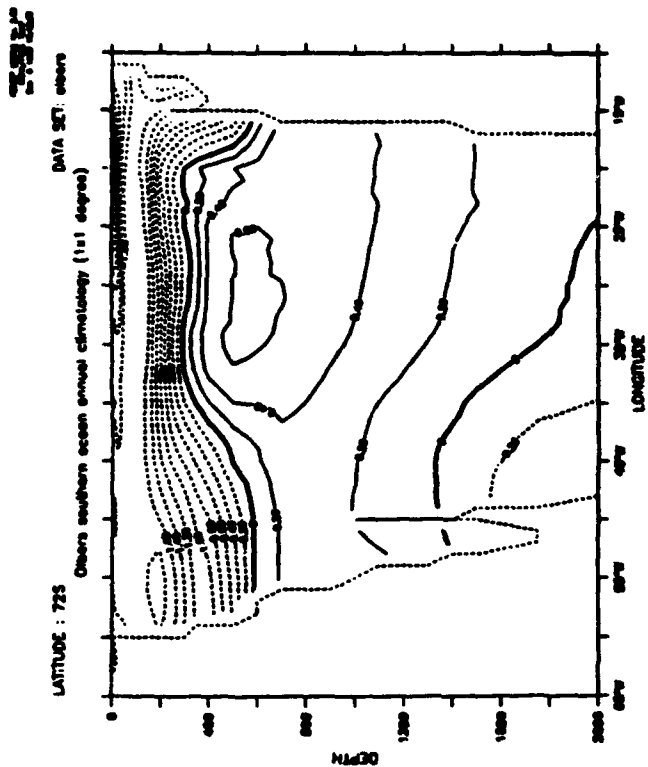
Figure 2.46 Potential Vorticity for area 150°W to 90°W
a.) Atlas Data b.) Half Degree Model Solution
c.) Quarter Degree Model Solution

G. WEDDELL SEA

The Weddell Sea is the area in the Antarctic which is the primary source of Antarctic Bottom Water. The western boundary current of the Weddell Gyre carries the Antarctic Bottom Water into the circumpolar belt to flood and chill the lower kilometer of the world's oceans. During the winter nearly all of the Weddell Gyre is covered by sea ice. In the gyre's western rim, however, a high concentration of perennial sea ice remains. Little data has been acquired from this region due to the nearly impenetrable ice cover.

Recently a US/Russian cooperative mission was deployed on an ice floe which drifted equatorward following the currents of the Weddell Gyre (Gordon, et al., 1993). This resulted in a unique opportunity to measure the currents of the western Weddell Sea and obtain temperature and salinity profiles which might add insight into the transport of Antarctic Bottom Water (AABW) northward.

From the observations the western boundary current appears to be over 400 km wide. The distribution of a temperature maximum along the western rim of the Weddell Gyre (Figure 2.46) (Gordon, et al., 1993) distinguishes two components of the western boundary current; a rim current which advects the warmest water from the eastern margins of the gyre to the western edge and a longer residence, interior component, which is essentially a recirculation of the inner hub of the Gyre. The rim current is believed to be more important to the overall water mass formation processes, as it provides salt to the continental margins required for the formation of AABW.



9

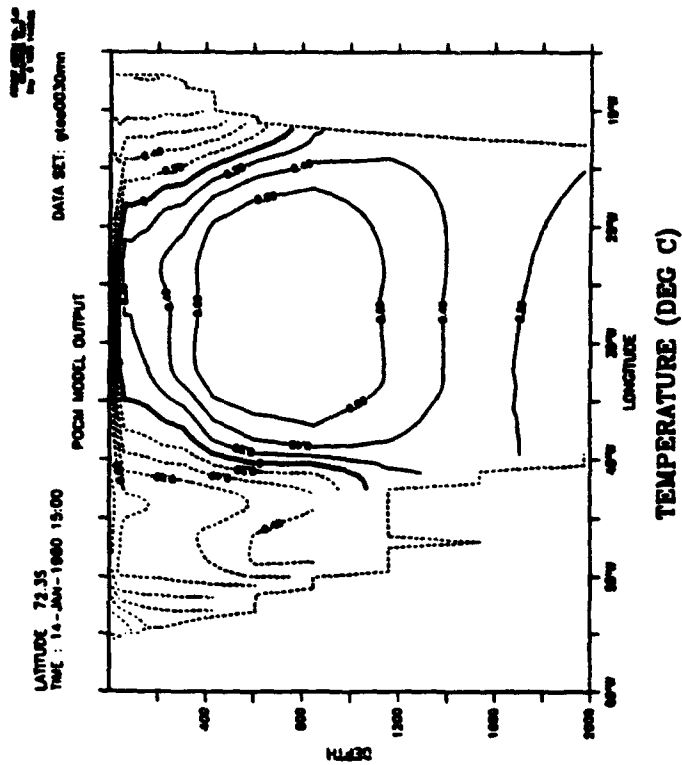
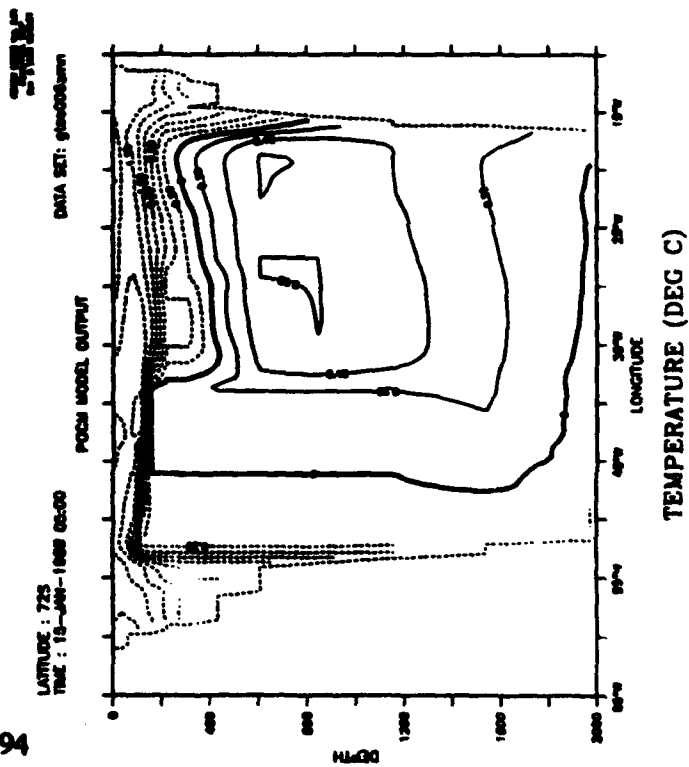


Figure 2.47 Vertical Temperature sections along 72°S
a.) Atlas Data b.) Half Degree Model Solution
c.) Quarter Degree Model Solution

In Figure 2.47 (a, b and c) , a vertical temperature section of the Weddell Sea, the half degree model solution shows a temperature maximum along the continental shelf which would also support the theory of a rim current. but neither the quarter degree model nor the observations show a similar maximum.

Transports of the western boundary current in the Weddell Sea, based on a mean bottom current of 1.3 cm/sec measured at 66.5 ° S and 41 ° W and upper level current measurements, are on the order of 40 Sv (Gordon et al., 1993) The mean 50 m depth northward current speed was about 5 cm/s in the western portion of the current dropping to about 1 cm/s farther to the east (Gordon et al., 1993). This is consistent with speeds predicted by both models .

In the half degree model transports calculated from the center of the gyre were 61 Sv. The quarter degree model transport was 51.2 Sv. This is consistent with the other transports calculated by the model. In general, the model transports are larger than the observations in the same proportion as those observed in the Drake Passage. In this case the flow is perhaps not as jet-like as the ACC and the more realistic bathymetry of the quarter degree model might make for more realistic transports.

1. Vertical Sections

a. Temperature along 72°S

In Figure 2.47 (a, b and c) the half degree model solution shows a temperature maximum along the continental shelf which would also support the theory of a rim current. but neither the quarter degree model or the observations show a similar maximum.

b. Salinity along 72°S

The surface salinity gradient in this area is strongest in the observations (Figure 2.48 a, b and c), weaker in the model solutions. This is in strong contrast to the other sectors of the study where in the vicinity of the ACC the gradient was greatest in the model solutions. The quarter degree model is in much closer agreement with the observations. Both the quarter degree model and the observations have a homogeneous deep layer of water below 400 m. Also in contrast to previous salinity sections, the surface layers in the Weddell Sea are fresher in the models than in the observations.

2. Area 4000 m Temperature

The observations and the model solutions are in surprisingly good agreement (Figures 2.49 a, b and c). The temperatures at this level are topographically dependent. If a sill is too high or low, the flow and hence the temperatures will be incorrect. Another reason for the good agreement shown is the time it would take for the model flow to influence the initialized values.

3. Circulation

a. Surface (37.5 m)

The circulation depicted in the quarter degree model (Figures 2.50 a and b, model only) also lend credence to the rim current theory as the current along the continental shelf is stronger than that of the gyre.

b. Deep (3575 m)

The deep circulation in the quarter degree model shows an interesting split in vicinity of 10°W and the continental shelf (Figures 2.51 a and b, model only). The stronger current remains to the south and circulates along the continental shelf; the

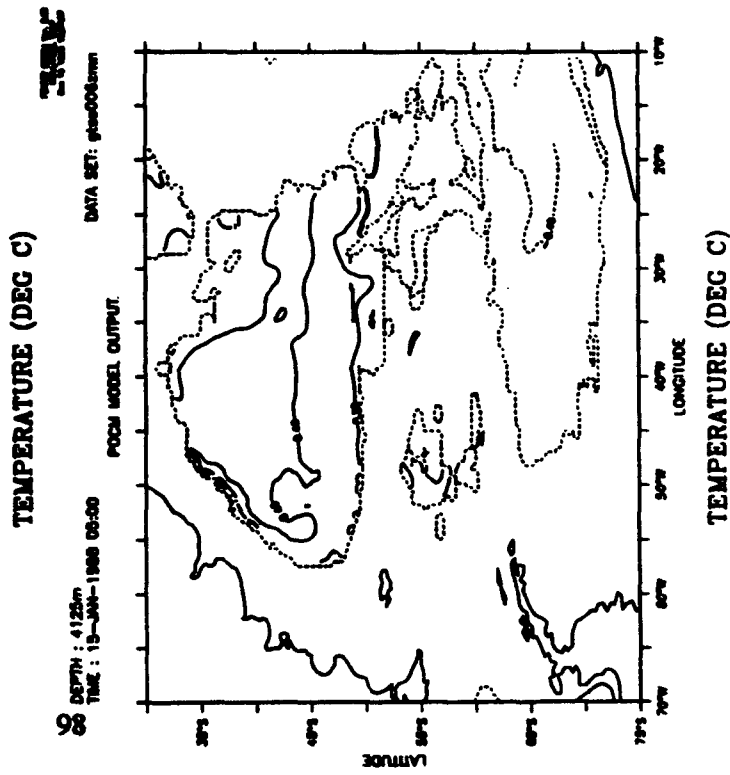
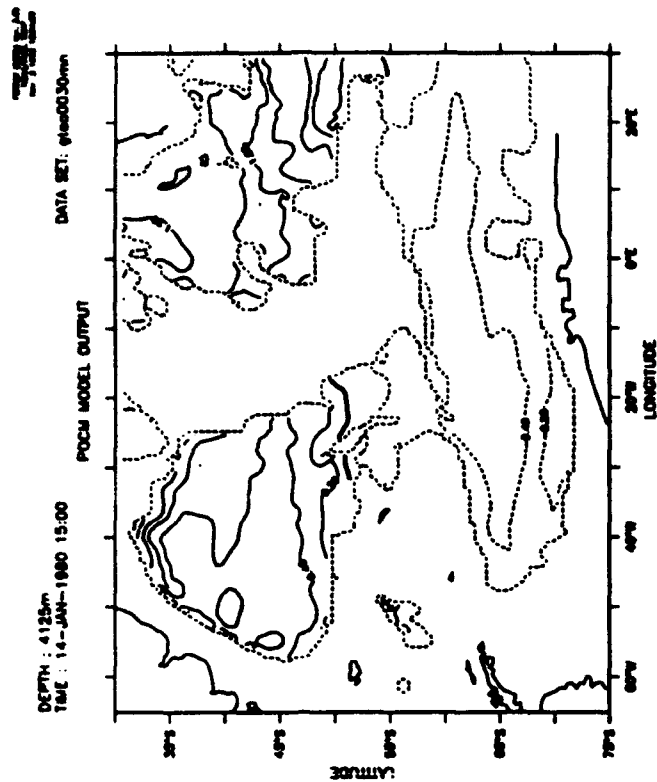
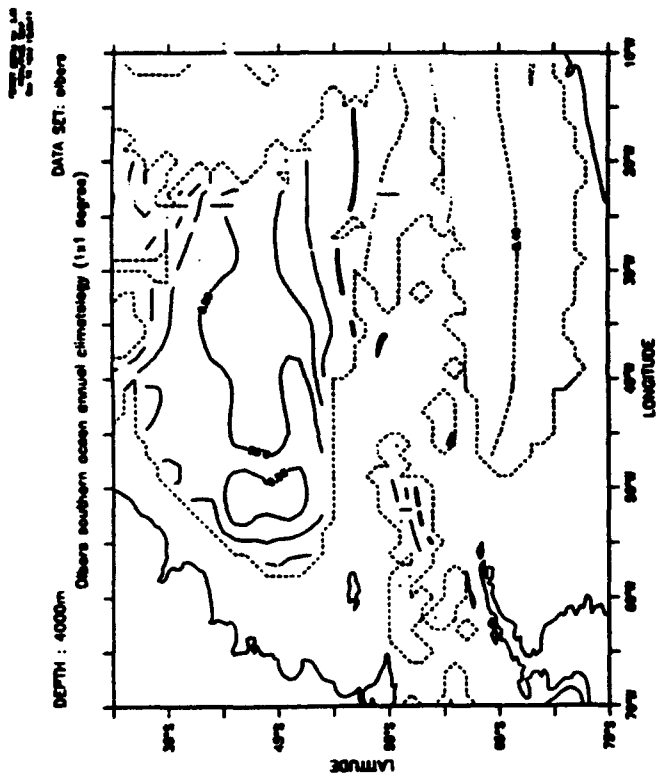


Figure 2.49 4000 m Temperature charts for Weddell Sea Area
 a.) Atlas Data b.) Half Degree Model Solution
 c.) Quarter Degree Model Solution

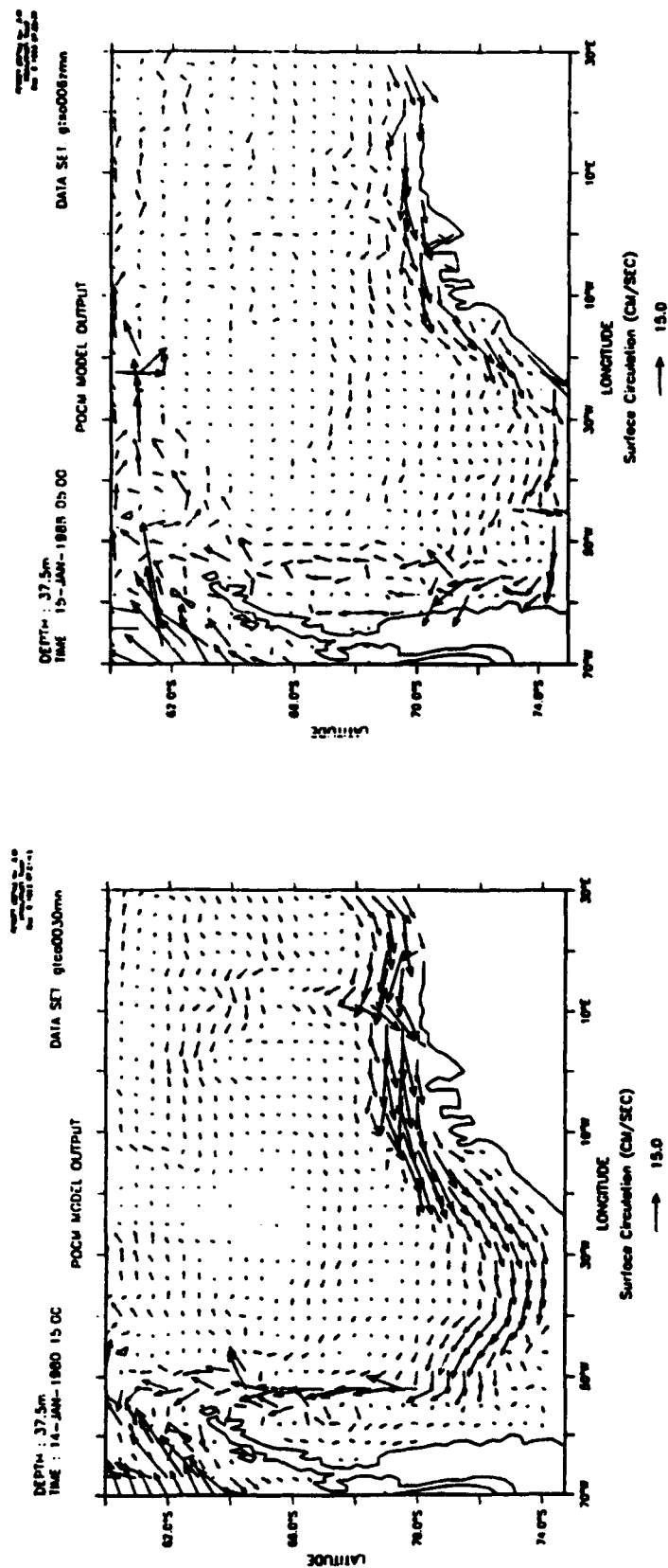


Figure 2.50 Surface Circulation in Weddell Sea Area
a.) Half Degree Model Solution b.) Quarter Degree Model Solution

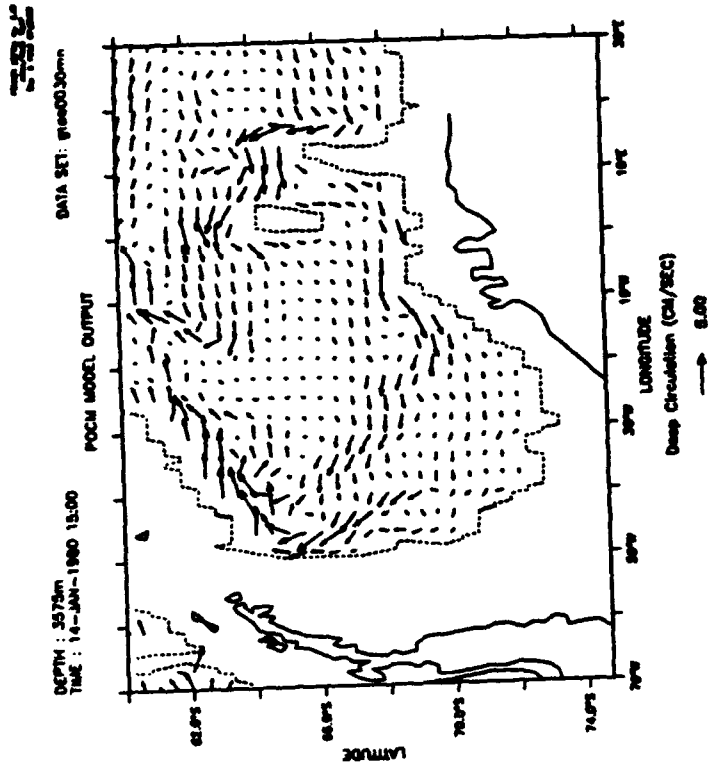
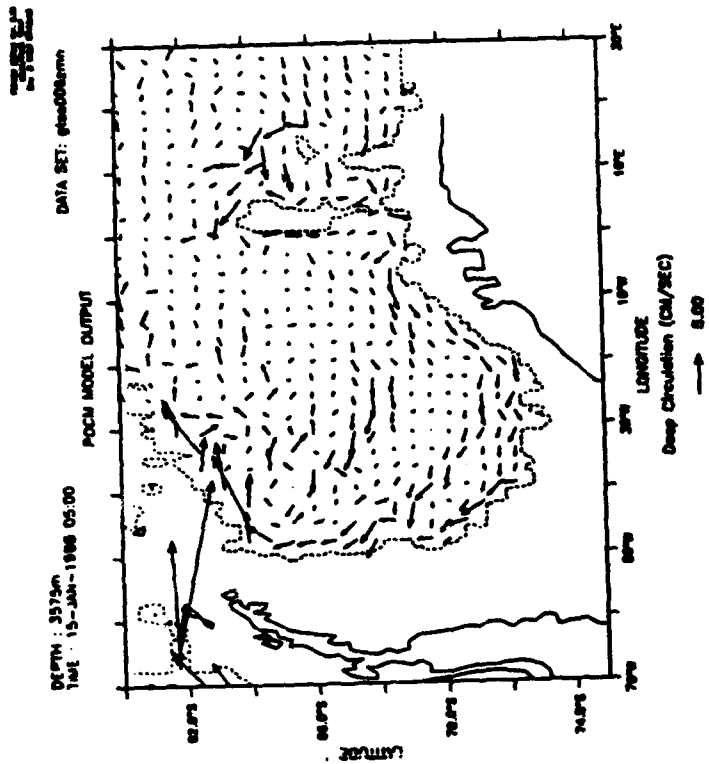


Figure 2.51 Deep Circulation in Weddell Sea Area
a.) Half Degree Model Solution b.) Quarter Degree Model Solution

interior gyre current continues to the north. In the half degree model there is only a single current and it is placed more towards the gyre than along the continental shelf.

H. THE TOTAL ACC

1. Transports

a. Mass Transports

Drake passage is one of the most studied areas of the Antarctic Circumpolar Current. This is because it is the most accessible portion of the ACC. It is also the one portion of the ACC that has a narrow choke point between the southern tip of South America and the continent of Antarctica. This makes it simpler to determine the mass transport of the current in this region. It may be simpler, but the measurement of the transport has historically not been a simple thing. The measurement of the current in the Drake passage is made difficult by the fragmented jet-like nature of the current. Even now there is great debate about whether the current has been well sampled enough to collect all the information necessary to measure the true transport. The observational data support a transport measured between 117 and 144 Sv (Whitworth, 1982). The transports measured between the southern tip of Africa and the Antarctic continent also give a similar value of 140 Sv (Whitworth and Nowlin, 1987). The Semtner - Chervin half degree model with ECMWF winds calculate a transport of 195.1 Sv in the Drake Passage south of Africa. This is reduced somewhat from the calculation of the Semtner - Chervin model with Hellerman and Rosenstein winds which gave a transport of 203 Sv for both the Drake Passage transport and the African transports. The major difference between these two sets of winds, is that in the ECMWF the polar easterlies which surround Antarctica south of 60°S are well represented and result in the easterly current

which would account for a slightly smaller transport calculation. The new quarter degree model transport calculation is somewhat higher, at 199.2 Sv. This may be a result of the enhanced resolution which can resolve more of that jet like flow. The increased grid resolution that modellers have been telling observationalists they need to sample the ACC may be a requirement for modellers as well. The FRAM (Fine Resolution Antarctic regional Model) calculated transports of around 200 Sv.

As discussed by the FRAM Group (1991) general circulation models have difficulty computing bottom pressure drags and torques in the presence of topography which results in a higher transport calculation.

b. Meridional Transports

Data simulated by ocean general circulation models have an advantage compared with data from observations in that it is almost continuous in time and space. Because of this it is possible to analyze numerical model data in ways which can give new insight to ocean circulation.

One of the new features that model data has highlighted is the series of cells that become apparent when the ocean velocity field is integrated zonally to give the meridional streamfunction. Such plots are used to illustrate the thermohaline circulation of the ocean. These plots represent the transport of angular momentum and not the water particle movement (Doos and Webb, 1992). In figures 2.52 a and b the meridional transport of the quarter degree and half degree models are shown.

A deep overturning cell driven by the circumpolar westerlies (recently termed the Deacon Cell) is also thought to be involved with the formation of

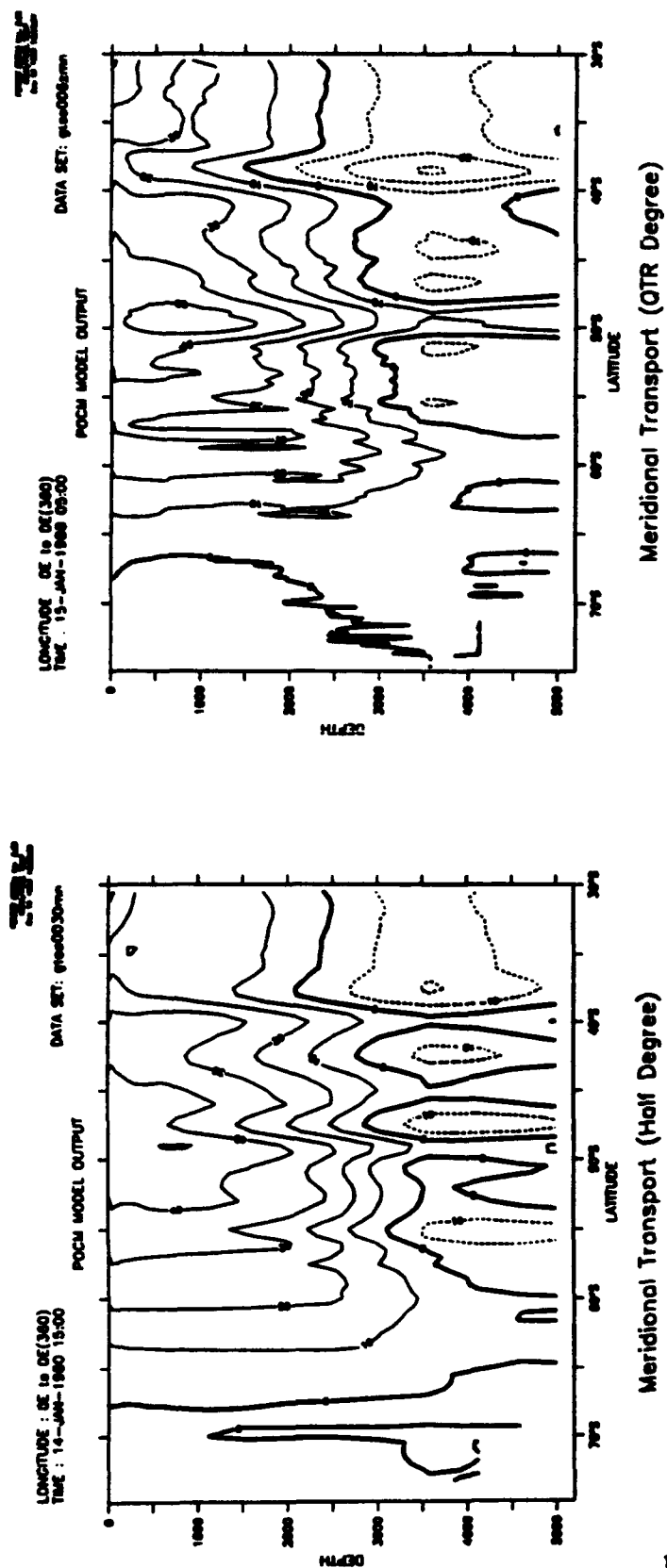


Figure 2.52 Meridional Transport
a.) Half Degree Model Solution b.) Quarter Degree Model Solution

deep water. The shape of the Deacon Cell, centered near 50°S in both models, has been shown to be highly influenced by the bathymetry of the Drake Passage gap (England, 1992). The quarter degree model bathymetry being more accurate results in a narrower and more shallow Deacon Cell. The differences between the quarter and half degree model seem primarily due to the improvement of eddy resolution. The half degree model presents an almost zonal flow, southward at the surface and northward at approximately 3000 m. In the quarter degrees model there are several vertical excursions indicating possible convection and eddy-mean exchange of angular momentum.

c. Meridional Heat Transport

T and V represent the instantaneous three day temperature and meridional velocity. An overbar represents the five or three year mean of these values. The mean of the meridional heat transport can then be decomposed into mean and fluctuating components.

$$\begin{aligned}\rho C_p \overline{VT} &= \rho C_p (\overline{V + V'}) (\overline{T + T'}) \\ &= \rho C_p (\overline{VT} + \overline{V'T'})\end{aligned}$$

The first term on the right is the meridional transport due to the mean current and the second term on the right is the meridional heat transport due to eddies. Figures 2.53a represents the half degree model mean and the eddy heat transport. Figure 2.53b represents the quarter degree model mean eddy heat transport. Figure 2.53 c displays both the half degree and quarter degree model for comparison. The FRAM meridional heat transport is shown in Figure 2.54 (FRAM group, 1991) and is very similar to the output of the half degree Semtner-Chervin model with Hellerman and Rosenstein winds (McCann, 1993).

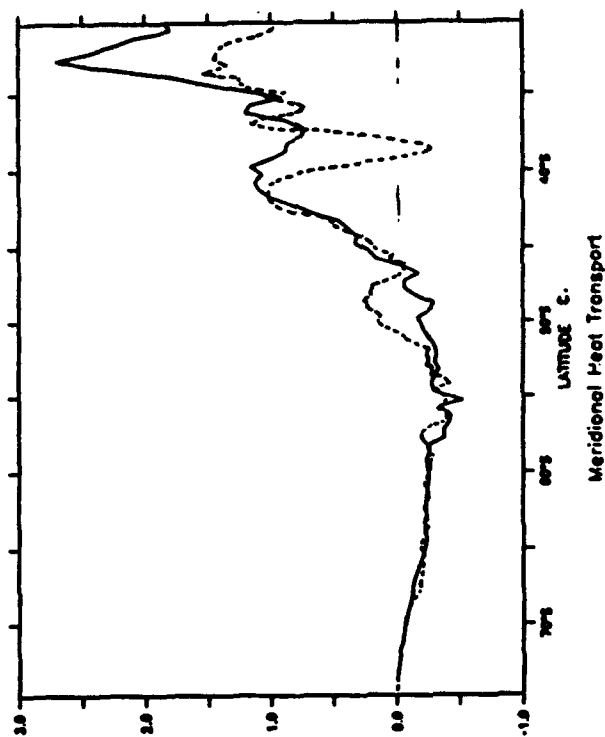
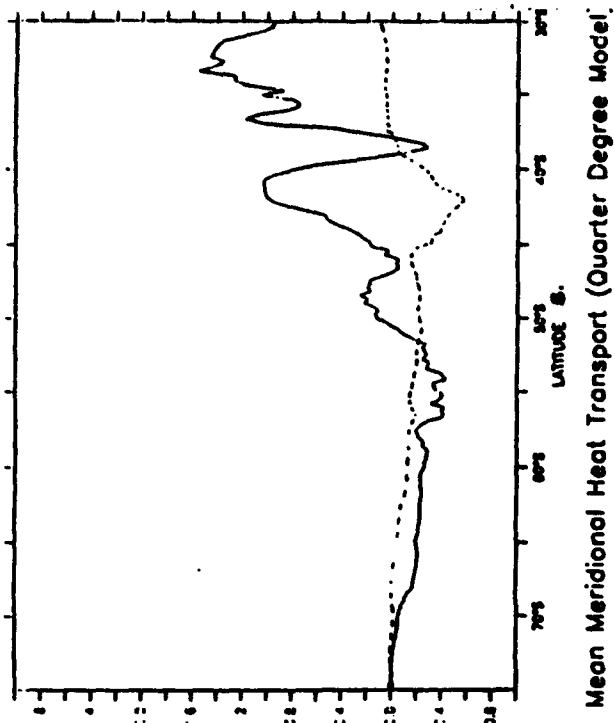
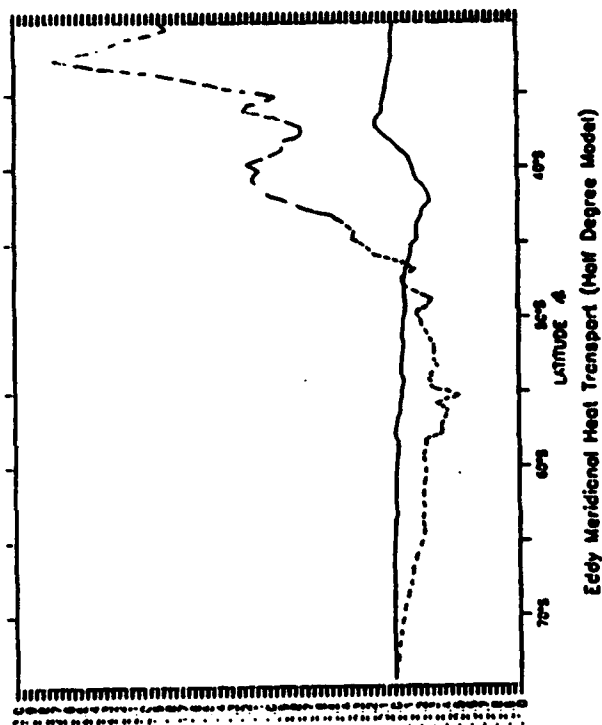


Figure 2.53 Meridional Heat Transport
 a.) Half degree model mean (dashed line)
 and Eddy (solid line) Heat Transport
 b) Quarter degree model mean (solid) and
 Eddy (dashed) Heat Transport
 c.) Half degree model mean (solid)
 and degree model mean (dashed)
 Heat Transport

Bryan (1991) compares a hierarchy of models of increasing resolution and concludes that eddies do not change the poleward transport of heat. Instead, they generate mean flows which tend to cancel the fluxes caused by eddies. This direct interaction between eddy and mean flow is supported by figures 2.53 a and b.

In comparison between the quarter degree and half degree model the quarter degree model shows a much smaller maximum near 35°S (1.55 pw vs. 2.7 pw) which are both in turn much larger than the FRAM solution which shows -.1 pw. This represents an equatorward transfer of heat. This feature does not appear in non-eddy-resolving simulations of the global circulation, perhaps because lateral diffusion dominates, forcing poleward transfer of heat. There is a possibility that equatorward heat transport may be a real feature of the southern ocean. A direct measurement of the ocean heat transport at 30°S gave a northward transport of 1.15 to 2.27 pw (Bennett, 1978). This is in the range of either the quarter or half degree model results. The ECMWF surface heat flux has also been compiled (Barnier, 1993). This data indicates that heat flux in the Northern Hemisphere is primarily negative while that in the Southern Hemisphere is primarily positive, which would also lend credence to an equatorward heat transport in the Southern Ocean.

In the quarter degree model there is a minimum (-.3 pw) located near 39°S that could be associated with the downwelling found at the Antarctic Convergence zone. This represents a poleward transfer of heat. There is also a minimum found in the half degree model but it is much weaker (.8 pw) and is found slightly more to the north along 37°S.

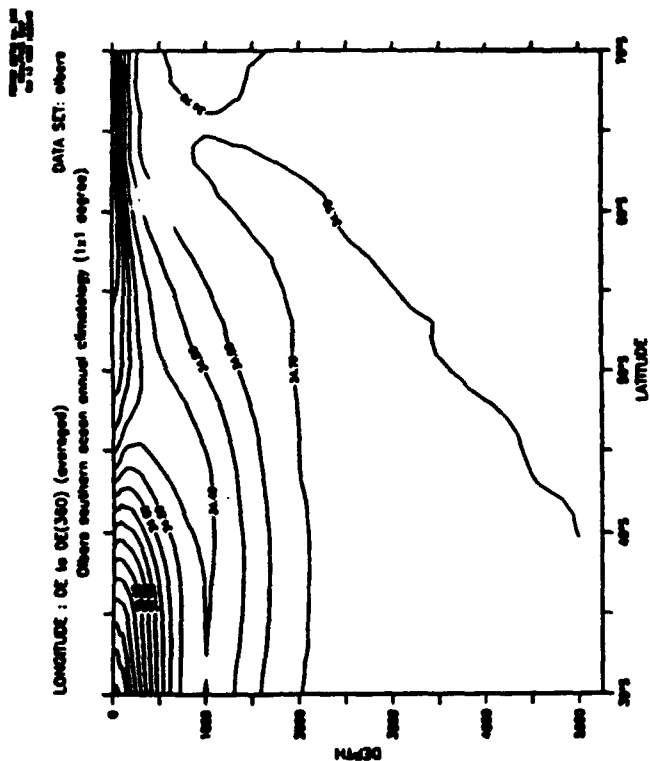
The FRAM solution also shows a minimum in region near 40°S but it is a relative minimum in the center of a maximum.

The heat transport in all the models go to zero near 70°S and the heat transport is poleward in all the models south of 45°S.

d. Zonal Salinity

Zonal salinity charts of the observations and the quarter and half degree models are shown to represent the models overall ability to create AAIW and AABW. See figure 2.54 a, b and c. In the observations the AAIW is represented by the low salinity tongue (34.40 psu) that extends from the surface near 50°S to 1000 m to the north near 35°S. In the half degree model the AAIW never quite completes the journey from the surface to 1000m. But a large pool of low salinity water is present in the half degree model at 1000m. This is primarily due to relaxation of the model parameters to observed Levitus values below 700m. The thermocline is free but the lower levels are forced back to observed values. In the quarter degree model, which is entirely free, the tongue of lower salinity water does appear to make the journey from the surface to the 1000 m level, although the tongue of water is more saline than those found in the observations at 34.6 ppt. The quarter degree model is not forced back to observed values. It is possible that given time the model will reach an even more realistic simulation of AAIW.

It is also worth noting is that the quarter degree model salinity gradient in the southern surface layer has become more spread out then the gradient in the half degree model.



108

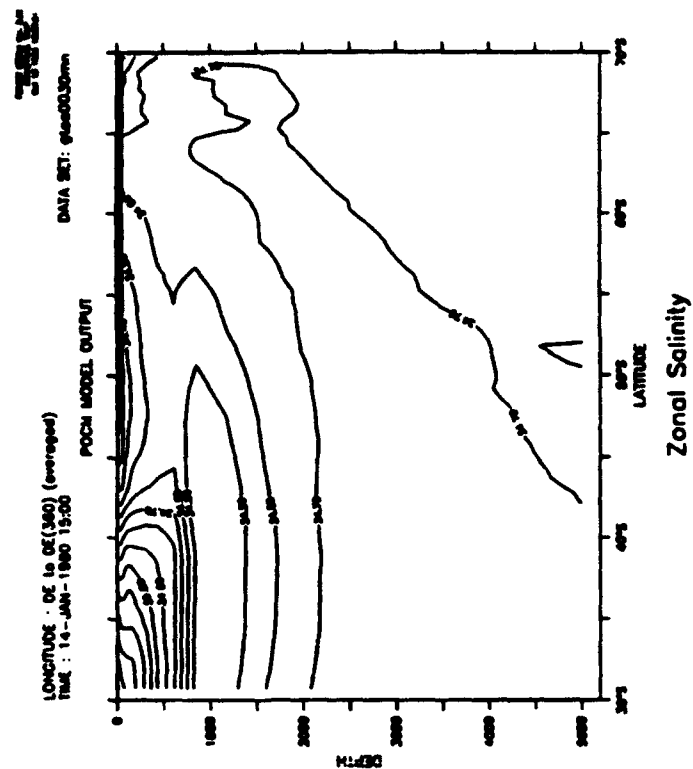
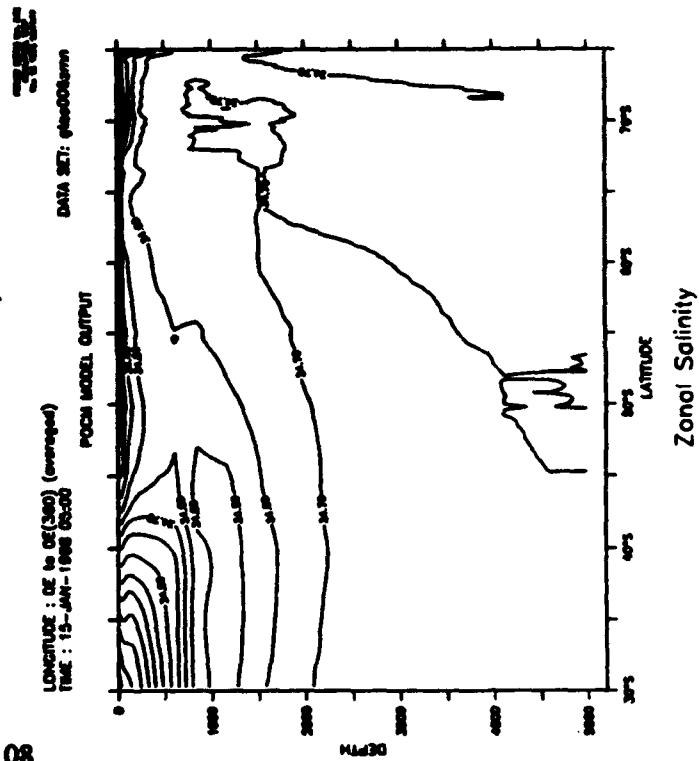


Figure 2.54 Zonal Salinities
a.) Atlas Data b.) Half Degree Model Solution
c.) Quarter Degree Model Solution

The Northern Deep Water represented by the 34.7 psu isohaline is well represented in both models with upwelling processes resulting in an upward hump near 65°S.

AABW although not shown in the observations also appears to be represented in both models as a lower salinity pool at depths below 3500 m.

e. Polar Projection Charts of the 100 m Temperatures

As was discussed in the regional analysis there are some discrepancies between the models and the observations. The 0° isotherm that surrounds the Antarctic continent extends much further to the north in the observations than in the model solutions (Figures 2.55 a, b and c). This could be due to the summertime bias in the Levitus data base which is more extreme than the summertime bias found in the Olbers data. The quarter degree model is better than the half degree model in this regard; perhaps because it is not as constrained to return to Levitus values as the half degree model is. The temperature gradients in the mid-latitudes are also stronger in the model solutions than in the observations, particularly in the Atlantic and Indian Oceans. The quarter degree model is also better in this regard than the half degree model. This could also be due to the forced return to Levitus values and perhaps given some time to run, the quarter degree model will correct this deficiency.

f. Polar Projection Charts of 100 m Salinity

The major discrepancy between the observations and the models throughout all of the regional analysis was the salinities in the surface layers of the Southern Ocean. This discrepancy is clearly shown in the polar salinity chart of the 100 m layer. The observations show a large area of low salinity water (34.0 psu) which almost

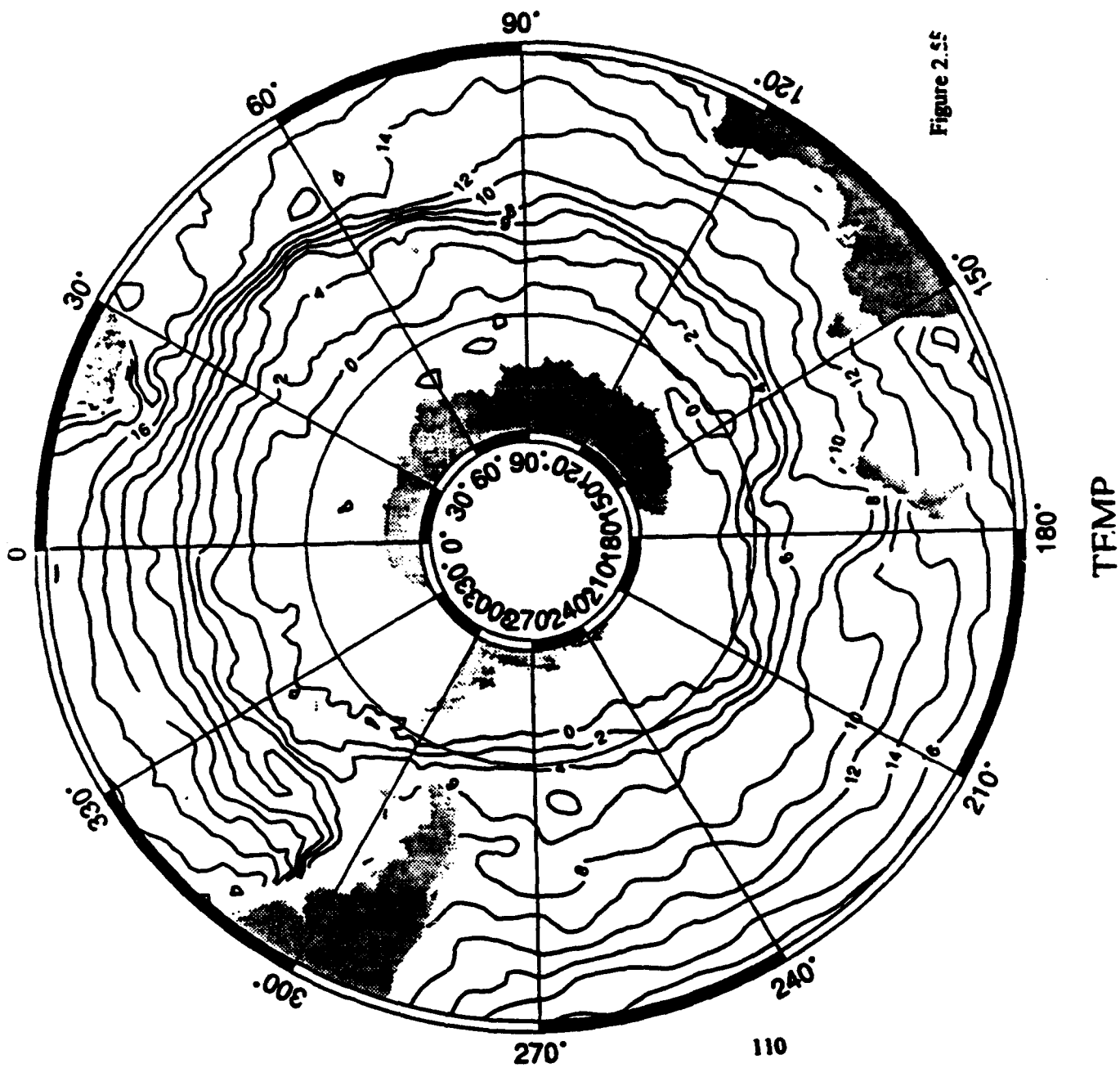


Figure 2.55 Polar 100 m Temperature Charts
a.) Atlas Data

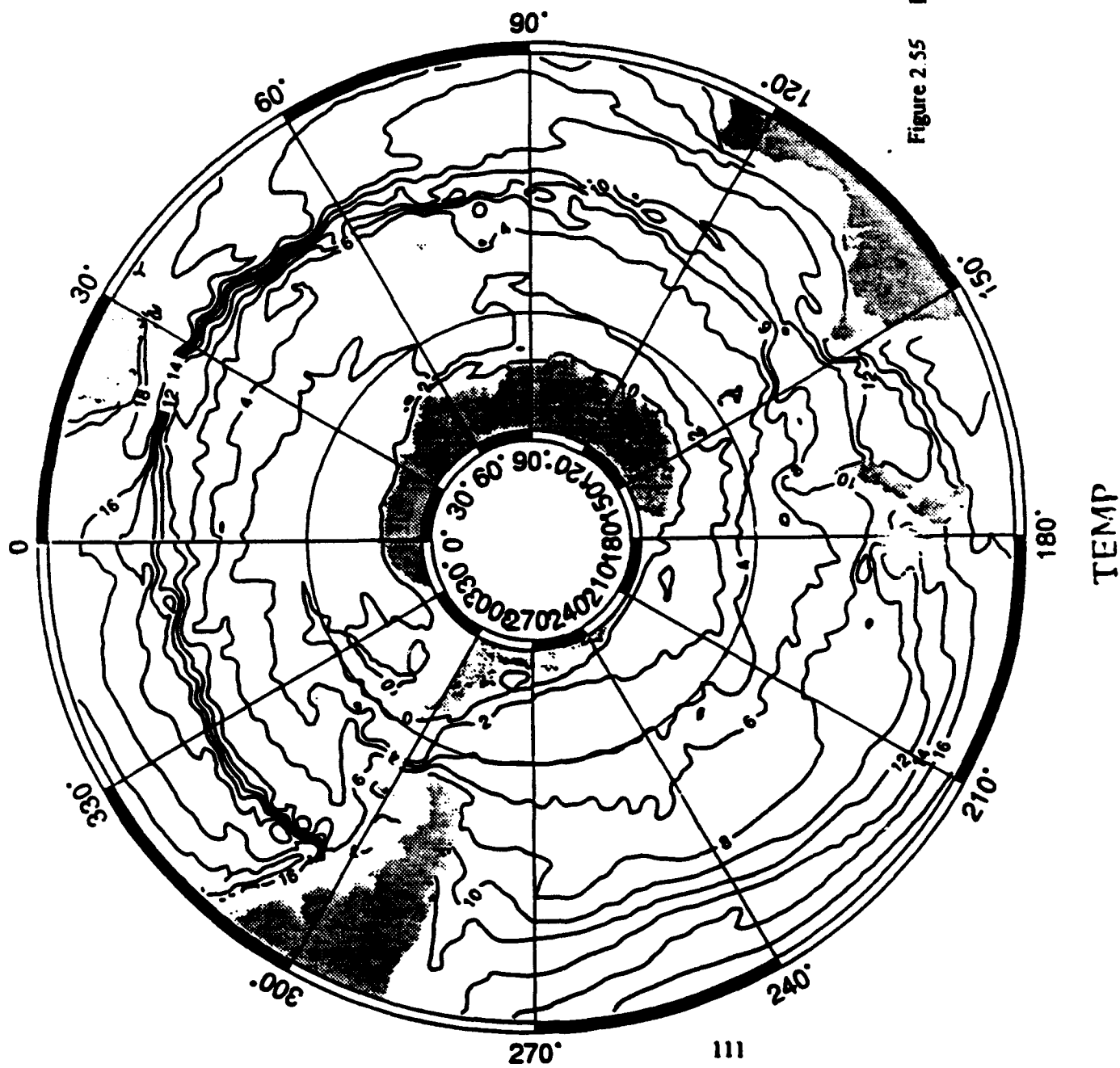


Figure 2.55 Polar 100 m Temperature Charts
b.) Half Degree Model Solution

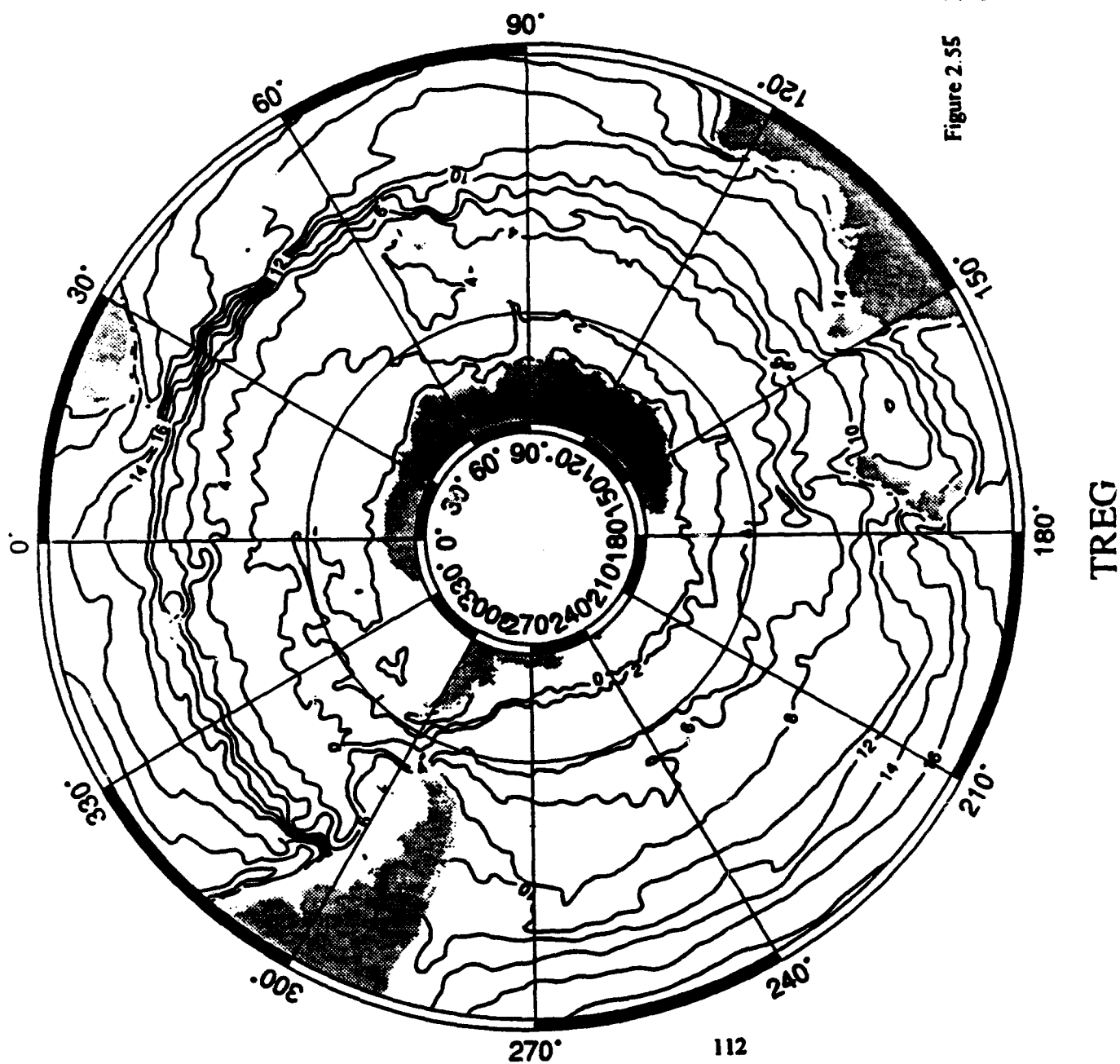


Figure 2.55 Polar 100 m Temperature Charts
c.) Quarter Degree Model Solution

TREG

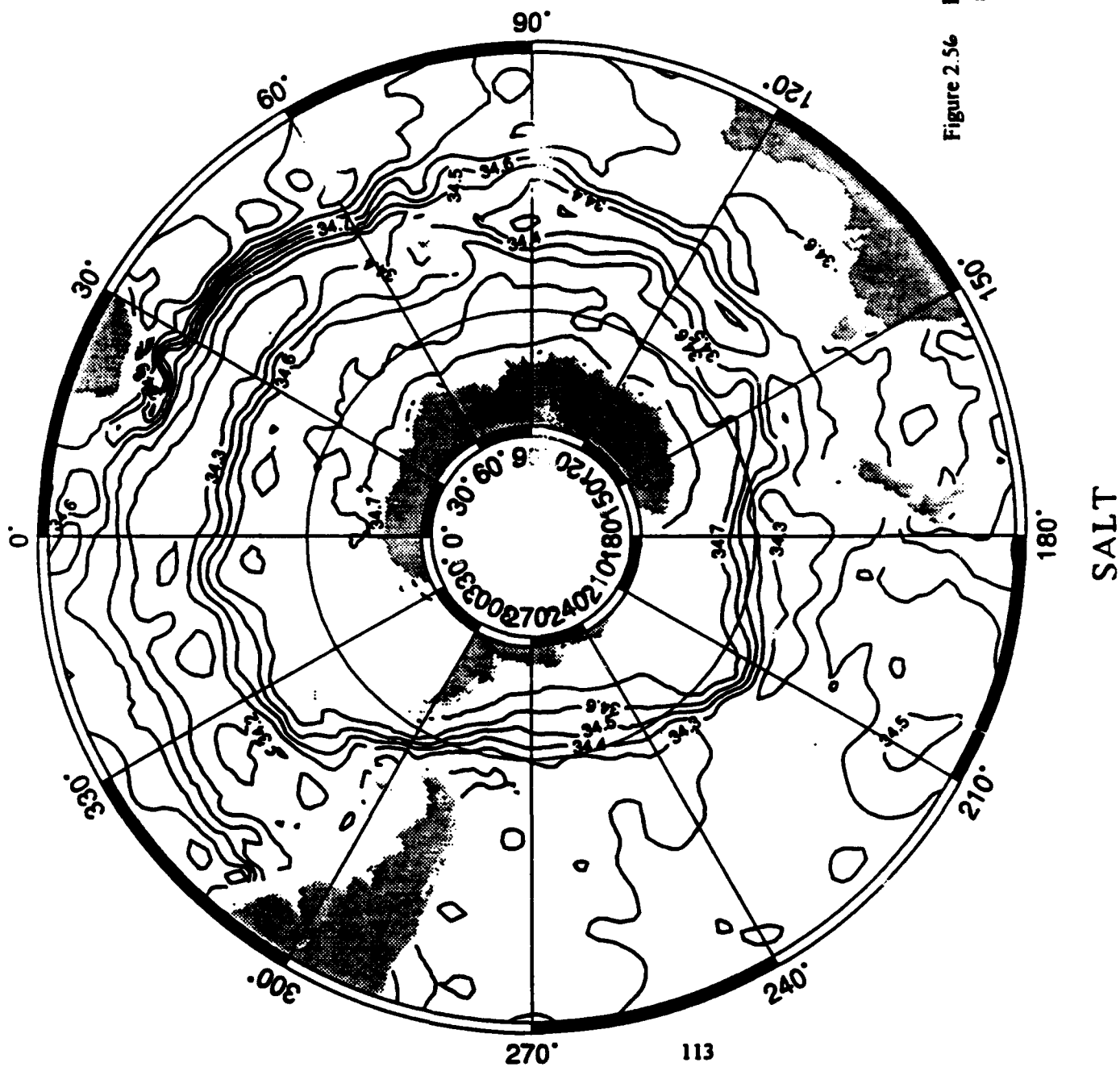


Figure 2.56 Polar 100 m Salinity Charts
a.) Atlas Data

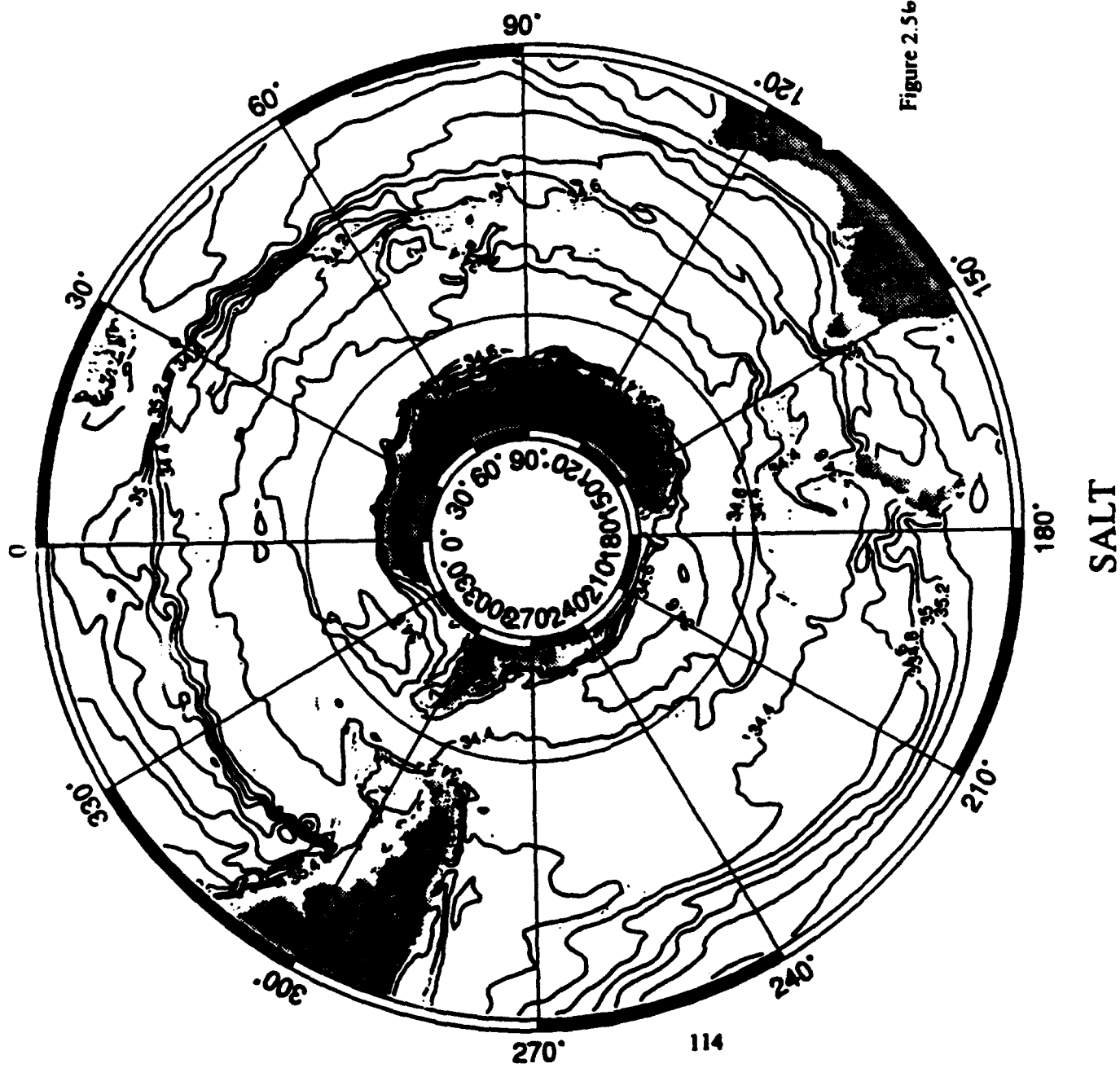


Figure 2.56 Polar 100 m Salinity Charts
b) Half Degree Model Solution

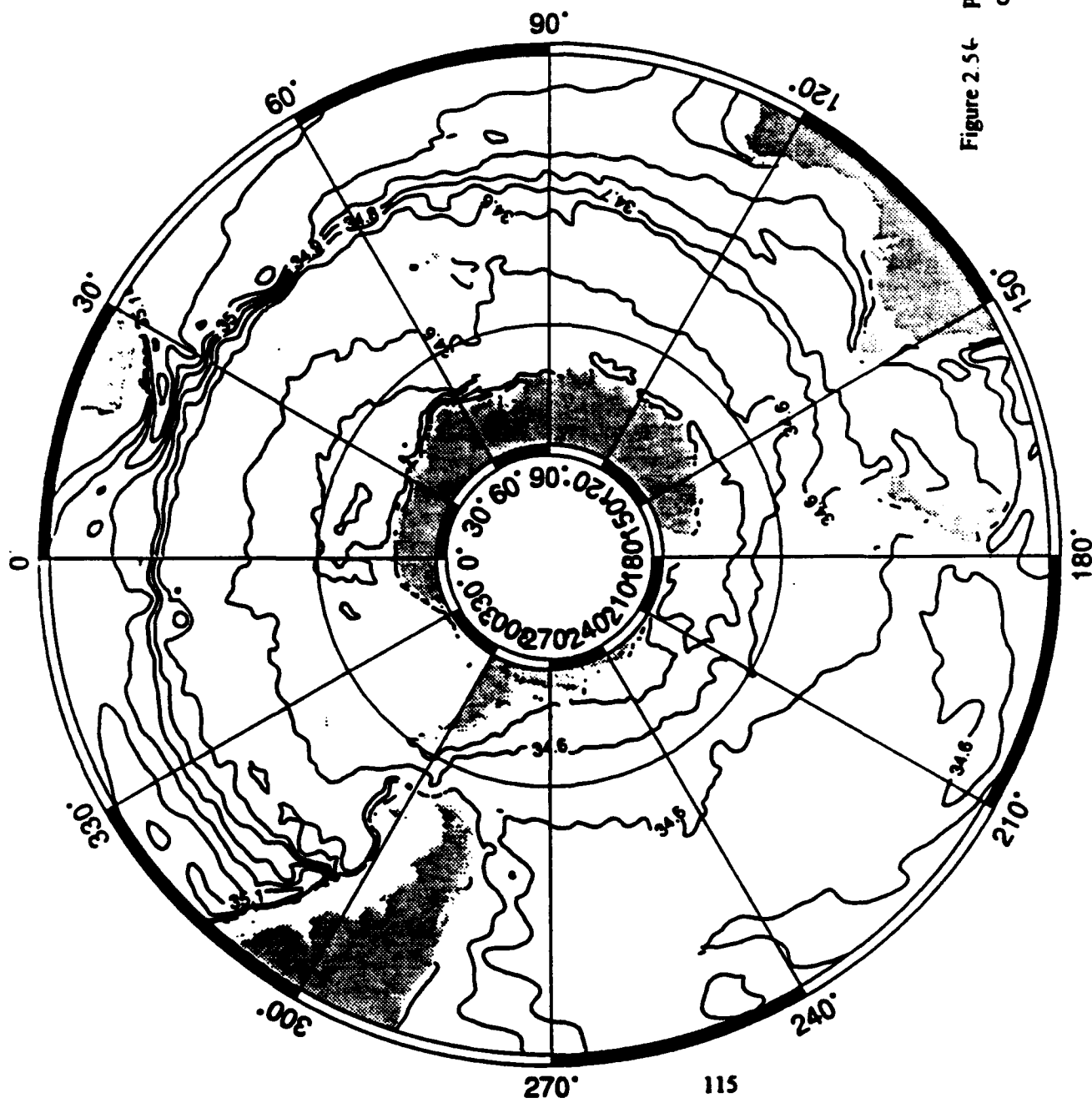


Figure 2.54 Polar 100 m Salinity Charts
c) Quarter Degree Model Solution

SREG

continuously circles the Antarctic continent from the Western Atlantic to the Central Pacific. The model solutions show the low salinity area of water at much higher salinities (34.4 ppt) and locates the low salinity water more to the north than in the observations. This results in a much more saline layer near the Antarctic continent in the model solutions than is observed.

The observations also show an area of higher salinity water (hatched area) in the Weddell and Ross Sea areas, associated with upwelling that is much smaller in the half degree model. The quarter degree model on the other hand has a larger area than the observations. The problems in this area have a lot to do with the parameterizations in the model for the melting of ice and its influence on the salinities. Another possibility is a problem with the mixed layer dynamics of the model or the surface fluxes that are used in the region. Additional observations in this area and new ECMWF gridded surface fluxes which will become available early next year might help make some improvements in this area.

III. CONCLUSIONS

Comparisons between the two model runs, a half degree resolution and a quarter degree resolution of the Semtner-Chervin eddy resolving global ocean model and the Hydrographic Atlas of the Southern Ocean (Olbers et al., 1993) observations are conducted by analyzing horizontal and vertical sections

The quarter degree model resolution, overall is a big improvement over the half degree model specifically in the areas of improved representation of Antarctic Intermediate Water (AAIW). In almost all regions the quarter degree model was closer to the observed temperature and salinity than the half degree model. The circulation of the quarter degree model especially at depth showed great improvement due primarily to the more realistic representation of bathymetry as well as the increase in resolution.

The quarter degree model, employing a Mercator grid, was interpolated forward from the half degree model initialization. For the last three years of the model run time, the resolution was improved to 0.25° on average and ECMWF winds were used. Also, no deep restoring in the last three years is introduced into the model. Another difference between the half degree model and the quarter degree model is that in the latter, the bathymetry is unsmoothed, so that not only is the resolution finer, the topography is more realistic.

The surface circulation also showed great improvement, especially in the Drake Passage region where bathymetry plays such a large role. In the Kerguelen plateau, Crozet Basin region, four fronts are discernible in the surface circulation, which is consistent with new observations (Park, et al., 1993). In the Weddell region the surface circulation in the quarter degree model is also consistent with new data obtained by the Weddell Ice Station group (Gordon, et al., 1993),

showing the presence of a stronger rim current which is also an improvement over the half degree model.

The surface salinity south of 55 ° S in the surface water above 400 m is of much higher salinity in the models than is observed. This could be due to problems in mixed layer dynamics in the model, inaccurate surface fluxes or inaccurate Levitus salinity values. Improvement in the model might be brought about by the new gridded surface flux data from ECMWF which will become available next year, increased number of observations of the Southern Ocean and the Weddell Sea during the WOCE initiative, and possibly an increase in vertical resolution which might help mixed layer dynamics.

Currently, a one sixth degree (on average) resolution model is being run at Los Alamos using the new 1024 node CM-5 computer. The grid has also been expanded to 78° North. It will be interesting to see whether the increase in horizontal resolution will continue to show the improvement in the circulation and property distribution patterns that has been demonstrated between the half degree and quarter degree model. Additionally the speed with which the Los Alamos machines are capable makes an operational, real-time, global ocean forecast model possible.

Other possible improvements include initiating the model with the Olbers (1993) data base in the Southern Ocean, rather than with the Levitus values. An increase in thermohaline observations in the Southern Ocean might lead to a more realistic simulation of the abyssal circulation as well.

LIST OF REFERENCES

- Barnier, B., L. Siefridt, and P. Marchesiello, Thermal forcing for a global ocean circulation model from a three year climatology of ECMWF analyses, submitted to *J. Marine Sciences*, Nov 1993.
- Bennett, A., Poleward heat fluxes in Southern Hemisphere Oceans *J. Phys. Oceanogr.*, **8**, 785-798, 1978.
- Boudra, D., K. Maillet, and E. Chassignet, Numerical modeling of Agulhas retroflection and ring formation with isopycnal outcropping, in *Mesoscale/Synoptic Structures in Geophysical Turbulence*, edited by J.C.J. Nihoul and B.M. Jamart, Elsevier Science Publishers B. V., Amsterdam, pp 315-334, 1989.
- Bryan, K., Poleward buoyancy transport in the ocean and mesoscale eddies, *J. Phys. Oceanogr.*, **16**, 927-933, 1986.
- Clarke, A., The dynamics of large scale, wind-driven variations in the Antarctic Circumpolar Current, *J. Phys. Oceanogr.*, **12**, 1092-1105, 1982.
- Cox, M., A primitive equation three dimensional model of the ocean, *Tech. Rep. 1, Ocean Group*, 250 pp., NOAA Geophys. Fluid Dyn. Lab., Princeton, NJ, 1984.
- Cox, M., A baroclinic numerical model of the world ocean: preliminary results, in *Numerical Models of Ocean Circulations*, National Academy of Sciences, pp. 107-120, 1975.
- Deacon, G., *The Antarctic Circumpolar Ocean*, Cambridge University Press, Cambridge, 1984.
- England, M., On the Formation of Antarctic Intermediate and Bottom Water in Ocean General Circulation Models, *J. Phys. Oceanogr.*, **22**, 918-926 1992
- The FRAM Group, An eddy resolving model of the Southern Ocean, *EOS Transactions of the AGU*, **72**, 169 and 174-175, 1991.
- Foldvik, A., and T. Gammelsrod, Notes on Southern Ocean hydrography, sea ice and bottom water formation, *Paleogeography, Paleoclimatology, Paleoecology*, **67**, 3-17, 1988.
- Forbes, C., K. Leaman, D. Olson, and O. Brown, Eddy and wave dynamics in the South Atlantic as diagnosed from GEOSAT altimeter data, *J. Geophys. Res.* **98**, 12,297-12,314, 1993.
- Gill, A., *Atmosphere-Ocean Dynamics*, Academic Press, Inc., Harcourt Brace Jovanovich, Publishers, 1982.
- Gordon, A., Seasonality of southern ocean sea ice, *J. Geophys. Res.* **86**, 4193-4197, 1981.
- Gordon, A., Weddell deep water variability, *J. Marine Res.* **40**, 199 -216, 1982.

- Gordon, A., and E. Molinelli, *Thermohaline and Chemical Distributions and the Atlas Data Set*, Columbia University Press, 1982.
- Gordon, A., The Southern Ocean and global climate, *Oceanus*, 31, 38-46, 1988.
- Gordon, A., B. Huber, and A. Field, Deep and bottom water of the Weddell Sea's western rim, submitted to *Nature*, 1993.
- Haney, R., Surface Thermal boundary condition for ocean circulation models, *J. Phys. Oceanog.*, 1, 241-248, 1971.
- Hastenrath, S., On meridional heat transports in the world ocean, *J. Phys. Oceanogr.* 12, 922-927, 1982.
- Haynes, P., Wind gyres in circumpolar oceans, *J. Phys. Oceanog.*, 15, 670-683, 1985.
- Hellerman, S., and M. Rosenstein, Normal monthly wind stress over the world ocean with error estimates, *J. Phys. Oceanog.*, 13, 1093-1104, 1983.
- Hoffman, E., and T. Whitworth III, A synoptic description of the flow at Drake Passage from year long measurements, *J. Geophys. Res.*, 90, 7177-7187, 1985.
- Johnson, T.J., Distribution of stress carried by mesoscale variability in the Antarctic Circumpolar current, 1992.
- Karolyi, D., and A. Oort, A comparison of Southern Hemisphere circulation statistics based on GFDL and Australian analyses, *Mon. Wea. Rev.* 115, 2033-2059, 1987.
- Keffer, T., The ventilation of the world's oceans: maps of the potential vorticity field, *J. Phys. Oceanog.*, 15, 509-523, 1985.
- Keffer, T., and G. Holloway, Estimating Southern Ocean eddy flux of heat and salt from satellite altimetry, *Nature*, 332, 624-626, 1988.
- Levitus, S. Climatological atlas of the world oceans, *NOAA Prof. Pap.* 13, U.S. Government Printing Office, Washington D.C., 1982.
- Mantyla, A., and J. Reid, Abyssal characteristics of the world ocean waters, *Deep Sea Res.* 30, 805-833, 1982.
- Marble, D., A model analysis of potential vorticity on isopycnal surfaces for the global ocean, Masters Thesis Sep 1993, Naval Postgraduate School, Monterey, CA.
- McCann, M., A. Semtner, and R. Chervin, Volume, heat, and salt budget transports from a global eddy-resolving model, *Climate Dyn.*, in press, 1993.

- Nowlin, W., and J. Klinck, The physics of the Antarctic Circumpolar Current, *Review Geophys.*, **24**, 469-491, 1986.
- Olbers, D., V. Gouretski, G. Seib, and J. Schroeter, *Hydrographic Atlas of the Southern Ocean*, Alfred Wegner Institute, Bremerhaven, 1992.
- Packanowski, R., S. Philander, Parameterization of vertical mixing in numerical models of tropical oceans, *J. Phys. Oceanogr.* **11**, 1443-1451, 1981.
- Patterson, S., Surface circulation and kinetic energy distributions in the Southern Hemisphere oceans from FGGE drifting buoys, *J. Phys. Oceanog.*, **15**, 865-880, 1985.
- Read, J., and R. Pollard, Structure and transport of the Antarctic Circumpolar Current and Agulhas return current at 40°E, *J. Geophys. Res.* **98**, 12281-12296, 1993.
- Reid, J., On the total geostrophic circulation of the South Atlantic Ocean: flow patterns, tracers, and transports, *Prog. Oceanog.* **23**, 149-244, 1989.
- Rintoul, S.R., South Atlantic interbasin exchange, *J. Geophys. Res.* **96**, 2675-2692, 1991.
- Semtner, A., History and methodology of modeling the world ocean circulation, in *Advanced Physical Oceanographic Numerical Modeling*, edited by J. O'Brien, pp. 23-26, Reidel Publishing, , 1986.
- Semtner, A., Finite difference formulation of a world ocean model, in *Advanced Physical Oceanographic Numerical Modeling*, edited by J. O'Brien, pp. 187-202, Reidel Publishing, 1986.
- Semtner, A., and R. Chervin, A simulation of the global ocean circulation with resolved eddies, *J. Geophys. Res.*, **93**, 15,502 - 15,521, 1988.
- Semtner, A., and R. Chervin, Ocean general circulation from a global eddy-resolving model, *J. Geophys. Res.*, **97**, 5493-5550, 1992.
- St.Pierre, D., On the effectiveness of the production of Antarctic Bottom Water in the Weddell and Ross Seas, Masters Thesis Sep 1989, Naval Postgraduate School, Monterey, CA.
- Szoeke, R., and M. Levine, The advective flux of heat by mean geostrophic motions in the Southern Ocean, *Deep Sea Res.*, **28**, 1057-1085, 1981.
- Tchernia, P., *Descriptive Regional Oceanography*, Pergamon Press, Oxford, England, 1980.
- Whitworth, T., III, and W. Nowlin, The net transport of the ACC through Drake Passage, *J. Phys. Oceanog.* **12**, 960- 971, 1982.

Whitworth, T., III, and W. Nowlin, Water masses and currents of the Southern Ocean at the Greenwich Meridian. *J. Geophys. Res.*, **92**, 6462-6476, 1987.

Wolff, J., E. Maier-Reimer, and D. Olbers, Wind driven flow over topography in a zonal β -plane channel: a quasi-geostrophic model of the ACC, *J. Phys. Oceanog.*, **21**, 236-263, 1991.

INITIAL DISTRIBUTION LIST

		<u>No. Copies</u>
1.	Defense Technical Information Center Cameron Station Alexandria, VA 22304-6145	2
2.	Library, Code 52 Naval Postgraduate School Monterey, CA 93943-5002	2
3.	Chairman, Department of Oceanography (Code OCCo) Naval Postgraduate School Monterey, CA 93943-5000	1
4.	Chairman, Department of Meteorology (Code ME/Hy) Naval Postgraduate School Monterey, CA 93943-5000	1
5.	Professor Albert J. Semtner Naval Postgraduate School Monterey, CA 93943-5000	1
6.	Stephen F. Ackley Cold Regions Research and Engineering Laboratory 72 Lyme Rd Hanover, NH 03755	1
7.	LT Rosemarie H. O'Carroll Naval Oceanography Command Facility P.O Box 85 NAS Jacksonville Jacksonville, FL 32212-0085	1
8.	Director Naval Oceanography Division Naval Observatory 34th and Massachusetts Avenue NW Washington, DC 20390	1
9.	Commander Naval Oceanography Command Stennis Space Center, MS 39522-5000	1

- | | | |
|-----|---|---|
| 10. | Commanding Officer
Naval Oceanographic Office
Stennis Space Center, MS 39529-5001 | 1 |
| 11. | Commanding Officer
Naval Polar Oceanography Center, Suitland
Washington, DC 20373 | 1 |
| 12. | Library
Department of Oceanography
University of Washington
Seattle, WA 98105 | 1 |
| 13. | Library Aquisitions
National Center for Atmospheric Research
P.O. Box 3000
Boulder, CO 80307 | 1 |